SYNTHESIS OF LIQUID LIGNIN POLYOL DESIGNED FOR FLEXIBLE POLYURETHANE FOAMS

By

Enoch Kofi Acquah

A DISSERTATION

Submitted to
Michigan State University
in partial fulfillment of the requirements
for the degree of

Chemical Engineering – Doctor of Philosophy

2025

ABSTRACT

Over the years, there has been a growing need for sustainable alternatives to replace petroleum-based polyols in the formulation of flexible polyurethane (PU) foams. Lignin, being the second most abundant natural polymer after cellulose, possesses various hydroxyl functionalities, making it a good polyol replacement. However, the incorporation of lignin in polyurethane flexible foams has been hampered by lignin's rigid structure, high hydroxyl value, poor solubility in co-polyols, and low reactivity towards isocyanate. Therefore, it is important to overcome these limitations to fully harness lignin's potential in flexible polyurethane foam applications. This study presents various modification strategies to synthesize liquid lignin polyols suitable for flexible PU formulations.

Lignin was first oxyalkylated using varying molar ratios of propylene carbonate (PC) (4, 5, and 10 equivalents (eq)), and the resulting liquid lignin polyols were directly incorporated into flexible PU foam formulations. While the inclusion of lignin polyols increased the biobased carbon content of the foams, excessive residual PC adversely affected key mechanical properties such as tensile strength, tear resistance, and compression force deflection (CFD). Fourier-transform infrared (FTIR) spectroscopy indicated that unreacted PC interfered with microphase separation, weakening intermolecular interactions and reducing the overall strength of the lignin-based foams. A lignin-to-PC molar ratio of 1:5 was identified as optimal, providing a balance between processability and thermomechanical performance.

Next, various co-polyols were used to further minimize PC loading in the lignin oxyalkylation reaction from 5 to 2eq. The results indicated that high ethylene oxide (EO)-based polyols showed the best compatibility with lignin oxyalkylation reaction and promoted lignin's phenolic hydroxyl group's reactivity with PC, while propylene oxide (PO)-based and bio-based polyols (such as

castor oil, soy polyols, and cardanol-based polyols) showed poor compatibility, resulting in a solid–liquid two-phase mixture during the reaction. Partial least squares (PLS) modeling (R^2Y = 86%, Q^2Y = 67%, using two components and cross-validation) revealed a strong positive correlation between the co-polyol's EO content and compatibility, and a strong negative correlation between compatibility and the co-polyol's average molecular weight. Following optimization of the oxyalkylation reaction, a flexible PU foam incorporating 20% lignin polyol in place of petroleum-based polyols demonstrated enhanced mechanical properties and met industry standards for automotive seating. Additionally, a foam formulation with 50% total polyol replacement, comprising 20% lignin polyol and 30% soy polyol, met all performance criteria except elongation at break, while showing improved CFD compared to commercial counterparts.

Finally, high-performance novel lignin-based polycarbonate polyols were prepared via a two-step process involving oxyalkylation of lignin with propylene carbonate, followed by transesterification with dimethyl carbonate. The resulting polycarbonate lignin polyols exhibited hydroxyl values (111–179 mg KOH/g) and viscosities (11,660–25,950 mPa.s) suitable for flexible PU foam formulations. In-depth Nuclear Magnetic Resonance (NMR) analysis confirmed the grafting of long polyether chains onto lignin during the oxyalkylation step and the introduction of multiple carbonate linkages at the end of the transesterification step. Foams were formulated by replacing up to 40% of petroleum-based polyols with synthesized polycarbonate lignin polyols. Additionally, flexible PU foams were prepared by replacing 60% of conventional polyol with a combination of synthesized lignin polyol and soy polyol. Formulated foams demonstrated superior mechanical properties, including enhanced tensile strength, and load-bearing properties, compared to petroleum-based foams. Additionally, the foams exhibited improved thermal stability, shock absorption, and biodegradability.

ACKNOWLEDGEMENTS

I express my sincere gratitude to my supervisor, Dr. Mojgan Nejad, for giving me the opportunity to learn under her guidance and to grow in all aspects of my life, including research, writing, presentation, and networking. I am also deeply grateful to my committee members, Dr. Rafael Auras (School of Packaging), Dr. Robert Ferrier (Chemical Engineering & Materials Science Department), and Dr. Ilsoon Lee (Chemical Engineering & Materials Science Department), for their invaluable feedback, comments, and suggestions.

Special thanks to Dr. Daniel Holmes (Department of Chemistry, MSU) for providing comprehensive training in polymer structural analysis using Nuclear Magnetic Resonance (NMR), which was instrumental throughout my research, I am also grateful to Dr. Amin Joodaky for his support in impact test analysis and to Mr. Larry Armbruster for his technical assistance and guidance. I extend my heartfelt thanks to Dr. Saeid Nikafshar for inspiring my passion for research and polymer chemistry. Additionally, I am grateful to my colleagues Maureen Afaglo, Mariia Bespalova, Kevin Dunne, Manasseh Agbedam, Sajad Nikafshar, Mohsen Siahkamari, Sadaf Mearaj, Rachel Schenck, Ella Yakubison, and our lab manager, Kory, for their support and encouragement.

Of course, I am immensely thankful to my parents and the Ishi Odamtten family for their unwavering prayers and support. I could not have achieved this without you. And finally, to my incredible wife, Richlove. Thank you for your patience, inspiration, unwavering support, care, and unconditional love. You are my greatest source of strength and my favorite person. Above all, I give thanks and glory to the Almighty God for His guidance, wisdom, and supernatural protection throughout my studies.

TABLE OF CONTENTS

LIST OF ABBREVIATIONS

PU – Polyurethane

PO – Propylene Oxide

EO – Ethylene Oxide

PC – Propylene Carbonate

PEG – Polyethylene Glycol

PEC – Polyether Carbonate

PPG – Polypropylene Glycol

SP – Soy Polyol

LP – Lignin Polyol

CNSL – Cashew Nut Shell Liquid

CO – Castor Oil

S – Syringyl

G – Guaiacyl

H – Hydroxyphenyl

LCC – Lignin Carbohydrate Complex

H-HW – Hydrolysis Hardwood

K-SW - Kraft Softwood

O-B – Organosolv Birch

OL – Oxyalkylated Lignin

TL – Transesterified Lignin

DBU - 1,8-Diazabicyclo 5.4.0 undec-7-ene

TBD - 1,5,7-Triazabicyclo[4.4.0]dec-5-ene

NMR – Nuclear Magnetic Resonance

HSQC – Heteronuclear Single Quantum Coherence

HMBC – Heteronuclear Multiple Bond Correlation

pMC - Percent Modern Carbon

OEM – Original Equipment Manufacturer

PPHP – Parts Per Hundred Polyol

Chapter 1: Introduction

1.1 Background

1.1.1 Polyurethane chemistry

Polyurethane flexible foams are utilized across various industries including automotive, furniture, packaging, medical devices, sporting goods, sound absorption, footwear and apparel, offering comfort, durability, and performance benefits in these applications.[1] Polyurethane is produced from a step-growth polymerization reaction between polyol and isocyanate, with or without catalysts. In flexible polyurethane foams, the polyol part forms the soft segment, whereas isocyanate forms the hard segment. Therefore, the properties of the final PU product can be tailored towards the target performance or end use by varying the properties of main components and additives.[2] The property of polyurethane foam largely depends on the hydroxyl value, functionality, and molecular weight of polyols as well as isocyanate types and amounts. [3]

Polyester and polyether polyols are primarily used for polyurethane synthesis, with the latter being mostly used in flexible foam formulation due to its resistance to hydrolysis.[4] Conventional polyether polyols are produced from the ring-opening polymerization of alkylene oxide in the presence of a basic catalyst and an initiator such as ethylene glycol, propylene glycol, sorbitol, or glycerol, based on the target functionality. [2] Generally, low hydroxyl value, high molecular weight, and low functionality (typically 2-3) polyols produce flexible and less crosslinked polymers whereas, high hydroxyl value, low molecular weight, and high functionality polyols yield rigid and highly crosslinked polymers.[3] Viscosity is another crucial physical characteristic, as it influences the processability of polyols,[5] which subsequently impacts the quality of the foam generated. Low polyol viscosities suitable for spray applications (Robotic heads) are generally preferred for flexible foams.[4]

In flexible polyurethane foam formulation, two main reactions take place: gelation and blow reactions. The gelation reaction occurs between polyol and isocyanate, forming urethane linkages, as illustrated in **Figure 1.1a**. The blow reaction, on the other hand, involves the reaction between water and isocyanate. Both reactions are exothermic. Water reacts with isocyanate to form thermally unstable carbamic acid, which decomposes into amine and carbon dioxide—the latter being essential for foam expansion. The resulting amines, which contain active hydrogen atoms, further react with isocyanate to introduce urea linkages into the polymer chain, as depicted in **Figure 1.1c**. The formation of polyurea linkages contributes to the hard segment of the foam, influencing its mechanical properties. [3]

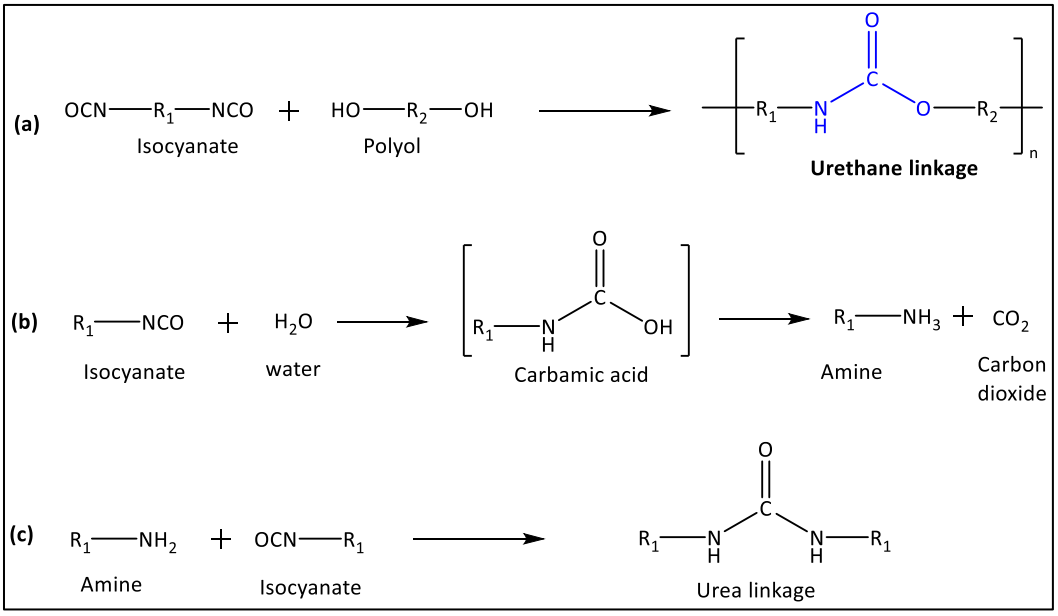

Figure 1.1: Chemistry of polyurethane flexible foam.

Despite the various applications of polyurethane flexible foams, the major drawback has been the source of feedstocks or raw materials. Currently, the majority of polyols are produced from fossil-based raw materials, directly utilizing toxic alkylene oxides such as propylene oxide.[2] This has

motivated researchers both from academia and industry to explore various sustainable alternatives to replace these petrochemicals, thus producing more sustainable foams.

Over the years, researchers have attempted to partially replace petroleum-based polyols with biobased alternatives such as castor oil, [6] rapeseed oil, [7] cashew nutshell liquid,[8] and palm oil. [9,10] Castor oil has been employed directly to produce PU foams due to the presence of hydroxyl groups in their fatty acid backbone.[6] Vegetable oils have also been extensively used to produce biobased polyols via various modification methods, with epoxidation and ring-opening being already employed by industries to produce soy polyols from soybean oil. [11–20] In this process, double bonds on the triglyceride chain of soybean oil are epoxidized in the presence of acetic/formic acid and hydrogen peroxide to yield hydroxyl groups required for PU applications. [21]

1.1.2 Lignin

1.1.2.1 Structure and Extraction Processes

Lignin is a complex natural polymer that accounts for about 30 wt.% of the biomass on a dry mass basis.[22] It is produced as a by-product of pulp and paper industry, and biorefineries.[23,24] Chemically, lignin is a multi-functional polymer containing of aliphatic, phenolic, and carboxylic hydroxyl groups.[25–28] It is primarily made up of three main monomeric phenolic subunits of syringyl (S), guiacyl (G) and *p*-hydroxyphenol (H) radically coupled via different ether and carbon-carbon linkages. [22,29–31]These linkages include *β*-O-4, *β*-5, and *β*-*β* linkages, with *β*-O-4 being the most abundant linkage in lignin.[32–40] The difference in monomers depends on the positions of methoxy group (MeO). [41] Guiacyl and syringyl have one and two methoxy group attached to lignin at ortho positions respectively as presented in **Figure 1.2**. The structure of lignin macromolecule and its linkages are shown in **Figure 1.3**.

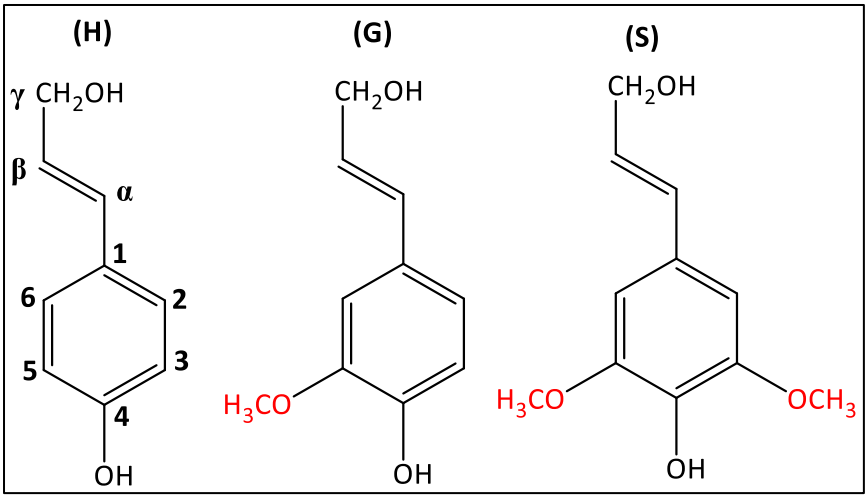

Figure 1.2: Structure of lignin monomeric units. H- p-hydroxyphenol, G-guiacyl, S-syringyl.

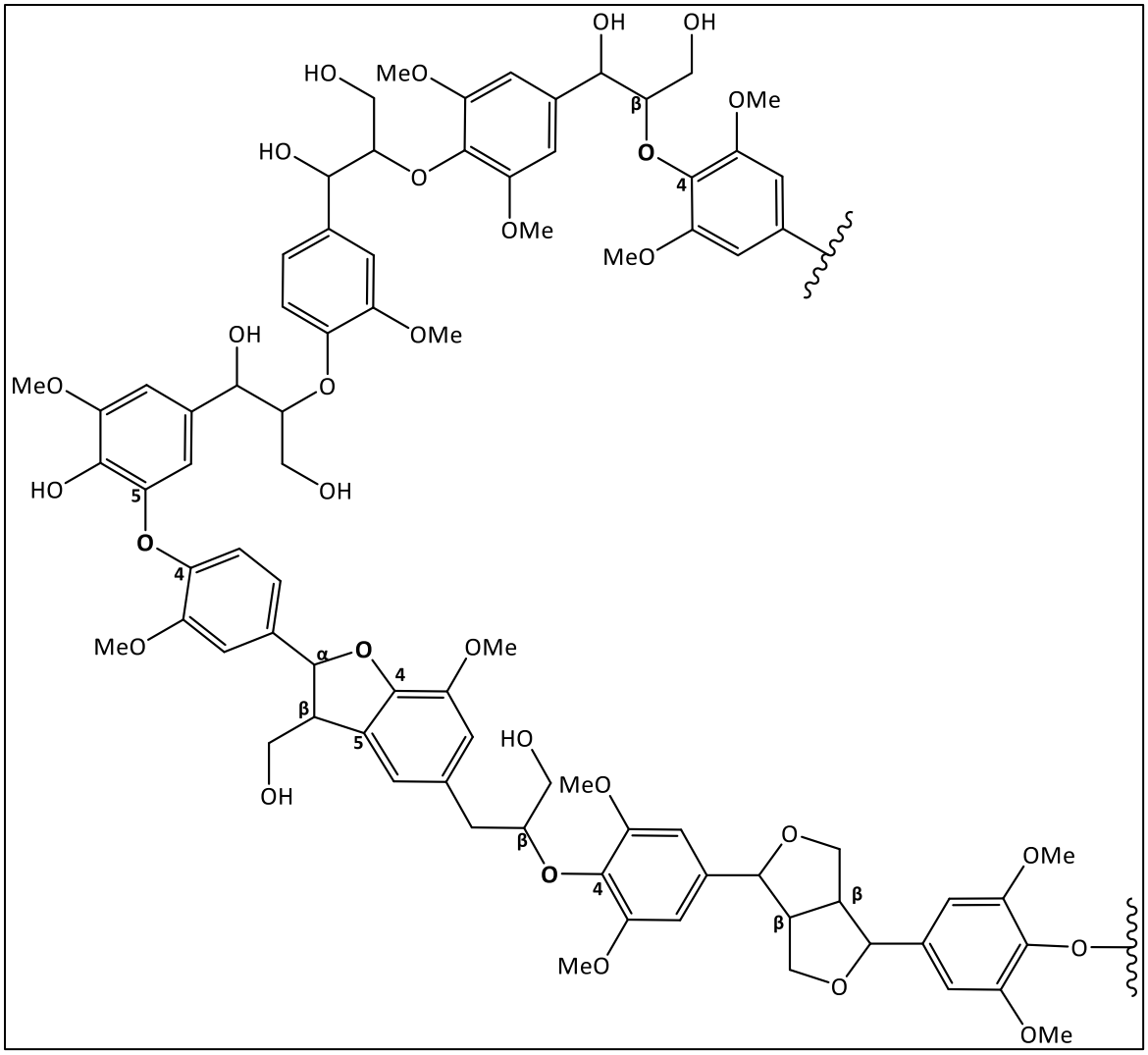

Figure 1.3: Structure of lignin macromolecule. [42]

The type and amount of subunit in lignin depends on the biomass source. G units, for instance, make up the majority of softwood lignins.[43] Conversely, herbaceous plants like wheat straw have all three monomers along with a high concentration of H units, in contrast to hardwood lignins, which are rich in G and S units and low in H units.[44] In addition, the proportion of lignin in different plant sources varies greatly, with grasses (15–24 wt.%), hardwood (18–26 wt.%), and softwood generally having the highest lignin concentration (25–32 wt.%). [45] Based on methoxy content and elemental analysis (C, H, O, S), the empirical formula of lignin can be deduced.

Lignin is extracted from biomass, typically as by-products, using different isolation processes. Kraft (using sodium hydroxide and sodium sulfite), soda (using sodium hydroxide), sulfite (using aqueous sulfur dioxide), and organosolv (using water and organic solvent) are the major delignification methods, with the kraft process being the most widely used.[46]

These lignin isolation methods have been exhaustively employed to break down the lignin carbohydrate complexes (LCCs) linkages,[38] resulting in lignin solubilized in the extraction media. These isolation processes have also been found to further chemically transform lignin, which significantly changes its properties.[29] The kraft process for instance, due to the severity of pulping condition, produces a significant depolymerization of easily altered β-O-4 ether linkages in lignin, resulting in a highly structurally modified lignin with high phenolic hydroxyl content.[46] It is important to also note that, lignin–carbohydrate complexes are not always completely broken down, resulting in a significant quantity of residual sugars in the isolated alkaline lignins.[47] This is particularly common in lignins produced from biorefineries. Additionally, the lignin fraction generally contains a sizable amount of residual minerals from the inorganic compounds used in the isolation process.[48]

On the other hand, organosolv pulping yields relatively high-purity lignins with considerably lower amounts of both residual carbohydrates and ash, making organosolv lignin ideal for various applications.[46,47] This pulping process is done with a mixture of water and an organic solvent, with or without the use of acid catalyst.[47] However, due to issues such as substantial equipment corrosion due to strong acid usage, high energy consumption from the solvent recovery process, and lower-quality pulp produced compared to the kraft process, this method is not currently used in the pulping industry.[49,50]

1.1.2.2 Lignin as a sustainable polyol replacement

Lignin, despite being the second most abundant natural polymer after cellulose, has received minimal attention in PU flexible foam formulations. Lignin can be an excellent precursor, typically as a polyol, for polyurethane synthesis due to the presence of hydroxyl functional groups. [51] The incorporation of lignin into various polyurethane products has been demonstrated in most cases to provide excellent performance benefits such as increasing the bio-based content of the polyurethane, increased ultraviolet (UV) stability, [52] antioxidant properties,[52] flame retardancy, [53–55] mechanical strength, [56] and thermal stability. [56]

Despite that, research on the utilization of lignin in flexible PU foams has been relatively limited, with only about 17 papers published on the application of lignin in flexible foams, [57–73] compared to the extensive research conducted on the application of lignin in rigid foams.[74,75] In a previously published paper by our group,[76] the performance of various lignin types in flexible PU foams was assessed while substituting 20 wt.% of petroleum-based polyols with various unmodified solid lignins. The results showed the addition of lignin improved tensile strength, tear strength, and compression force deflection. [76] Despite lignin's potential to enhance mechanical strength in materials, its high hydroxyl value, [48,77] functionality, [48,77] and glass transition temperature (Tg) [77,78] can negatively impact the flexibility and resilience of flexible foams. Additionally, its crosslinked structure can reduce the ultimate elongation of flexible PU foams, limiting its incorporation into such applications. Another significant challenge is lignin’s three-dimensional structure, which makes its hydroxyl groups less accessible for reaction with isocyanate.[79] Also, its solid nature and poor solubility in co-polyol [80] primarily cause it to act as a filler, increasing the rigidity of flexible foams. Therefore, overcoming these challenges is essential for harnessing lignin's potential as a sustainable polyol in PU flexible foam formulations.

1.2 Research Objectives

The main objectives of this thesis are summarized below:

1. Synthesize and characterize lignin polyols via oxyalkylation using propylene carbonate and evaluate their feasibility in flexible polyurethane foam formulations without further purification.
2. Incorporate co-polyols as reactive components to reduce unreacted propylene carbonate content in oxyalkylated lignin polyols.
3. Develop high-performance lignin-based polyols with low hydroxyl values and workable viscosities for polyurethane flexible foam application.
4. Evaluate the integration of soy polyol to increase the biobased carbon content, and characterize the resulting foams for thermomechanical properties, morphology, shock absorption, and biodegradability.

Chapter 2: Direct Incorporation of Propylene Carbonate Oxyalkylated Lignin Polyol in Flexible Polyurethane Foam Formulation

Abstract

This study explores the feasibility of incorporating propylene carbonate (PC) oxyalkylated lignin polyol directly into flexible polyurethane (PU) foam formulations. Different lignin-to-PC molar ratio polyols were prepared, and the hydroxyl value, viscosity, and unreacted PC content were measured. Synthesized lignin polyols were then used to formulate flexible PU foams and analyzed for its thermomechanical properties to assess the effect of unreacted PC content. The results indicated that excessive unreacted PC adversely affected mechanical performance, leading to reductions in tensile strength, tear resistance, and compression force deflection (CFD). Additionally, it contributed to inferior thermal properties compared to conventional foams. Fourier-transform infrared (FTIR) spectroscopy further revealed that unreacted PC disrupted microphase separation, weakening intermolecular interactions and reducing foam strength.

2.1 Introduction

Polyurethane (PU) flexible foams are widely used across industries such as automotive, furniture, packaging, and footwear owing to their comfort, resilience, and mechanical performance. These foams are formed via a step-growth polymerization reaction between polyols and isocyanates.[3] In flexible PU foams, polyols (primarily polyether-based) constitute the soft segment, while isocyanates form the hard segment. By adjusting the chemical structure and ratio of these components, the final foam properties can be precisely tailored.[2] The mechanical and thermal behavior of PU foams is primarily governed by polyol characteristics such as hydroxyl value, molecular weight, and functionality, along with the isocyanate type and stoichiometric ratio. Typically, polyols with low hydroxyl value, high molecular weight, and low functionality produce soft and flexible foams, whereas those with high hydroxyl value and functionality result in rigid, and highly crosslinked networks.[3]

Despite their widespread use, conventional polyols are predominantly petroleum-derived and synthesized from toxic, non-renewable feedstocks such as propylene oxide (PO) and ethylene oxide (EO).[2] This has raised environmental and safety concerns, prompting the search for more sustainable alternatives. This has led to the development of bio-based polyols from soybean oil,[11–20] rapeseed oil,[7] cashew nut shell liquid,[8] and palm oil[9,10] through chemical modification strategies such as epoxidation/ring opening,[81] Mannich reaction,[82] and novolac/ propoxylation chemistry.[83] Castor oil, due to its intrinsic hydroxyl groups within the triglyceride backbone, has also been used directly in flexible PU foam formulations without further modification.[6]

Among emerging bio-based feedstocks, lignin has gained considerable attention for PU applications due to its natural abundance, aromatic structure, and inherent hydroxyl content.[51] As the second most abundant biopolymer after cellulose, lignin offers several advantages when

incorporated into PU materials, including enhanced flame retardancy [53–55] and improved thermo-mechanical properties. [56] However, its use in flexible PU foams remains underexplored compared to rigid foams. Only a limited number of studies (~17 publications) have examined lignin's potential in flexible foams. [57–73] Prior work from our group demonstrated that incorporating 20 wt.% of various unmodified lignins into flexible PU foams improved tensile and tear strength, as well as compression force deflection. [76] Despite these promising findings, the direct use of solid lignin in flexible PU foams is limited by several chemical and structural drawbacks. Its high hydroxyl value and functionality contribute to increased stiffness and reduced flexibility. [48,77] Additionally, the presence of sterically hindered phenolic hydroxyl groups hinders lignin's reactivity towards isocyanates.[79] Poor solubility in co-polyols can further lead to phase separation,[84] causing lignin to act more as a filler than a reactive polyol at higher loadings. Overcoming these challenges is essential to unlock lignin's potential as a renewable polyol for flexible PU foam production.

To address these limitations, two major lignin modification techniques have been widely investigated: liquefaction [85–87] and oxyalkylation. [88–93] Liquefaction involves the solvolytic breakdown of lignin using polyhydric alcohols such as polyethylene glycol, [85] glycerol,[85] ethylene glycol, [86] or a mixture of polyols, [85,87,94] at elevated temperatures (150–250 ^{o}C), often in the presence of acid catalysts such as sulfuric acid and hydrochloric acid. This method improves lignin's solubility and reactivity; however, it suffers from drawbacks such as high solvent demand (typically a 1:5–1:9 lignin-to-solvent ratio), complex degradation pathways, [58,69,70,72] and the formation of unwanted byproducts like 4-hydroxy benzoic acid, vanillic acid, syringic acid, vanillin, coniferyl alcohol, syringaldehyde, sinapyl alcohol, 3,5-dimethoxyphenol, and ferulic

acid. [86] These side reactions complicate process control and limit its application in flexible PU foam.

Oxyalkylation, especially with propylene oxide (PO), has proven effective in enhancing lignin's reactivity by converting phenolic hydroxyls into more reactive aliphatic ones, improving both solubility and compatibility in PU systems. [70] However, PO presents significant industrial limitations due to its high toxicity, low boiling point, and harsh reaction conditions (6–27 bar, 140–280 °C). [95] Furthermore, uncontrolled homopolymerization of PO can produce heterogeneous polyol mixtures with inconsistent properties. [80]

To mitigate these issues, cyclic carbonates have recently emerged as safer and more sustainable oxyalkylation agents. They offer low toxicity, [96,97] high boiling points, [96] and biodegradability, [98] and can be synthesized from captured carbon dioxide,[99] aligning with green chemistry principles. Like alkylene oxides, cyclic carbonates can react with lignin's phenolic and carboxylic hydroxyl groups to generate more reactive aliphatic hydroxyl groups,[73] thereby enhancing lignin's suitability for flexible PU foam applications. However, the direct incorporation of cyclic carbonate oxyalkylated lignin polyol into flexible PU foams remains underexplored. Most research has focused on the isolation and purification of the modified lignin for characterization,[88,93,100,101] without testing its performance in an actual flexible PU foam formulation.

A recent publication by our group demonstrated the direct incorporation of propylene carbonate (PC) oxyalkylated lignin polyols, with hydroxyl values ranging from 105 to 163 mg KOH/g, into flexible PU foams, replacing up to 30% of petroleum-based polyol. [73] While that study showed technical feasibility, the influence of residual unreacted PC on foam properties was not fully addressed. Since PC is relatively inert in PU reactions, its retention may impact foam performance. Therefore, understanding the effect of unreacted PC content is crucial for optimizing formulations

using unpurified oxyalkylated lignin polyols. This study aims to bridge this knowledge gap by systematically synthesizing PC-oxyalkylated lignin polyols using varying molar ratios of PC (4, 5, and 10 equivalents) and incorporating them, without purification, into flexible PU foam formulations. The goal is to evaluate the influence of PC molar ratio on polyol properties (hydroxyl value, viscosity, and unreacted PC content) and foam performance, including mechanical strength, thermal stability, and the degree of microphase separation. Additionally, foams containing both lignin and soy polyol were developed to increase the biobased carbon content.

2.2 Materials and Method

2.2.1 Materials

Huntsman Corporation generously supplied polyether polyol (MW 6000 Da, hydroxyl value 28 mg KOH/g), propylene carbonate, and isocyanate. Momentive Performance Materials provided the gelation catalyst, blowing catalyst, and siloxane surfactant. Cargill supplied soy polyol (BIOH 2828). Analytical reagents, including cyclohexanol (99% purity), pyridine (HPLC grade), and 2-chloro-4,4,5,5-tetramethyl-1,3,2-dioxaphospholane (TMDP), were purchased from Sigma-Aldrich. Additionally, chromium (III) acetylacetonate, deuterated chloroform, HPLC-grade tetrahydrofuran, dimethyl carbonate (99% purity), and acetic anhydride were obtained from Fisher Scientific. Tokyo Chemical Industry (TCI) supplied 1,8-Diazabicyclo [5.4.0] undec-7-ene (DBU). Kraft softwood lignin sample was obtained from Ingevity, with their properties detailed in **Table**s **A1** and **A2** in Appendix A.

2.2.2 Lignin Characterization

2.2.2.1 Ash Content

The ash contents of lignin samples were measured according to TAPPI T 212 om-93 standard method. Briefly, each oven-dry lignin sample (1–2 g) was added to a pre-weighed crucible and heated in a muffle furnace. The temperature was gradually increased from room temperature to 525 °C at a ramp rate of 5 °C min^{-1} and then kept at 525 °C for 4 h. After cooling in a desiccator, the ash content was determined as the ratio of residual mass in the crucible compared to the initial mass of the dry lignin.

2.2.2.2 Elemental Analysis

Lignin samples were dried overnight at 100-105 °C and prepared according to the Association of Official Analytical Chemists (AOAC) Official Methods 922.02 and 980.03. Samples were analyzed using an Inductive-Coupled Plasma Atomic Emission Spectroscopy (ICP-AES) with a Thermo Scientific iCAP 6000 series 6500 Duo.

2.2.2.3 Hydroxyl Content Determination

The hydroxy content of lignin and the synthesized lignin polyols were evaluated using Phosphorus-31 Nuclear Magnetic Resonance Spectroscopy (^{31}P NMR). [102] A solvent mixture of pyridine and chloroform-d (1.6:1, v/v) was prepared, and an internal standard was made by dissolving approximately 22 mg of cyclohexanol in 1 mL of the solvent. Additionally, 5 mg of chromium (III) acetylacetonate was dissolved in 1 mL of the solvent, and about 30 mg of the lignin sample was dissolved in 500 μL of the same solvent. After vortexing all solutions together for 30 seconds at 3000 rpm, 100 μL each of the chromium (III) acetylacetonate solution and the internal standard were added to the lignin solution. Then, 100 μL of 2-chloro-4,4,5,5-tetramethyl-1,3-2-dioxaphospholane (TMDP) was added, followed by another 30-second mixing in the vortex. The

final mixture was transferred to a 5 mm Wilmad NMR tube and analyzed using an Agilent DDR2 500 MHz NMR spectrometer. Data were collected using a 90° pulse angle, a relaxation delay of 5 seconds, and 128 scans. Hydroxy content was quantified using MNova software (Mestrelab), by calculating the ratio of the integrated area of the cyclohexanol peak (145.3-144.9 ppm) to the various lignin hydroxy groups: aliphatic (149.1-145.4 ppm), condensed phenolic (144.6-143.3 and 142.0-141.2 ppm), syringyl phenolic (143.3-142.0 ppm), guaiacyl phenolic (140.5-138.6 ppm), p-hydroxyphenyl phenolic (138.5-137.3 ppm), and carboxylic acids (125.9-134.0 ppm).

2.2.2.4 Molecular Weight Distribution

The molecular weight distribution of the lignin sample was analyzed using gel permeation chromatography (GPC) with tetrahydrofuran (THF) as the mobile phase. To ensure proper solubilization, the lignin samples were first acetylated by mixing 1 g of lignin in a 50-50 v/v% pyridine-acetic anhydride solution for 24 hours at room temperature. Afterward, the samples were precipitated with hydrochloric acid, washed with deionized water, and dried under vacuum. The dried sample was then dissolved in HPLC-grade THF at a concentration of 5 mg/mL and filtered through a 0.45 μm syringe filter. The filtrate was injected into the GPC system, which used three Ultrastyragel columns for separation, with a flow rate of 1 mL/min. The system was calibrated using polystyrene standards with known molecular weights (ranging from 162 to 42400 Da), and the sample molecular weight was calculated using Empower GPC Software.

2.2.2.5 Glass Transition Temperature (Tg)

Differential Scanning Calorimetry (DSC) of lignin sample was conducted using a standard aluminum pan and lid. Approximately 8 mg of each sample was weighed and analyzed using a TA DSC instrument under nitrogen. The testing protocol involved equilibrating the sample at 25°C,

ramping the temperature at 20 °C/min to 200 °C, cooling at 20 °C/min back to 25 °C, holding isothermal for 10 minutes, and then ramping again at 20°C/min to 230°C.

2.2.3 Polyol Synthesis

Oven-dried lignin was mixed with a 4eq molar ratio of propylene carbonate (PC), with respect to the total hydroxyl value of lignin, in a Parr Reactor (Model 4524, 0.6L capacity). Then 0.05 molar ratio of 1,8-Diazabicyclo [5.4.0] undec-7-ene catalyst was added to the mixture. The reactor was purged with nitrogen gas for 5 minutes to completely remove air trapped in the reactor. The mixture was heated at 150 °C for 1.5 hours, mixing at 400 rpm. The gas outlet valve was opened occasionally to vent carbon dioxide produced from the reaction to avoid pressure build-up in the reactor. At the end of the reaction, the product mixture was allowed to cool to room temperature. The reactions were repeated for two batches of lignin polyols made with 1:5 and 1:10 molar ratios of lignin to PC.

2.2.4 Polyol Characterization

2.2.4.1 Hydroxyl Value (OHV)

The hydroxy contents of the polyol were measured using ^{31}P NMR spectroscopy, using a method similar to that used for lignin characterization. The polyol's hydroxyl value (OHV), measured in mg KOH/g, was computed by multiplying the total hydroxyl content (mmol/g) by 56.1 (mass of potassium hydroxide (KOH)).

2.2.4.2 Viscosity

The viscosity of developed polyols was assessed at ambient temperature employing a Discovery HR-1 hybrid rheometer manufactured by TA Instruments. A 40 mm stainless steel Peltier plate geometry with a 1 mm gap was utilized, with samples sandwiched between the plates and trimmed

before analysis. Viscosity measurements were conducted under a constant shear rate of 50 s^{-1}, with the recorded viscosity representing the average value over 60 seconds.

2.2.4.3 Unreacted PC Content

The quantification of unreacted PC content in the polyol at the end of the oxyalkylation reaction was conducted gravimetrically. Initially, the mass of a ceramic crucible filter, with a pore size of 10-15 µm, was measured. Subsequently, 1 g of each polyol was combined in a 50 mL beaker with 20 mL of acidified water (pH 2) and vigorously agitated using a magnetic stirrer until the modified lignin precipitated entirely. Following precipitation, the mixture was subjected to vacuum filtration using ceramic filters and subsequently washed with excess distilled water. The resulting samples were left to dry overnight in a vacuum oven at 85 °C and subsequently cooled in a desiccator. The mass of the dry-modified lignin was computed by subtracting the mass of the dry ceramic crucible filter from the combined dry mass of the precipitated lignin and filter. Consequently, the unreacted PC content was calculated using equation (2.1).

$$Unreacted\ PC\ content\ (\%) = (1 - \frac{m_{filter\ residue}}{m_{lignin\ polyol}}) \times 100 \qquad [2.1]$$

2.2.5 Foam Formulation

Synthesized lignin polyol was directly used, without further purification, to formulate flexible PU foams. Twenty parts per hundred of the petroleum-based polyols (pphp) were replaced with the synthesized lignin polyol. Foams containing both synthesized lignin polyol and soy polyol were also formulated to increase the biobased carbon content of the developed foams. The isocyanate index was set at 80 for all foams due to the relatively high hydroxyl value of the synthesized lignin polyols. In a 12-ounce paper cup, 100 g of polyol blend, water (2 pphp), gelation catalyst (0.53 pphp), blow catalyst (0.32 pphp), and surfactants (1 pphp) were mixed at 3000 rpm using an overhead high-speed stirrer for two minutes. Finally, the calculated amount of isocyanate was

added using a disposable plastic syringe and mixed at 3000 rpm for another 3-5 seconds. The mixture was then quickly poured into a silicone mold conditioned at 65 °C and left to cure at room temperature for about 30 minutes before demolding. After removing the foams from the mold, they were left to post-cure for 2 days at room temperature, as recommended by the industry. Samples were cut into various sizes required for mechanical testing according to the ASTM D3574 standard test method. It is important to note that the foams were specifically formulated for automotive carpet flooring and panel insulation applications. **Figure 2.1** shows the foams formulated with and without lignin polyol.

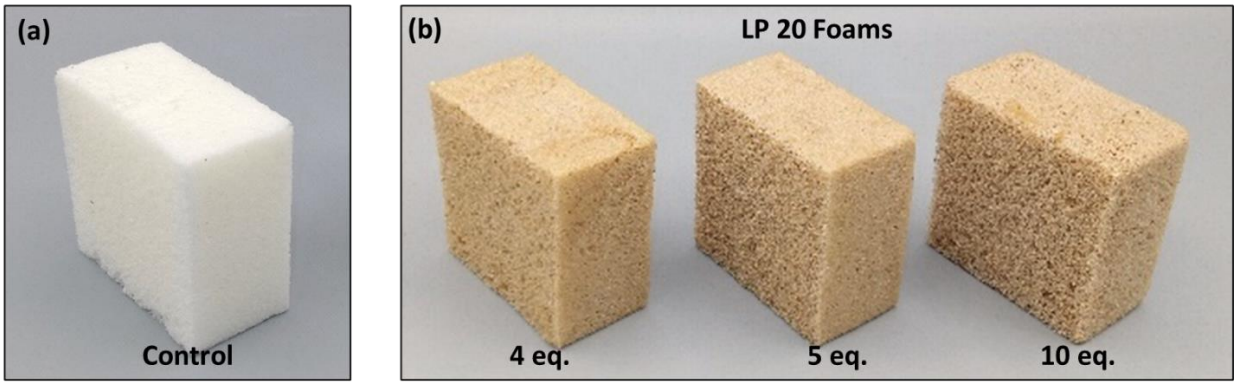

Figure 2.1: Flexible polyurethane foams produced by replacing 20% of petroleum-based polyols with propylene carbonate (PC) oxyalkylated lignin polyols (LP 20), synthesized at different PC molar ratios (4, 5, and 10 eq.).

2.2.6 Foam Characterization

2.2.6.1 Apparent Density and Compression Force Deflection

The Compression Force Deflection (CFD) of the foam samples were evaluated following ASTM D3574. [103] 50mm x 50mm x 25mm foam blocks were cut, and their dimensions were precisely measured with calipers (for density calculation). The samples were then placed on an Instron universal testing machine, and the platen separation was set to the foam height as shown in **Figure 2.2a**. The samples were then compressed to 75% of their initial height as part of "pre-flex" to pop open any closed cells in the foam, after which it was then allowed to recover for at least 5 ± 1 minutes. After recovery, the samples were compressed again to 25% strain, and the stress was measured after 1 minute of relaxation. This was repeated at 50% and 65% strain. The compression force deflection (CFD) was reported as stress after 1 minute of relaxation at 50% strain, whereas the support (sag) factor was calculated as a ratio of 65% CFD to 25% CFD. The apparent density of the foam samples was calculated based on the mass and volume of the CFD test specimen. Six replicates of each foam sample were tested.

2.2.6.2 Tensile Strength

The tensile strength of the foam samples was evaluated following the ASTM D3574. Foam specimens were first cut to a thickness of about 10 mm in the direction of the foam rise. Using a hydraulic press equipped with a die, the samples were shaped into a dog-bone form as defined by ASTM D412A. Precise measurements of the sample width and thickness were taken using calipers. The specimens were then secured in an Instron 5585H universal testing machine as shown in **Figure 2.2b**, outfitted with a 10 kN load cell, and held in place with hydraulically operated grips. The grip distance, set at 80 mm, served as the initial length for determining strain. The samples

were then elongated at a speed of 500 mm/min, with the maximum stress and elongation at the break being reported.

2.2.6.3 Tear Resistance

The tear resistance was also measured according to ASTM D3574. A foam prism was cut with dimensions 25.4 x 25.4 x 152.4 mm. A 40 mm incision was created into the long dimension of the foam, parallel to the foam rise direction, and the foam thickness was recorded parallel to this slit. The foam was then placed into an Instron universal testing machine, with each grip holding one of the cut foams, as shown in **Figure 2.2c**. The sample was then pulled apart at 500 mm/min, until the tear propagated 120 mm or the tear cut through the foam. The tear strength was computed by dividing the maximum tear force by sample thickness.

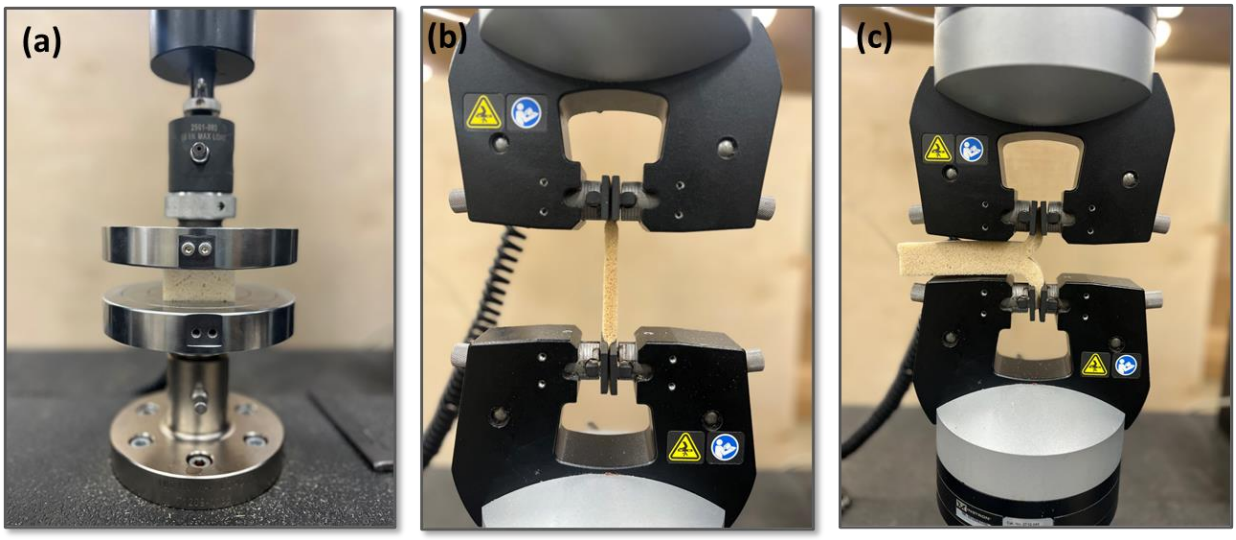

Figure 2.2: Mechanical property testing configurations (ASTM D3574) for measuring (a) compression force deflection (CFD) and support factor, (b) tensile strength and elongation at break, and (c) tear strength of polyurethane flexible foams.

2.2.6.4 Fourier Transform Infrared (FTIR) Spectroscopy

The infrared spectra of foam samples were acquired using a PerkinElmer Spectrum Two FT-IR Spectrometer, in Attenuated Total Reflectance (ATR) mode. 10 mm thick foam samples were compressed at the same force level during measurement to ensure that the ATR crystal maintained adequate contact with the foam, and spectra were collected from 400-4000 cm^{-1} using 32 scans.

2.2.6.5 Thermogravimetric Analysis (TGA)

The thermal degradation of foam samples was investigated using a TGA55 (TA Instruments) thermogravimetric analyzer. 7-10 mg of each foam sample was placed in a platinum pan and heated to 800 °C at a rate of 10 °C/min. The weight loss % thermogram and its derivative were recorded.

2.2.6.6 Biobased Carbon Content Measurement

The foam samples were sent to Beta Analytic Inc. (Florida, USA), in which the bio-based content of the samples were measured according to the ASTM D6886-22 test method using the radiocarbon isotope (Carbon-14). The result was obtained by measuring the ratio of radiocarbon in the material relative to a National Institute of Standards and Technology (NIST) modern reference standard (SRM 4990C). The ratio was calculated as a percentage and was reported as percent modern carbon (pMC). The value obtained relative to the NIST standard was normalized to the year 1950 AD so an adjustment was required to calculate a carbon source value relative to today. In the standardized terminology, adjusted results were reported as % biobased carbon, calculated from pMC by applying a small adjustment factor for ^{14}C in carbon dioxide in the air.

2.3 Results and Discussion

2.3.1 Polyol Properties

^{31}P NMR spectra of lignin polyol, presented in **Figure 2.3,** revealed a significant reduction in phenolic (137 to 144.6 ppm) and carboxylic (134 to 135.9 ppm) hydroxyl (OH) groups of lignin after the oxyalkylation reaction. This transformation occurs due to the reaction between lignin's phenolic OH groups and propylene carbonate (PC), resulting in the formation of aliphatic OH groups and the release of carbon dioxide as illustrated in **Figure 2.4a**. Previous studies have shown that lignin's aliphatic hydroxyl groups, depending on the reaction condition, can also react with PC, leading to the incorporation of carbonate linkages into the structure.[93] However, lignin polyol synthesized using 4 and 5 equivalent (eq.) PC molar ratios exhibited some trace phenolic OH moieties, suggesting that slightly longer reaction times may be necessary for complete conversion. Although the synthesized polyols exhibited high aliphatic OH content (95–100%), trace phenolic OH groups may hinder reactivity, as isocyanates preferentially react with aliphatic hydroxyl groups.[104]

Additionally, several narrow peaks appear in the aliphatic OH region of the ^{31}P NMR spectra, likely corresponding to oligomeric glycols such as propylene glycol, which may have formed due to transesterification side reactions (see **Figure 2.4b** for scheme) occurring as the reaction progressed. Another possible source of oligomeric glycols in the lignin polyol is the reaction between residual moisture and PC, as illustrated in **Figure 2.4c**. These glycols typically function as chain extenders in polyurethane foams, increasing the length of the hard segment due to its low molecular weight and influencing the degree of phase separation within the cured polymer. [105–107] As a result, the synthesized lignin polyol consists of a mixture of oxyalkylated lignin, some quantities of low-molecular-weight glycols, and excess unreacted PC, which acts as a solvent. The

^{31}P NMR spectra was then integrated to determine the total hydroxyl content and hydroxyl value (OHV) of the polyols, as summarized in **Table 2.1**.

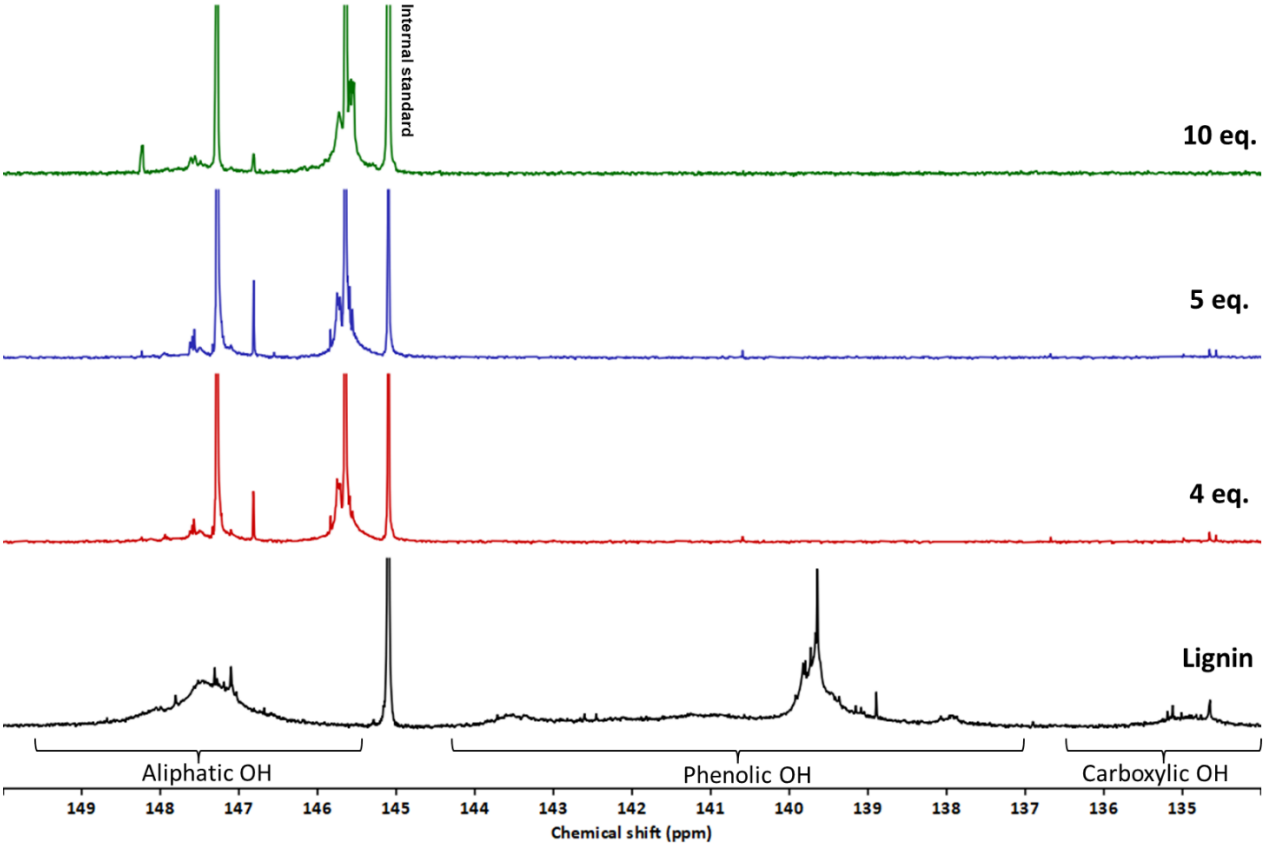

Figure 2.3: ^{31}P NMR spectra of lignin and propylene carbonate oxyalkylated lignin polyols synthesized using 4, 5 and 10 equivalent molar ratios of propylene carbonate. Samples were phosphitylated prior to analysis.

As seen in **Table 2.1**, the viscosity of lignin polyol decreases as the molar ratio of PC increases. This is attributed to the increasing concentration of unreacted PC in the resulting lignin polyols, which also act as solvent. Another contributing factor to this trend, particularly in 4 eq. molar ratio polyols, could be associated with a possible transesterification side reaction, which may have led to lignin crosslinking. At lower PC molar ratios, it's possible the electrophilic carbonyl group in PC may have competed with the carbonyl group in the carbonate linkages (formed from the

reaction between lignin aliphatic OH group and PC) for nucleophilic attack by DBU-activated lignin's aliphatic OH group. This competition increases the likelihood of chain coupling reactions. Given the structure and size of the lignin macromolecule, the probability of a reverse reaction becomes increasingly low due to the steric hindrance effect. The scheme for the chain coupling reaction is illustrated in **Figure 2.4b**.

Table 2.1: Properties of oxyalkylated lignin polyols at different propylene carbonate (PC) molar ratios (4, 5, and 10 eq): Hydroxyl value, aliphatic hydroxyl content, viscosity, and unreacted PC content.

PC molar ratio (eq.)	**Hydroxyl Value (mg KOH/g)**	**Aliphatic OH content (%)**	**Viscosity (Pa.s)**	**Unreacted PC content (%)**
4	176	95	38,320 ± 80	63 ± 2
5	158	96	6140 ± 50	69 ± 3
10	42	100	70 ± 10	79 ± 1

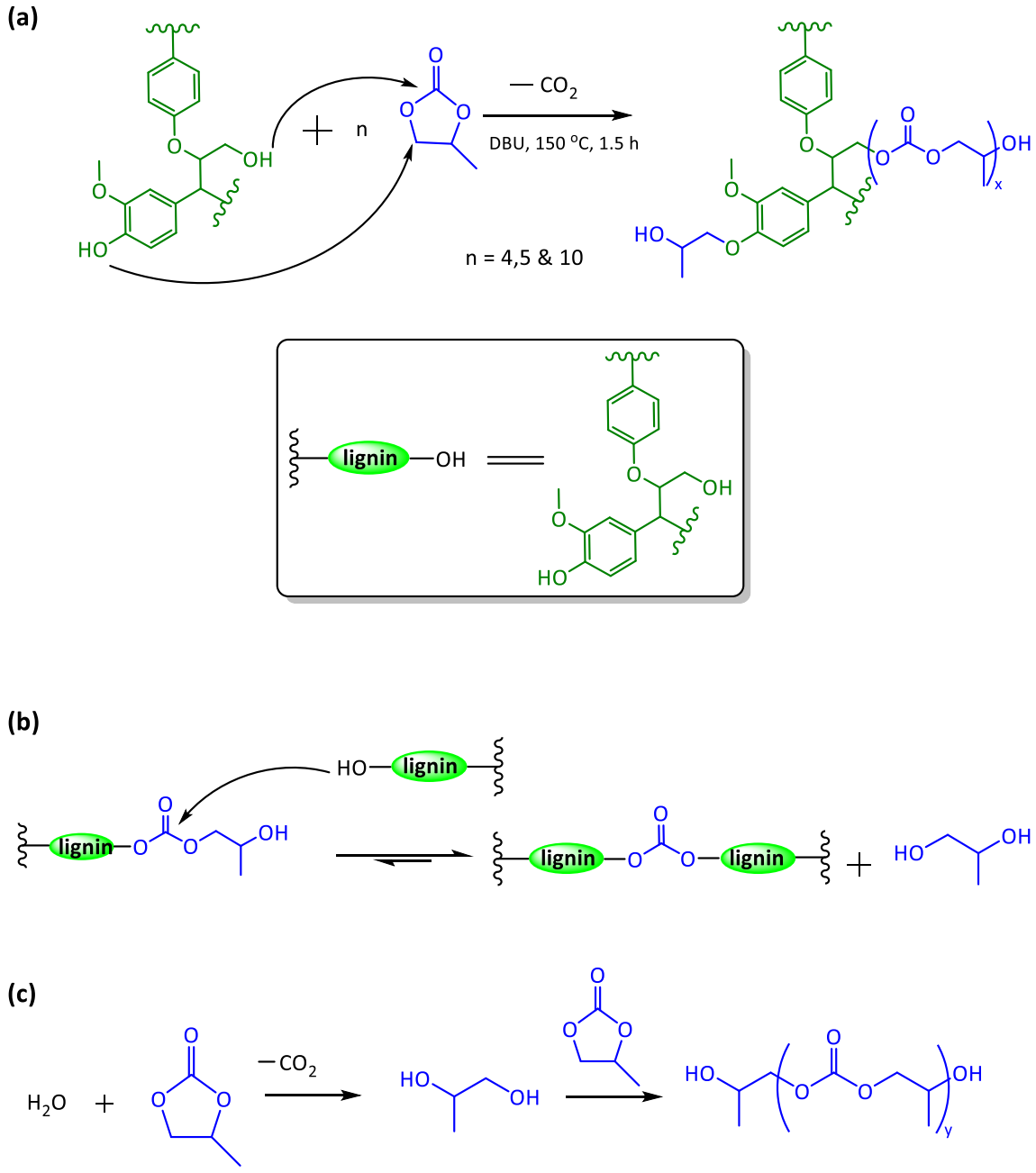

Figure 2.4: Reaction pathways in the lignin-propylene carbonate system: (a) Reaction of lignin's phenolic and aliphatic hydroxyl groups with propylene carbonate's alkyl and carbonyl carbons, respectively; (b) Transesterification side reaction, resulting in lignin chain coupling and propylene glycol formation; (c) Ring-opening reaction between water and propylene carbonate, leading to oligomeric glycol formation.

2.3.2 Foam Properties

2.3.2.1 Mechanical Properties

The three lignin polyols, synthesized using varying amounts of PC molar ratios, were directly incorporated into a flexible PU foam formulation by replacing 20% of petroleum-based polyols. The mechanical properties of the foams were measured according to the ASTM D3574 standard testing, and the results are presented in **Figure 2.5**. Their performance was also compared with the Original Equipment Manufacturer (OEM) standard requirements for PU flexible foams used for under carpet flooring and panel insulation of cars. As seen in **Figure 2.5a**, there was no significant difference in the density values among all lignin-based foams. Overall, the densities of all foam samples fell within the required density range of 30 to 100 kg/m^3.[76]

The compressive force deflection (CFD), which indicates the foam's resistance to deformation under load, varied depending on the PC content in the polyol. Despite the aromatic structure and high OHV of lignin polyols, their respective CFD values were significantly lower compared to the control foam (without lignin polyol). This decrease in CFD can be attributed to the high levels of unreacted PC (63–79%) in the synthesized lignin polyols. As the PC molar ratio increases, the CFD value decreases, confirming a direct relationship between these two parameters. Among the lignin-based foams, only the foam formulated with 4 eq. lignin polyol achieved a CFD value that met the standard requirement. Meanwhile, the support factor, which indicates the foam's cushioning performance, remained unaffected by the PC molar ratio.

Tensile strength, which measures a foam's ability to withstand tension, was significantly affected by the unreacted PC content. Foams formulated with synthesized lignin polyols exhibited considerably lower tensile strength compared to the control foams. This outcome was unexpected, given the rigid structure of lignin and the relatively high hydroxyl value of the synthesized lignin

polyols (42–176 mg KOH/g) compared to conventional polyols (28 mg KOH/g), which would typically enhance crosslinking density. Additionally, the ultimate elongation of lignin-based foams was lower than that of the control foams. This suggests that unreacted PC may have acted as a plasticizing agent, thereby reducing the foam's overall strength. PC molecules may have diffused in between the urethane and urea chains in the foam, increasing free volume within the polymer matrix and weakening secondary molecular interactions, such as hydrogen bonding between polymer chains. This disruption in chain interactions likely contributed to the reduced tensile strength observed in lignin-based foams. Among the lignin-based foams, only the foam formulated with 4eq. PC lignin polyol achieved a tensile strength value (55 kPa) that met the standard requirement.

Tear strength, which reflects a foam's resistance to crack propagation, was also affected by the unreacted PC concentration. Foams containing lignin polyols exhibited lower tear strength compared to the control foams without lignin polyol. Among the lignin-based foams, a decreasing trend in tear resistance was observed as the amount of unreacted PC in the lignin polyol increased. Notably, foam formulated with 10 eq. PC lignin polyol failed to meet the standard requirements for carpet flooring and panel insulation applications. [103]

The mechanical properties results demonstrate that the presence of unreacted PC in synthesized lignin polyols negatively impacts the foam's overall strength, particularly tensile strength, tear strength, and compression force deflection (CFD). Based on these findings, the maximum allowable PC molar ratio, out of the three tested, for synthesizing oxyalkylated lignin polyols while maintaining acceptable mechanical performance is 5 eq.

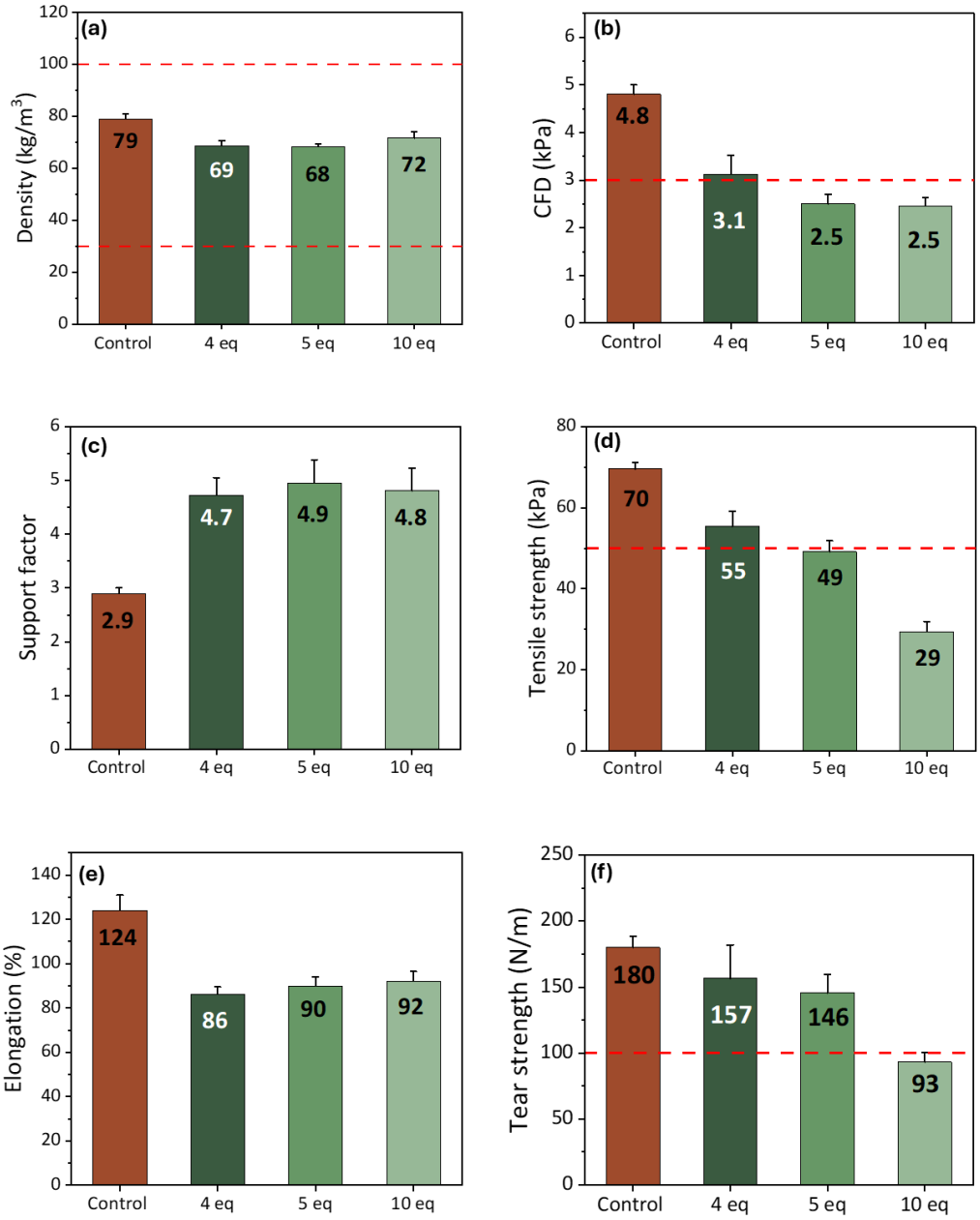

Figure 2.5: Mechanical properties (ASTM D 3574) of flexible polyurethane foams with 20% petroleum-based polyol replacement using propylene carbonate oxyalkylated lignin polyols: (a) density, (b) compression force deflection (CFD) at 50% strain, (c) support factor, (d) tensile strength, (e) elongation at break, and (f) tear strength. Lignin polyols were synthesized at varying propylene carbonate molar ratios (4, 5, and 10 eq.).

2.3.2.1.1 Impact of Soy Polyol

To further increase the biobased carbon content in lignin-based foams, soy polyol (29 mg KOH/g) was incorporated, replacing up to 20% of conventional petroleum-based polyols while maintaining a fixed lignin polyol content of 20%. The 5 eq.-based lignin polyol was selected over the 4 eq polyol due to its lower viscosity, which facilitated processing and blending with the soy polyol. The mechanical properties of the lignin-soy-based PU (LP-SP) flexible foams are summarized in **Table 2.2**. As the soy polyol content increased, the foam's tear strength and elongation at break decreased, while all other properties remained largely unchanged. This behavior may be attributed to the secondary aliphatic OH group in the soy polyol, which has lower reactivity toward isocyanate compared to the primary aliphatic OH group in conventional polyols. Additionally, the mid-position of the OH functionality in soy polyol introduces additional steric hindrance. Despite these effects, the foam prepared by replacing 40% of conventional polyols (20% lignin-polyol and 20% soy-polyol) met all standard requirements for PU foams used for under-carpet flooring and insulation panel, except for tensile strength.

Table 2.2: Mechanical properties (ASTM D3574) of flexible polyurethane foams with partial replacement (up to 40%) of petroleum-based polyol by a blend of propylene carbonate (PC) oxyalkylated lignin polyol (20% fixed) and soy polyol (0-20%). Lignin polyol was synthesized at 5 eq. PC molar ratio.

Mechanical Property	**Desired range**	**Unit**	Lignin polyol (5 eq.) based PU foams		
			L 20	**LP 20-SP10**	**LP 20-SP20**
Density	30-100	kg/m^3	68 ± 1	74 ± 4	71 ± 5
Tear strength	≥100	N/m	146 ± 14	141 ± 24	120 ± 20
Compression Force Deflection	3-12	kPa	2.5 ± 0.3	3.0 ± 0.6	3.0 ± 0.3
Support factor	-	-	4.9 ± 0.4	4.9 ± 0.7	4.4 ± 0.4
Tensile strength	≥50	kPa	49 ± 3	48 ± 2.7	47 ± 1.9
Elongation at break	≥60	%	90 ± 11	86 ± 10	75 ± 5

2.3.2.2 Fourier Transform Infrared Spectroscopy

A key characteristic of flexible PU foam is microphase separation, which plays a crucial role in determining its mechanical properties.[108–110] This phenomenon occurs due to the inherent incompatibility between the soft segments (polyol) and the hard segments (isocyanate-derived structures).[111] Microdomains start to emerge when the concentration of urethane and urea hard segments exceeds a specific solubility limit. These microdomains are held together by hydrogen bonding interactions, which enhance structural integrity and contribute to the foam's rigidity. [108] Studies have shown that during the foaming process, hard segments undergo microphase separation, resulting in the formation of microdomains with an average spacing of 5–10 nm.[112]

Researchers commonly use Fourier-transform infrared (FTIR) spectroscopy to analyze the extent of microphase separation in flexible PU foams. This technique provides insights into hydrogen bonding interactions within the polymer matrix. [113–115]

All developed foams exhibited an N-H bond stretching at 3350 cm^{-1}, confirming the successful introduction of urethane linkages in the foam matrix as seen in **Figure 2.6a**. The absence of the free isocyanate peak at 2270 cm^{-1} in lignin-based foams indicates that they were fully reacted by lignin's OH groups. The FTIR spectra revealed a significant distinction between the control foams and the lignin-based foams, particularly in the carbonyl region, as shown in **Figure 2.6b**. One of the most noticeable differences was the intensity of the free urethane carbonyl peak at 1730 cm^{-1}, which was highest in control foam. This result was unexpected, given that lignin polyols have a higher OHV than conventional polyols, which should theoretically lead to an increased number of free urethane linkages due to their reaction with isocyanates. However, the spectra suggest the presence of strong intermolecular interactions within the lignin-based foams, as evidenced by their higher hydrogen-bonded urethane carbonyl intensity around 1700 cm^{-1} and high monodentate urea carbonyl absorption around 1650 cm^{-1}. [113] While the bidentate urea peak around 1625 cm^{-1} was very weak in all foams, the increased intensity of monodentate urea in lignin-based foams strongly indicates disordered urea phase aggregation, suggesting that lignin-based foams exhibit a lower degree of microphase separation compared to the control foams.

Among the lignin-based foams, the foam produced using polyol synthesized with a 10 eq lignin polyol exhibited the lowest intensity of free urethane and free urea bands. However, it displayed the highest monodentate urea intensity at 1650 cm^{-1}. Also, as the PC molar ratio increases, the intensity of the monodentate urea band increases. This trend indicates a disruption in hydrogen bond connectivity within the urea microphase domains of lignin-based foams. An explanation for

this disruption is the presence of unreacted PC in the lignin polyols, which may have interfered with urea aggregation. Due to the polarity of PC, it likely interacts with other polar segments in the foam, particularly urethane and urea linkages, through hydrogen bonding as presented in **Figure 2.6c**, thereby weakening the interconnection between polymer domains. These dipole-dipole interactions enable PC to diffuse across polymer chains, increasing the spacing in the microdomain and lessening the cohesive forces that give PU foam its strength. This explains why the lignin polyol-based foams demonstrated inferior mechanical properties, despite their relatively high hydroxyl values.

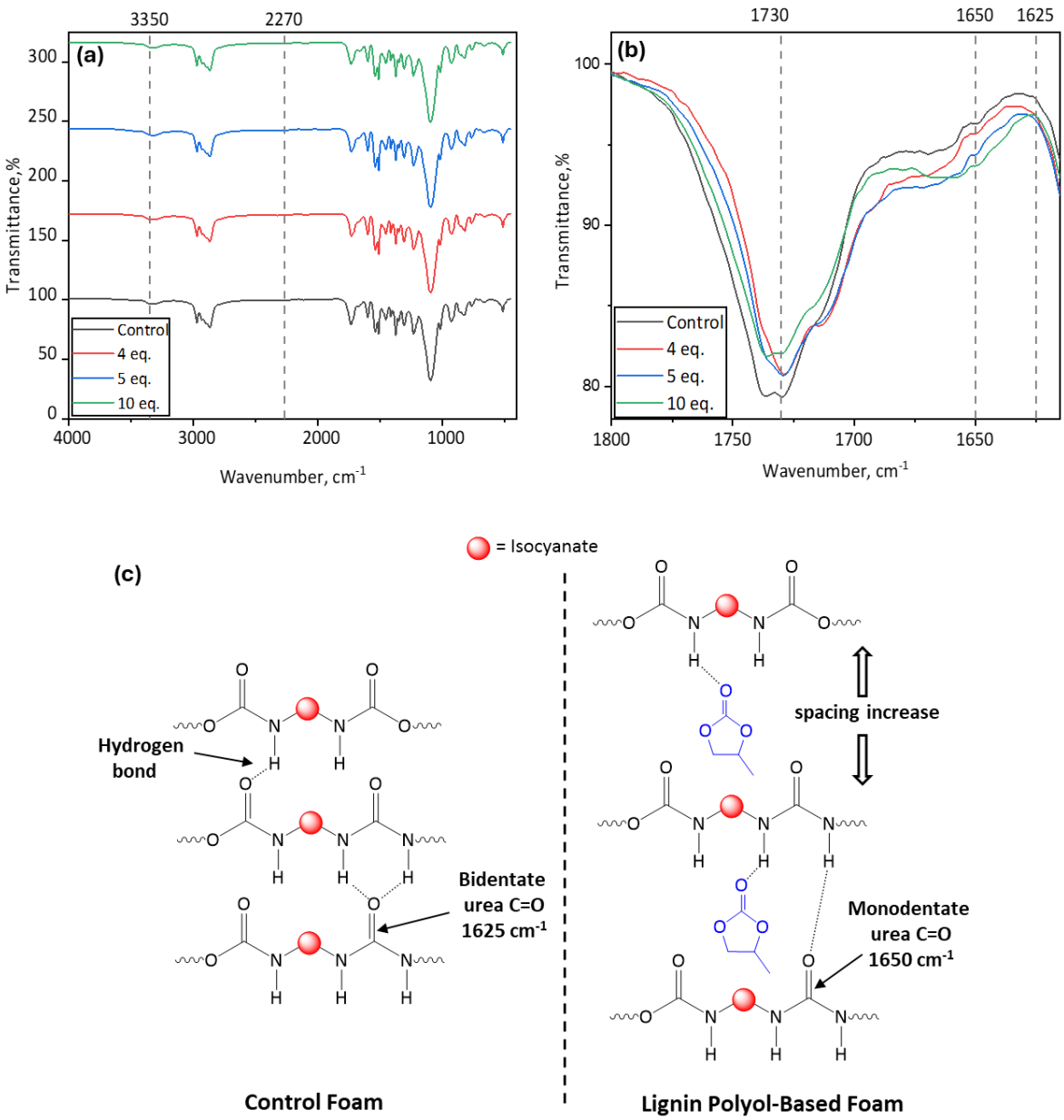

Figure 2.6: FTIR analysis of PU flexible foams with lignin polyol (20% petroleum-based polyol replacement): (a) full spectra, (b) carbonyl region, and (c) schematic representation of propylene carbonate (PC) hydrogen bonding in hard segment domains. Lignin polyols synthesized at 4, 5, and 10 eq. PC ratios.

2.3.2.3 Thermogravimetric Analysis (TGA)

Figure 2.7 presents the thermogravimetric (TG) and derivative thermogravimetric (DTG) analysis curves of the foams. Both the control and lignin polyol-based foams exhibited similar thermal degradation behavior. The first major weight loss, occurring between 265–306 °C, is attributed to the degradation of urethane bonds. [116] The second stage of decomposition, observed between 359–369 °C, corresponds to the breakdown of the soft segments. [117] Notably, the soft segment degradation temperature was higher in the lignin-based foams than in the control foams, due to the rigid aromatic structure of lignin, which is more resistant to volatilization.

Among the lignin-based foams, the soft segment degradation temperature remained constant (369 °C), regardless of the type of lignin polyol used. However, at the soft segment DTG peak temperature, the lignin-based foams decomposed at a faster rate than the control foams, with the foams formulated using 10 eq lignin polyol exhibiting the highest peak intensity. A decrease in peak intensity was observed as the PC molar ratio decreased, indicating that the accelerated decomposition of lignin-based foams at 369 °C is due to the presence of residual PC in the foam matrix, which acted as a plasticizer. As previously seen in the FTIR results, PC disrupts microphase separation between polymer domains, reducing interconnectivity, weakening the foam structure, and ultimately increasing its thermal degradation rate. At 800 °C, the char residue content was higher in the lignin-based foams compared to the control foam without lignin. Among the lignin-based foams, 10 eq lignin polyol produced the foam with the lowest char content, while the 4 eq and 5 eq formulations showed no significant difference in residue levels. The reason for this trend can be associated with the lignin content in the synthesized lignin polyol, with the 10-eq. lignin polyol containing the least amount of modified lignin.

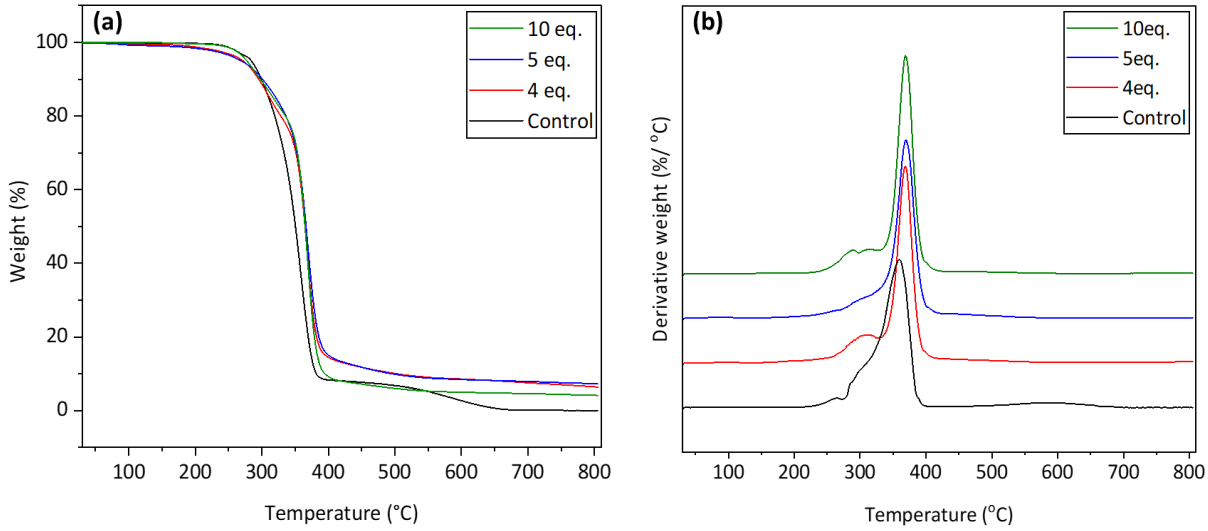

Figure 2.7: Thermogravimetric analysis (TGA) of flexible PU foam with lignin polyol (20% petroleum-based polyol substitution), N_2 environment: (a) thermogram and (b) differential thermogravimetric (DTG) curve. Lignin polyols synthesized at different PC molar ratios (4, 5, and 10eq.).

2.3.2.4 Biobased Carbon Content

Figure 2.8 presents the carbon content results for the synthesized lignin polyols and their corresponding flexible PU foams. As expected, both lignin and soy polyol were 100% biobased, as they are derived entirely from renewable sources. Lignin, a natural polymer found in wood cell walls,[23] and soy polyol, produced via soybean oil epoxidation, [118] contribute significantly to the renewable carbon content of PU formulations. Among the synthesized lignin polyols, the 4eq lignin polyol (40%) exhibited a higher biobased carbon content than the 5eq polyol (34%). For LP 20 foams, the biobased carbon content ranged from 4% to 5%, depending on the lignin polyol used in the formulation. This relatively low percentage is due to the high proportion of petroleum-derived components, such as PC and oligomeric glycols, in the synthesized lignin polyol. However, incorporating soy polyol increased the biobased content to 13–20%, depending on the

loading ratio. In contrast, the commercial polyol showed the lowest biobased carbon content (1%), likely attributable to the glycerol initiator used in its production. Since polyols typically constitute 60–70% of the total weight in flexible PU foams, these findings highlight the potential of lignin- and soy-based polyols to enhance renewable carbon content, offering a more sustainable alternative to conventional petroleum-based polyols.

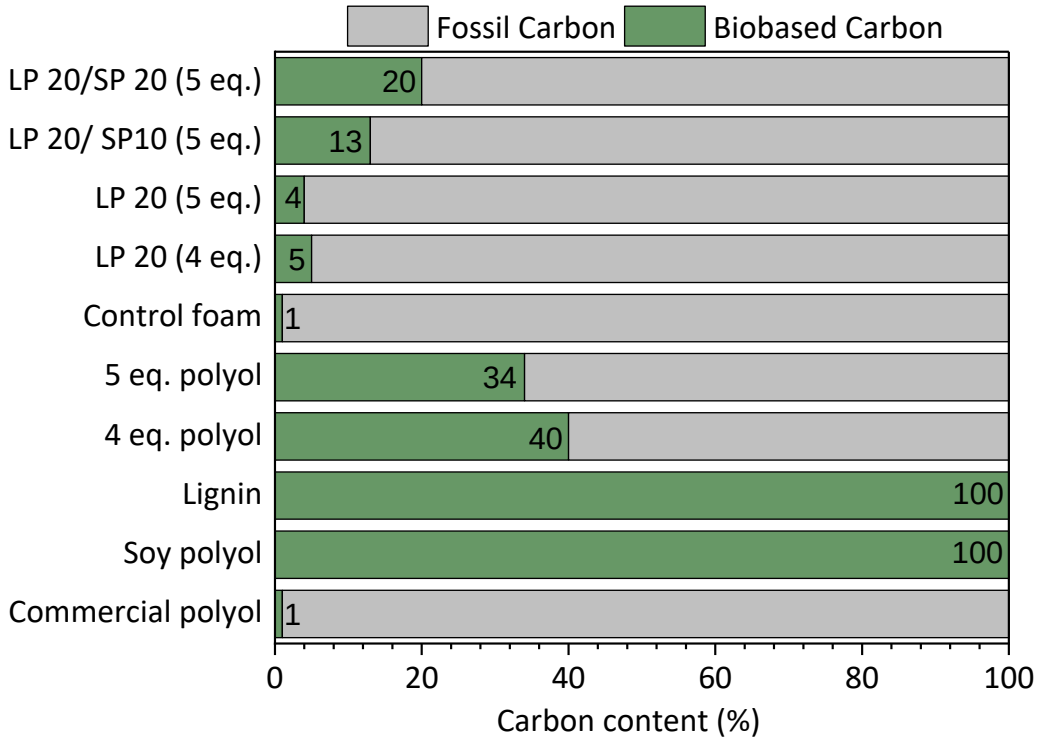

Figure 2.8: Biobased carbon content of polyols (petroleum-based, soy and lignin) and their respective PU flexible foams.

2.4 Conclusions

This study investigated the direct incorporation of propylene carbonate (PC)-oxyalkylated lignin polyols into flexible polyurethane (PU) foam formulations without additional purification. Varying the PC molar ratio (4, 5, and 10 eq.) yielded lignin polyols with distinct hydroxyl values, viscosities, and residual PC content, all of which significantly influenced the resulting foam properties. The findings demonstrated that while lignin polyols successfully enhanced the bio-based content of the foams, excessive unreacted PC adversely affected mechanical performance, particularly in tensile strength, tear resistance, and compression force deflection. Furthermore, residual PC disrupted microphase separation and accelerated thermal decomposition. In conclusion, the PC retention strategy successfully prevented lignin precipitation while facilitating direct application of oxyalkylated lignin polyols in PU foam formulations. However, this approach resulted in compromised foam performance due to residual PC content. To optimize this system, future investigations should focus on incorporating compatible co-polyols during the lignin oxyalkylation process. This modification could potentially reduce unreacted PC levels while preserving the essential mechanical and thermal properties of the resulting PU flexible foams.

Chapter 3: Selecting the Right Co-Polyol for Lignin Oxyalkylation and Its Application in Polyurethane Flexible Foam

Abstract

This study investigated the use of co-polyols to minimize unreacted propylene carbonate content in oxyalkylated lignin polyols, thereby mitigating its negative impact on flexible polyurethane (PU) foam properties. Various co-polyols with different structural units were systematically evaluated for their compatibility and performance in the lignin oxyalkylation process. Results demonstrated that high ethylene oxide (EO)-based polyols most effectively solubilized lignin and improved its reactivity with propylene carbonate, whereas propylene oxide (PO) and bio-based polyols showed poor compatibility with the reaction. The optimized lignin polyols successfully replaced 20% of petroleum-based polyols in flexible PU foam formulations, with the resulting foams meeting all standard requirements for automotive seating applications. Furthermore, a foam formulation incorporating a 50% replacement of petroleum-based polyols (using a combination of lignin polyol (20%) and soy-polyol (30%)) satisfied all specifications except elongation at break, while exhibiting improved compression force deflection characteristics.

3.1 Introduction

Polyurethane (PU) is a versatile polymer with widespread applications in foams, coatings, adhesives, sealants, and elastomers. It is synthesized via step-growth polymerization between polyols and isocyanates. In PU chemistry, polyols constitute the soft segments, while isocyanates form the hard segments. By adjusting the properties of these components and additives, the final PU product can be precisely tailored for specific performance requirements or end-use applications. [2] Polyester and polyether polyols are the two primary types used in PU synthesis, with polyether polyols generally preferred due to their superior hydrolysis resistance.[4] Conventional polyether polyols are produced through the ring-opening polymerization of alkylene oxides, catalyzed by bases and initiated by compounds such as ethylene glycol, propylene glycol, sorbitol, or glycerol, depending on the desired functionality. [2] Despite the versatility of PU flexible foams, a significant limitation lies in their reliance on petroleum-based feedstocks. Consequently, the industry is increasingly shifting toward sustainable, bio-based alternatives. Various plant-derived oils, including castor oil,[6] rapeseed oil,[7] cashew nut shell liquid,[8] soybean oil, [11–20] and palm oil [9,10] have been explored as potential polyol sources, either used directly or through chemical modification.

Among bio-based options, lignin has emerged as a promising polyol substitute due to its high hydroxyl group content. As the second most abundant natural polymer, lignin constitutes approximately 30% of plant biomass (by dry weight). [22] It is primarily obtained as a byproduct of the pulp and paper industry, where it is often burned for energy generation. [23,24] Structurally, lignin contains diverse hydroxyl functionalities (phenolic, aliphatic, and carboxylic), [25–28] making it a suitable natural polyol. Utilizing lignin in PU production not only provides a pathway to valorize this underused resource but also helps reduce emissions associated with its combustion. However,

several structural limitations hinder lignin's direct use as a polyol in PU synthesis. The primary challenge is the low reactivity of its sterically hindered phenolic hydroxyl groups toward isocyanates.[79] Additionally, lignin's three-dimensional structure restricts hydroxyl group accessibility, [79] while its solid-state nature and poor solubility in co-polyols often lead to phase separation. [80] Addressing these challenges is critical to unlocking lignin's full potential as a sustainable polyol for PU applications.

Oxyalkylation with alkylene oxide[80] and cyclic carbonates[88–93,101] has emerged as a promising method to enhance lignin's reactivity toward isocyanates, by converting sterically hindered phenolic to aliphatic hydroxyl groups. Cyclic carbonates are generally preferred over alkylene oxides due to their low toxicity, [96,97] biodegradability, [98] and high boiling point.[96] Furthermore, cyclic carbonates can be derived from carbon dioxide captured from the atmosphere, contributing to a more environmentally friendly production process.[96,119,120] In oxyalkylation process, lignin undergoes ring-opening polymerization with cyclic carbonates, [121] where hydroxyl groups nucleophilically attack either the alkyl or carbonyl carbon, depending on their type. [91] More acidic hydroxyl groups (e.g., phenolic and carboxylic OH) preferentially attack the alkyl carbon, forming hydroxyalkyl ether units and releasing carbon dioxide. In contrast, aliphatic hydroxyl groups react at the carbonyl carbon site, generating carbonate linkages. [91,122] Due to their high solvency, cyclic carbonates act as both reactants and solvents, dissolving lignin, thus accelerating the reaction. [93] However, the carbonyl carbon pathway is less favorable due to its reversibility, [91,122,123] leaving significant amounts of unreacted cyclic carbonate in the product. This necessitates a precipitation step to isolate the modified lignin.[100] Despite this challenge, few studies have explored retaining unreacted cyclic carbonates and using the mixture directly as a polyol replacement in PU foam applications. [92 73]

For instance, Viera et al. [92] incorporated propylene carbonate (PC)-oxyalkylated lignin polyol, with OH value of 257 mg KOH/g, into rigid PU foams as a 100% replacement for petroleum-based polyols. However, the resulting foams exhibited significantly lower compressive strengths compared to conventional rigid foams, attributed to the plasticizing effect of residual PC and its oligomers, which counteracted lignin's inherent rigidity. Similarly, Dunne et al.[73] recently tested PC-oxyalkylated lignin polyols, with OH values ranging from 105–163 mg KOH/g, in flexible PU foams at up to 30% replacement levels. They observed reduced tensile and tear strengths with increasing lignin polyol content, along with a lower soft-segment glass transition temperature compared to the control. These findings highlight the detrimental impact of excess unreacted PC, which lacks the active hydrogen needed to react with isocyanate crosslinking, limiting its suitability for flexible PU foam formulations.

To address this issue, one promising strategy is the use of co-polyols, which could reduce the amount of cyclic carbonate needed to perform the oxyalkylation reaction while ensuring the lignin polyol remains viable for direct PU flexible foam synthesis. Although some studies have employed low-molecular-weight polyethylene glycol (150–400 g/mol) as a co-polyol, [124,125] none have systematically investigated how co-polyol structure and properties influence the oxyalkylation reaction. This study aims to bridge that gap by evaluating the compatibility of various petroleum- and bio-based co-polyols with lignin oxyalkylation and their effects on the resulting polyol properties. A secondary objective is to optimize the reaction to produce a lignin polyol suitable as a "drop-in" replacement for conventional polyols in flexible PU foams for automotive seating applications.

3.2 Materials and Method

3.2.1 Materials

Polyether polyols, including Jeffol G 31-28, Jeffol PPG 2801, and Jeffol FE 41-42, as well as propylene carbonate, polymeric MDI (Rubinate M), and foaming catalysts, were generously provided by Huntsman Corporation. Pluracol 1070 was kindly supplied by BASF. The cashew nuts shell liquid (CNSL)-based polyol, NX-9001 LV, was provided by Cardolite, while the soy polyol, BIOH 2828, was obtained from Cargill. Potassium carbonate, dimethyl carbonate, polyethylene glycols, and polypropylene glycol (PPG 1000) were purchased from Fisher Scientific and used as received. The siloxane-based surfactant was supplied by Momentive Performance Materials. 1,8-Diazabicyclo [5.4.0] undec-7-ene (DBU) was purchased from Tokyo Chemical Industry (TCI), and 1,5,7-triazabicyclo [4.4.0] dec-5-ene (TBD) and castor oil were obtained from Sigma-Aldrich. Lignin samples were sourced from Fortum Bio2X, West Fraser, and Sweetwater Energy, and their properties are summarized in **Tables B1** and **B2** in Appendix B.

3.2.2 Lignin Characterization

Various analytical techniques were employed to characterize lignin and assess its composition and properties. The ash content was measured following the TAPPI T 212 om-93 standard method, where lignin samples were heated at 525 °C for 4 hours, and the residual mass was recorded. Elemental composition was analyzed using Inductively Coupled Plasma Atomic Emission Spectroscopy (ICP-AES). The hydroxyl group content was determined via Phosphorus-31 Nuclear Magnetic Resonance (^{31}P NMR) spectroscopy, following established protocols. [126–129] Molecular weight distribution was evaluated using gel permeation chromatography (GPC), with prior acetylation to improve solubility in tetrahydrofuran (THF). All analyses were performed in triplicate, and the average values were reported.

3.2.3 Polyol Synthesis

3.2.3.1 Oxyalkylation in the Presence of Co-Polyol

Oven dried lignin sample was mixed with 2 equivalent (eq.) molar ratio (with respect to total hydroxyl group in lignin) of propylene carbonate (PC) in a Parr Reactor (Model 4524, 0.6L capacity). Co-polyol was added to the mixture to obtain 30% lignin loading. 0.05 eq. of catalyst was added to the mixture. The reactor was purged with nitrogen for 5 minutes to completely remove air trapped in the reactor. The mixture was heated at 150 ^{o}C for 1.5 hours, mixing at 400 rpm. The gas outlet valve was opened occasionally to vent carbon dioxide produced from the reaction to avoid pressure build-up in the reactor. A model polyether carbonate polyol (PEC) was synthesized to study the effect of carbonate linkage on the lignin oxyalkylation process.

3.2.3.2 Synthesis of Polyether Carbonate Polyol (PEC)

A 100 g of polyethylene glycol (PEG 400) was mixed with 36 g of dimethyl carbonate (DMC). 3.48 g of 1,5,7-Triazabicyclo [4.4.0] dec-5-ene catalyst was added to the reaction mixture and heated at 85 °C under reflux for 4 hours. At the end of the reaction, the produced methanol and unreacted DMC were removed completely at 90 ^{o}C under vacuum, but the catalyst was retained at the end of the reaction. For this reason, no additional catalyst was required in the oxyalkylation step.

3.2.3.3 Oxyalkylation Without Co-Polyol (Ligol 3)

Oven-dried lignin sample was mixed with 5 equivalent (eq.) molar ratio (with respect to total hydroxyl group in lignin) of PC in a Parr Reactor (Model 4524, 0.6L capacity) and 0.05 eq. of catalyst was added to the mixture. The reactor was purged with nitrogen for 5 minutes to completely remove air trapped in the reactor. The mixture was heated at 150 ^{o}C for 1.5 hours,

mixing at 400 rpm. The gas outlet valve was opened occasionally to vent carbon dioxide produced from the reaction to avoid pressure build-up in the reactor.

3.2.4 Polyol Characterization

3.2.4.1 Hydroxyl value

The hydroxy contents of the polyol were measured using ^{31}P-NMR spectroscopy, using a method similar to that used for lignin characterization.[102] The hydroxyl value (OHV), measured in mg KOH/g, of the polyol was computed by multiplying the total hydroxyl content (mmol/g) by 56.1.

3.2.4.2 Viscosity

The viscosity of developed polyols was assessed at ambient temperature employing a Discovery HR-1 hybrid rheometer manufactured by TA Instruments. A 40 mm stainless steel Peltier plate geometry with a 1 mm gap was utilized, with samples sandwiched between the plates and trimmed before analysis. Viscosity measurements were conducted under a constant shear rate of 50 s^{-1}, with the recorded viscosity representing the average value over a 60-second period.

3.2.4.3 Determination of Co-Polyol Ethylene Oxide Content

The polymerized ethylene oxide content of the polyether co-polyols used in this study was determined according to the ASTM D4875-11 standard.[130] ^{13}C NMR spectroscopy was utilized instead of ^{1}H NMR to clearly distinguish signals from the initiator from those of ethylene oxide and propylene oxide. Samples for analysis were prepared by dissolving approximately 100 mg of polyether co-polyols in 600 µL of deuterated dimethyl sulfoxide (DMSO-d_6) and mixed using a vortex at 3000 rpm for 30 seconds. For samples insoluble in DMSO-d_6, deuterated acetone was used, with results remaining consistent regardless of the solvent. A total of 600 µL of the final solution was then transferred to a 5 mm Wilmad NMR tube for analysis. The NMR spectra was acquired using an Agilent DDR2 500 MHz NMR spectrometer equipped with a 7600AS

autosampler and operated with VnmrJ 3.2 A software. Data acquisition included a relaxation delay of 4 seconds and 1024 scans. The ratio of propylene oxide to ethylene oxide (PO/EO) was calculated using equation (3.1) and the ethylene oxide weight percent (EO %) was calculated using equation (3.2). Where B^1 is the area of PO methylene and methine carbons (76.9 to 72 ppm), B area of EO methylene carbons (71.9 to 67.8 ppm), C^1 is area of PO terminal methine carbon (67.0 to 65.0 ppm), C is the total area of terminal EO carbons (61.5 to 60.3 ppm), and F is the area of terminal EO carbon of EO capped block (60.8 to 60.5 ppm). 58 and 44 are the molar mass of propylene oxide and ethylene oxide respectively.

$$PO/EO = \frac{B^1 + C^1 - F}{B + C + F} \quad [3.1]$$

$$\%\, EO = \left(\frac{44}{58\left(\frac{PO}{EO}\right) + 44}\right) \times 100 \quad [3.2]$$

3.2.4.4 Propylene Carbonate Conversion

The consumption of propylene carbonate by PEG over time was quantified using Proton Nuclear Magnetic Resonance (^{1}H NMR) spectroscopy. Sample preparation followed a standardized protocol: an internal standard solution was prepared by dissolving 50 mg of 1,3,5-trioxane in 1 mL of deuterated dimethyl sulfoxide (DMSO-d_6). For analysis, approximately 40 mg of the sample was dissolved in 0.6 mL of DMSO-d_6 and mixed using a vortex at 3000 rpm for 30 seconds. Subsequently, 100 µL of the internal standard solution was added to the sample and vortexed under the same conditions to ensure uniform mixing. A total of 650 µL of the final solution was then transferred to a 5 mm Wilmad NMR tube for analysis. The NMR spectra was analyzed using an Agilent DDR2 500 MHz NMR spectrometer equipped with a 7600AS autosampler and operated with VnmrJ 3.2 A software. Data acquisition involved a relaxation delay of 10 seconds and 64 scans. The percentage of PC consumed was calculated using Equation (3.3), where A_o and A_t

correspond to the initial and final integrated area of the proton signals within the range of 4.72 to 4.86 ppm, respectively.

$$PC\ consumed\ (\%) = (\frac{A_o - A_t}{A_o}) \times 100 \qquad [3.3]$$

3.2.5 Fourier Transform Infrared (FTIR) Spectroscopy

The infrared spectra of synthesized lignin polyols (Ligol) were measured with a PerkinElmer Spectrum Two FT-IR Spectrometer, in Attenuated Total Reflectance (ATR) mode. Few drops of lignin polyols were placed on the ATR crystal and data was collected using 32 scans. Spectrum was processed with a baseline correction and noise-reduction algorithm after data collection.

3.2.6 Foam Formulation

Twenty parts per hundred polyol (pphp) of petroleum-based polyols were replaced with synthesized lignin polyol (Ligol 1, 2, and 3) to produce flexible polyurethane foams (A, B, and C) as presented in **Figure 3.1**. For these foams, the isocyanate (NCO) index was fixed at 100. A high-speed overhead mixer was used to combine polyol blend, water, catalysts, and surfactants for two minutes at 3000 rpm in a 12-ounce paper cup. The calculated amount of isocyanate was then added using a disposable plastic syringe and mixed at 3000 rpm for 3–5 seconds. The mixture was quickly poured into a silicone mold preconditioned at 65 °C and allowed to cure at room temperature for approximately 30 minutes before demolding. After demolding, the foam was left to post-cure at room temperature for at least two days. Foam samples were then cut into mechanical testing specimens, ensuring the removal of the outer skin, for further characterization. Based on the results, an optimized version of Foam B (B-Opt) was formulated by reducing the NCO index to 85. Additionally, a foam formed by replacing 50% of conventional polyol with a combination of lignin polyol (LP) and soy polyol (SP) was formulated to increase the biobased content.

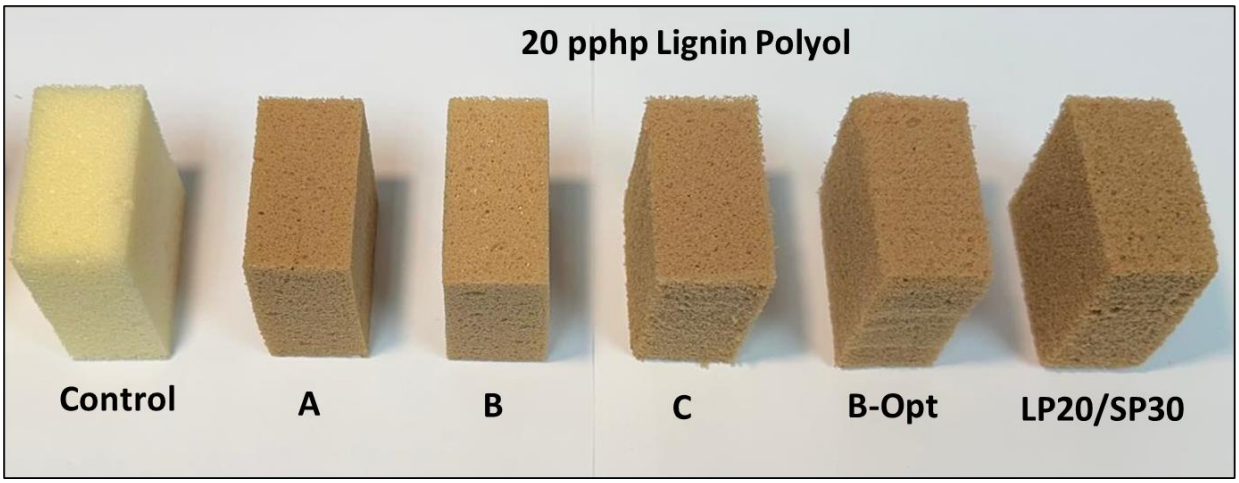

Figure 3.1: Formulated lignin-based flexible polyurethane foams. **LP**-Lignin polyol, **SP**-Soy polyol.

3.2.7 Mechanical Property Testing

The foam samples were cut into mechanical testing specimens without any skin present. These samples were then subjected to property characterization using an Instron Universal Testing machine based on the ASTM D3574 test standard,[131] to assess their physical and mechanical properties, including density, compression force deflection (CFD), support factor, tensile strength, ultimate elongation at break, and tear strength. The values obtained were then compared to the control foams made without lignin polyol and the Original Equipment Manufacturer (OEM) standard requirements for automotive seating applications. Six replicates of each foam sample were tested, and the average and standard deviations were reported.

3.2.7.1 Hysteresis Loss

Foam samples were cut into a similar geometry as CFD test, and their dimensions were precisely measured with calipers. The samples were then placed on an Instron universal testing machine, and the platen separation was set to the foam height. The samples were then compressed to 75% of their initial height at a strain rate of 50 mm/min (loading). The platen was then released from the sample at the same strain rate (unloading). The energy for loading and unloading was computed

by calculating the area under their respective stress-strain curve. The percentage hysteresis loss was calculated as the ratio of energy loss to loading energy multiplied by 100.

3.3 Results and Discussion

3.3.1 Catalyst Screening

A catalyst screening (potassium carbonate (K_2CO_3), 1,8-Diazabicyclo 5.4.0 undec-7-ene (DBU), and 1,5,7-Triazabicyclo 4.4.0 dec-5-ene (TBD)) study was conducted to identify a suitable catalyst for the oxyalkylation reaction **(Figure 3.2)**. Each catalyst was tested under identical conditions, including catalyst loading (0.05 eq.), PC molar ratio (2 eq.), temperature (150 ^{o}C), and reaction time (2 hours), using polyethylene glycol (PEG), with molecular weight 200 g/mol, as the oxyalkylation co-polyol. PC was chosen as the preferred cyclic alkyl carbonate for this study due to its liquid state at room temperature, making it more suitable than ethylene carbonate. The significant reduction of phenolic (137.3–144.6 ppm) and carboxylic hydroxyl (134–135.9 ppm) peaks in the synthesized lignin polyols, as observed in the ^{31}P NMR spectra **(Figure 3.3)**, confirms the conversion of these functional groups into aliphatic hydroxyl groups. Additionally, the appearance of two distinct peaks at 147.3 and 145.6 ppm suggests the formation of propylene glycol or oligomeric glycols, likely resulting from moisture-induced reactions with PC or transesterification side reactions (see **Figure B2** in Appendix B for scheme). Furthermore, the peak around 147.1 ppm corresponds to the aliphatic hydroxyl group of the PEG used in the oxyalkylation reaction. These findings indicate that the synthesized lignin polyol contains modified lignin, co-polyol, oligomeric glycols, and lower amounts of unreacted PC.

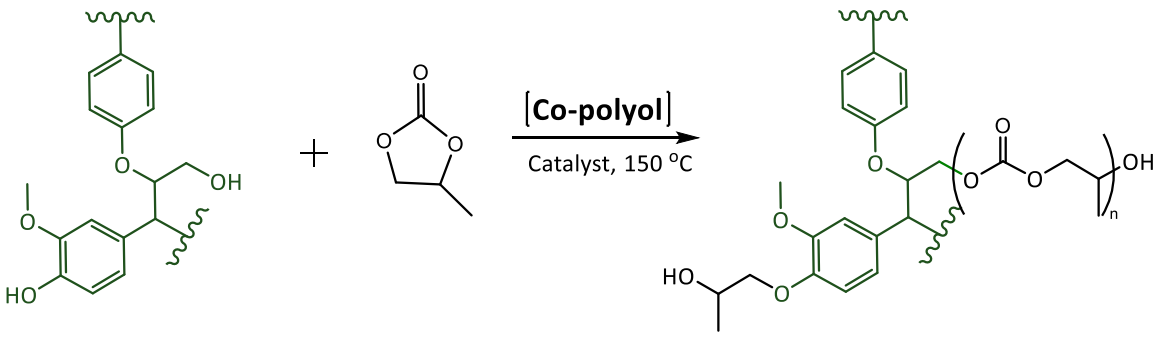

Figure 3.2: Synthesis of propylene carbonate oxyalkylated lignin polyol in the presence of co-polyol.

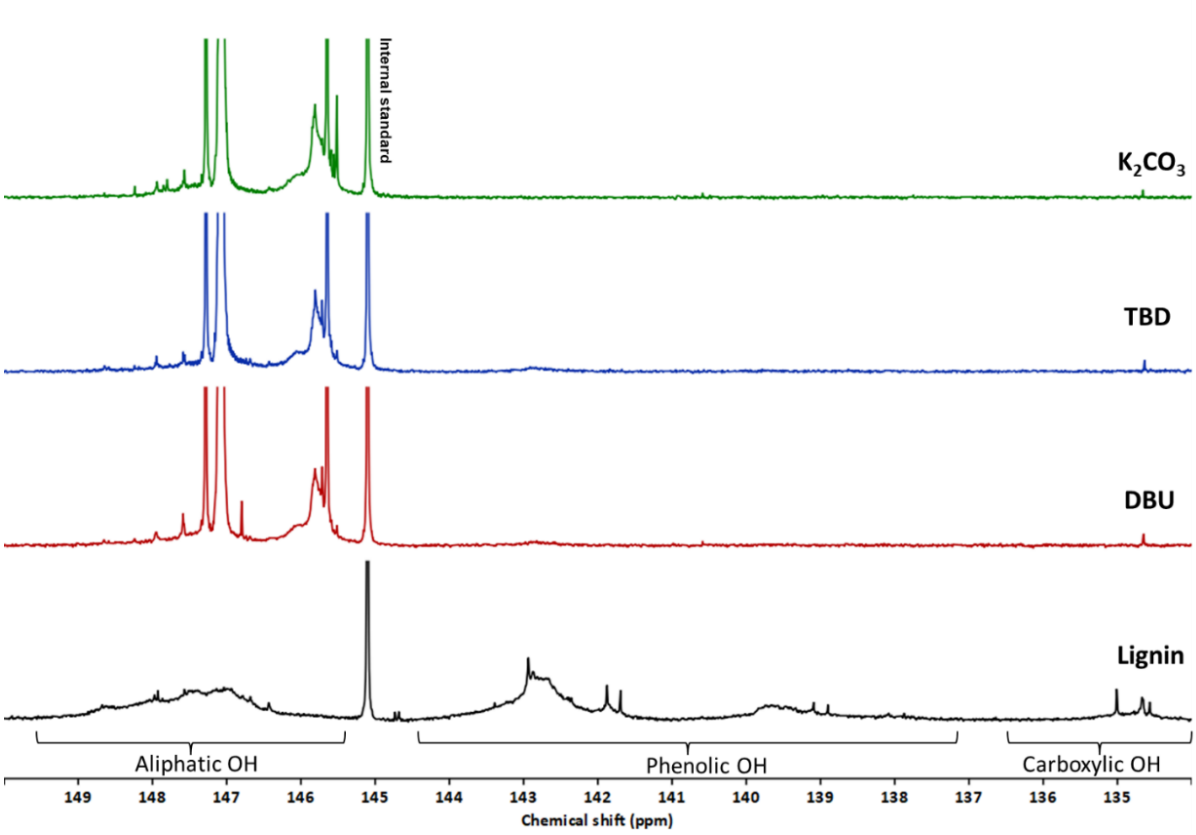

Figure 3.3: ^{31}P NMR spectra of solid unmodified lignin (H-HW) and synthesized lignin polyol catalyzed by DBU, TBD, and potassium carbonate. **Reaction condition:** 2eq. propylene carbonate, 0.05eq. catalyst, 150 °C, 2 hours reaction time, 30% initial lignin loading, and PEG 200 as co-polyol. Samples were phosphitylated prior to analysis. **H-HW**-Hydrolysis Hardwood.

The efficiency of each catalyst was determined by measuring the aliphatic hydroxyl content of the synthesized lignin polyol. As summarized in **Table 3.1**, the aliphatic hydroxyl content, an indicator of the degree of phenolic conversion, was highest (98%) in the K_2CO_3 catalyzed lignin polyol compared to those catalyzed by DBU and TBD at the same reaction time (2 hours). However, the K_2CO_3 catalyzed reaction produced a significantly more viscous lignin polyol than its DBU and TBD-catalyzed counterparts. This high viscosity can be attributed to K_2CO_3 promoting lignin transesterification,[93] which induces lignin chain coupling, thereby increasing polyol viscosity. Studies have shown that this side reaction can increase the molecular weight of lignin by up to 3.7 times, resulting in non-homogeneous fragments with a high polydispersity index (PDI). [93] The lignin polyols catalyzed by DBU and TBD exhibited comparable aliphatic hydroxyl content and viscosity. Based on these findings, DBU and K_2CO_3 were selected for further studies. The effect of reaction time on lignin oxyalkylation was then investigated to determine the best duration for subsequent studies. As shown in **Table 3.1**, there was no significant change in hydroxyl value, but the viscosity of the polyol increased as the reaction progressed in both K_2CO_3 and DBU-catalyzed oxyalkylation reactions. This trend can be attributed to the decreasing concentration of PC in the reaction mixture. As the reaction proceeds, more PC reacts with the aliphatic hydroxyl groups present in both lignin and PEG, thereby reducing PC content while increasing the overall polyol viscosity.

Table 3.1: Effect of catalyst type and reaction time on propylene carbonate oxyalkylated lignin polyol's hydroxyl value (OHV), aliphatic OH content, and viscosity. **Reaction condition:** 2 eq. ratio propylene carbonate, 0.05 eq. catalyst, 150 ^{o}C, 30% initial lignin (H-HW) loading, and polyethylene glycol (MW 200) as co-polyol. **H-HW=**Hydrolysis Hardwood.

Catalyst type	**Time (h)**	**Total OHv (mgKOH/g)**	**Aliphatic OH content (%)**	**Viscosity (mPa.s)**
DBU	2	368	97	4100 ± 30
DBU	1.5	365	94	2600 ± 30
TBD	2	397	97	3810 ± 50
K_2CO_3	2	381	98	11,800 ± 220
K_2CO_3	1.5	374	98	9400 ± 150
K_2CO_3	1	371	98	7000 ± 100

To confirm the reaction between PC and PEG, the oxyalkylation reaction was performed in the absence of lignin, and the conversion of PC was monitored using ^{1}H NMR every 30 minutes over a two-hours period. The ^{1}H NMR spectra (see **Figure B1** in Appendix B**)** revealed the appearance of a new proton signal at 0.9 ppm, which corresponds to the methyl pendant group formed from the reaction between PEG and PC. The increasing intensity of this methyl proton peak over time indicates continuous reaction between PEG and PC. Additionally, new methylene proton signals emerged at 3.49 and 4.06 ppm. Meanwhile, the characteristic PC peak around 4.8 ppm decreased in intensity as the reaction progressed, confirming its continuous consumption by PEG. By integrating the peak at 4.8 ppm, the amount of PC consumed was quantitatively determined, as summarized in **Table B3** (Appendix B).

Another contributing factor to the excessively high lignin polyol viscosity at longer reaction time, particularly in the potassium carbonate catalyzed reaction, is the lignin chain coupling or transesterification side reaction (see **Figure B2** in Appendix B for scheme). This side reaction not only increases polyol viscosity but also elevates the overall hydroxyl value due to the production of propylene glycol as by-product. Given that propylene glycol has a theoretical hydroxyl value of 1474.6 mg KOH/g, its excessive presence through side reactions can significantly increase lignin polyol's hydroxyl value, which is unfavorable for flexible PU foam applications, where low hydroxyl values are required. Therefore, K_2CO_3 was found to be the most sensitive to reaction time, as evidenced by its sharp increase in viscosity. Consequently, DBU was determined to be the more suitable oxyalkylation catalyst, aligning with the findings reported by Kühnel et al.[93] A reaction time of 1.5 hours was selected for subsequent study since it resulted in a lignin polyol with low viscosity (2600 mPa.s) and considerably high aliphatic hydroxyl content (94%).

3.3.2 Oxyalkylation in the Presence of Co-Polyol

An initial experiment utilizing lignin to PC molar of 1:2 without co-polyol yielded a gelled material which was difficult to process, however, the introduction of a co-polyol in the oxyalkylation reaction produced a homogeneous lignin polyol with workable viscosity (2600 to 11,800 mPa.s). Therefore, the incorporation of co-polyols is an essential step to minimize PC usage in the oxyalkylation reaction and obtain a lignin polyol that can be used directly in foam formulation without further purification. Based on this, various co-polyols with different chemical structures **(Figure 3.4)**, molecular weights, functionalities, and hydroxyl values were evaluated for their compatibility with the oxyalkylation process and impact on overall lignin polyol properties. **Table 3.2** summarizes the properties of the co-polyols used. Among these, only castor oil, soy and cashew nuts shell liquid (CNSL) polyols are bio-based. CNSL-based polyols are typically produced from

cardanol via the novolac chemistry, followed by ethoxylation of phenolic hydroxyl groups to introduce aliphatic hydroxyl functionalities.[83] Similarly, soy polyol is derived from soybean oil through epoxidation and subsequent ring-opening reactions.[81] In contrast, castor oil already contains aliphatic hydroxyl groups in its triglyceride backbone, so there is no need for further modification.[132]

Table 3.2: Hydroxyl value, OH functionality (f), molecular weight (Mw), ethylene oxide (EO) content and chemistry of co-polyols evaluated.

Co-polyol	**Description/source**	**OHv (mgKOH/g)**	**f**	**Mw (Da)**	**EO content (%)**	**Structure/ linkages**
PEG_{200}	Polyethylene glycol	561	2	200	100	EO
PEG_{400}		281	2	400	100	EO
PEG_{600}		187	2	600	100	EO
PEG_{1000}		112	2	1000	100	EO
PPG_{1000}	Polypropylene glycol	112	2	1000	0	PO
PO/EO-A	Propylene glycol initiated EO capped	40	2	2801	17.3	PO/EO
PO/EO-B	Glycerol initiated EO capped	28	3	6000	16.6	PO/EO
PO/EO-C		170	3	1000	75.1	PO/EO
PO/EO-D		42	3	4000	75.9	PO/EO
PEC	Polyether carbonate	138	2	813*	-	EO/carbonate
CNSL Polyol	Cashew nut shell liquid	175	3.8	-	-	Novolac polyol
Soy Polyol	Soybean oil	29	-	933	-	Ester
CO polyol	Castor oil	168	3	933	-	Ester

*Mw of polyether carbonate (PEC) polyol was calculated based on measured hydroxyl value and functionality.

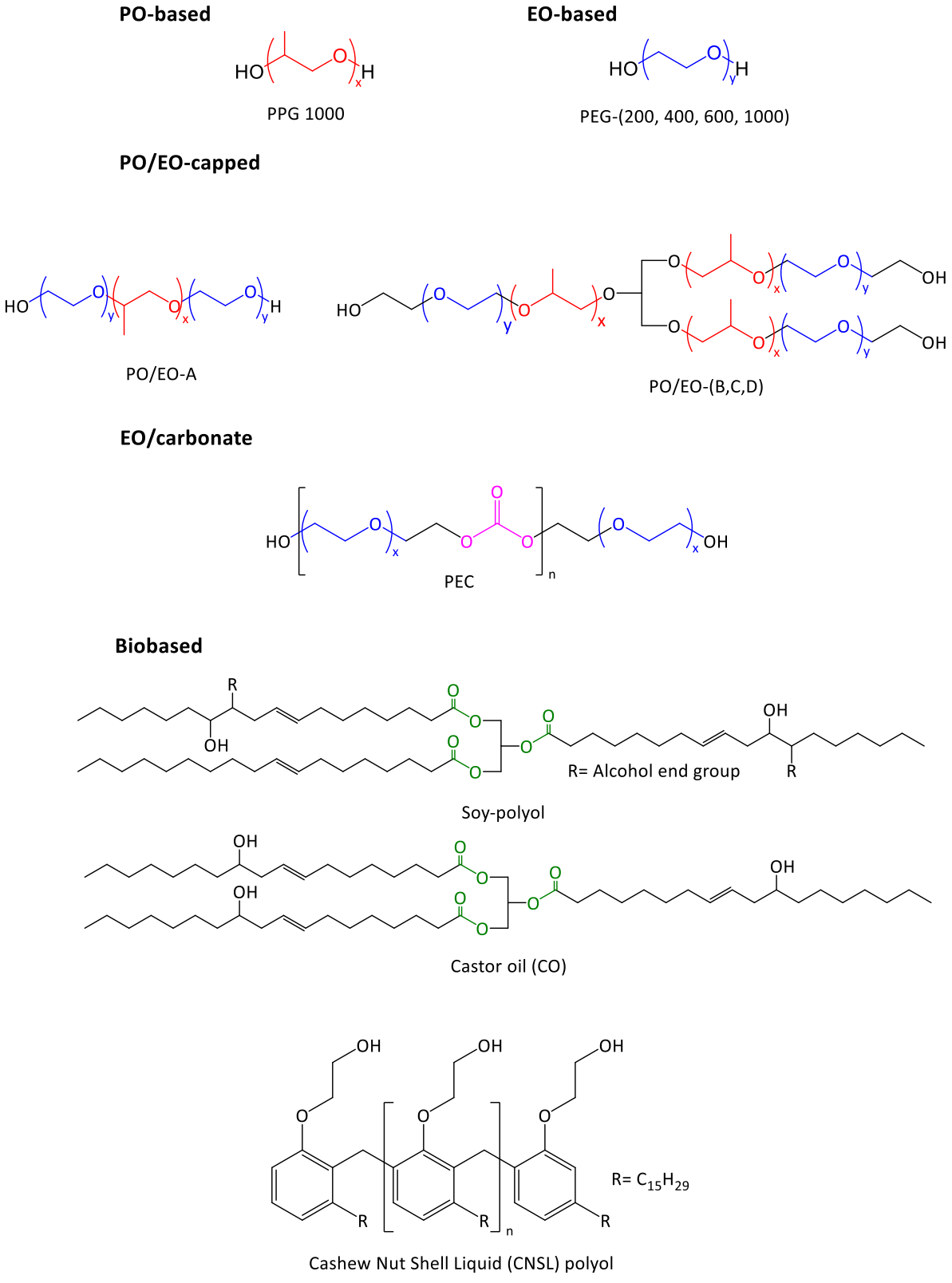

Figure 3.4: Chemical structure of co-polyols tested in lignin oxyalkylation reaction.

3.3.2.1 Role of Co-Polyol Structure

The role of co-polyol structure and properties in lignin oxyalkylation was investigated to guide the selection of an appropriate co-polyol for achieving the desired lignin polyol properties. Considering the target application, it is essential to determine which co-polyol can be effectively incorporated into the reaction. Ethylene oxide (EO)-based polyols demonstrated remarkable compatibility with the lignin oxyalkylation process, producing a uniform lignin polyol. This indicates that EO-polyol enhances lignin solubility and provides an effective medium for its reaction with propylene carbonate. The high aliphatic hydroxyl content (85–94%) of EO-based lignin polyols, as shown in **Figure 3.5**, further confirms their role in facilitating the oxyalkylation reaction. In contrast, propylene oxide (PO)-based polyols were incompatible with the oxyalkylation process. When polypropylene glycol (PPG, MW 1000 Da) was used as the co-polyol, the reaction produced a two-phase liquid-solid mixture, as shown in **Figure 3.5c**, indicating that lignin was insoluble in the PO-based polyol. The presence of a dark liquid phase suggests that lignin is only partially dissolved in the PC/PO-based polyol mixture. This poor solubility can be attributed to the steric hindrance caused by the hydrophobic methyl pendant groups, [133] which reduce the co-polyol's ability to polarize and interact effectively with lignin's hydroxyl groups.

Co-polyols with different ratios of EO and PO were then evaluated. It is important to know that these polyols tested are EO-capped polyols. In other words, they were initially polymerized with PO and terminated with EO. This is usually done in industry to achieve a polyol with a primary hydroxyl group, thereby increasing their reactivity towards isocyanate. When these polyols were used in the lignin oxyalkylation reaction, it exhibited an interesting behavior. At low EO content, such as in PO/EO-A (16.6%) and PO/EO-B (17.4%), lignin exhibited self-aggregation, forming a two-phase mixture similar to that seen with purely PO-based polyols. In contrast, when the EO

content was higher, as in PO/EO-C (75.1%), lignin self-aggregation was not observed, resulting in a uniform lignin polyol. This behavior is likely attributed to the lower concentration of hydrophobic PO methyl side groups, which otherwise reduce polarity and compatibility. This clearly demonstrates that the compatibility of PO/EO-capped polyols with the oxyalkylation process is directly related to their ethylene oxide content. However, due to the limited number of co-polyols tested, it was not possible to determine the minimum EO content required to prevent lignin aggregation and phase separation. Additionally, polyols with random or alternating PO/EO block structures were not assessed, leaving the influence of block configuration on the oxyalkylation reaction unexplored. EO/carbonate-based polyol (PEC) also demonstrated excellent compatibility with the oxyalkylation process, likely due to the presence of highly polar carbonate linkages that can form strong hydrogen bonds[134] with lignin hydroxyl groups, thereby enhancing lignin (H-HW) solubility. This finding suggests that polar repeating units reduce the tendency of lignin to self-associate, aligning well with previous studies [135] that have shown lignin's high solubility in aprotic polar solvents.

Biobased polyols, such as cashew nuts shell liquid (CNSL)-based polyol, castor oil and soy polyol, were found to be incompatible with the oxyalkylation reaction. The incorporation of soy polyol and castor oil led to the formation of a two-phase mixture, likely due to the presence of ester linkages in the triglyceride backbone. These ester linkages form weak hydrogen bonds with lignin hydroxyl groups, which are further destabilized by repulsive electrostatic interactions with the adjacent carbonyl groups.[136] In contrast, the CNSL-based polyol resulted in a hard, gelled material at the end of the reaction, as shown in **Figure 3.5d**. The exact mechanism behind this behavior remains unclear but may be attributed to a chemical interaction, possibly a transesterification side reaction between a CNSL polyol adduct, formed from the reaction of CNSL aliphatic hydroxyl

groups with PC, and lignin hydroxyl groups. The long hydrophobic hydrocarbon pendant group may have also contributed to the incompatibility of the biobased polyols in the oxyalkylation reaction. When a co-polyol containing 50 w% castor oil and 50 w% PEG 400 was used, it produced a homogeneous oxyalkylated lignin polyol. This presents an opportunity to enhance the biobased content in the final PU product by blending EO-based polyols with biobased polyols prior to the oxyalkylation reaction.

As shown in **Figures 3.5a** and **b**, co-polyols with higher molecular weights resulted in lignin polyols with lower total hydroxyl values, reduced aliphatic hydroxyl content, and increased viscosity. The decrease in aliphatic hydroxyl content indicates a reduction in the lignin dissolution rate in co-polyol due to chain entanglement from high-molecular-weight co-polyols. This diminished dissolution likely slowed the lignin oxyalkylation reaction, leading to a lower aliphatic hydroxyl content in the final product. When co-polyols with similar molecular weights, such as PEG 1000 and PO/EO-C, were compared, they produced lignin polyols with similar hydroxyl values but different aliphatic hydroxyl contents and viscosities. PO/EO-C co-polyol exhibited lower viscosity and higher aliphatic hydroxyl content than PEG 1000-based lignin polyol, as shown in **Figure 3.5a**. These differences can be directly attributed to the repeated EO units in PEG 1000 which tend to crystallize.[137] This implies that while EO content is the primary factor in selecting a co-polyol for lignin oxyalkylation, an excessively high EO content results in a lignin polyol with high viscosity and low aliphatic hydroxyl content. It is evident that the properties of the resulting lignin polyols were primarily influenced by the molecular weight of the co-polyol, while the behavior of the co-polyol in the oxyalkylation reaction depended on its hydrogen bonding potential. Based on this principle, the compatibility of co-polyols in the lignin oxyalkylation process, ranked according to the hydrogen bonding potential of their structural units

with unmodified or PC-modified lignin, follows the order: Carbonate > EO > PO/EO > Ester > PO.

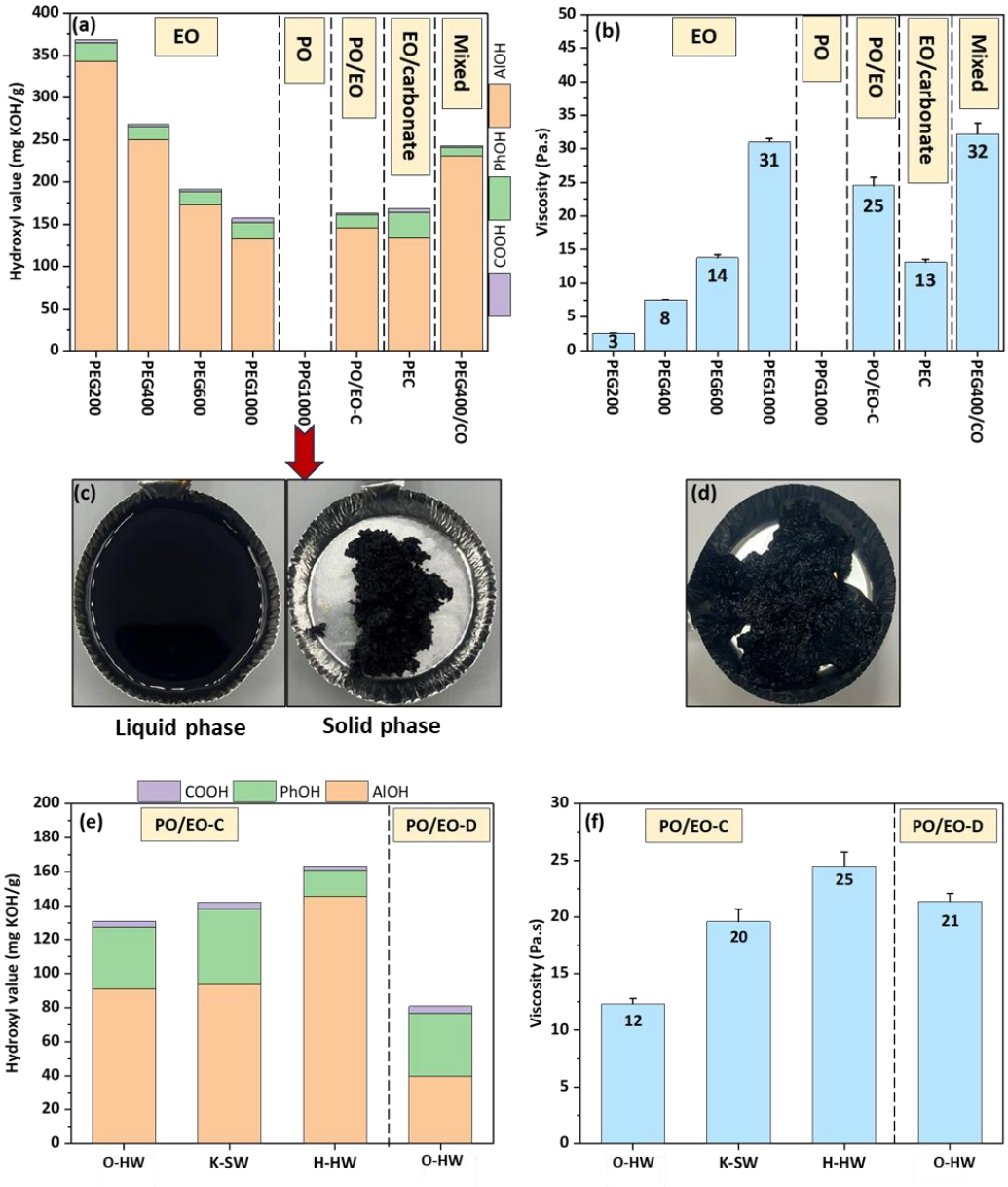

Figure 3.5: Effect of co-polyol structure on oxyalkylated lignin polyol's (a) hydroxyl value, aliphatic OH content, and (b) viscosity. (c) A two-phase liquid-solid mixture formed from a PO-based lignin oxyalkylation reaction. Liquid phase (left) and solid phase (right). (d) Gelled product from cashew nutshell liquid (CNSL)-based lignin oxyalkylation reaction. (e) Role of lignin type on hydroxyl value, aliphatic OH content, and (f) viscosity of PO/EO capped polyol-based oxyalkylated lignin polyol.

3.3.2.2 Role of Lignin Type

Three different lignin types, including organosolv hardwood (O-HW), kraft softwood (K-SW), and hydrolysis hardwood (H-HW) lignins, were independently used in the oxyalkylation reaction with PO/EO-C as the co-polyol to understand the impact of lignin type. The uniform lignin polyol obtained in all cases confirms PO/EO-C's compatibility with all lignin types, highlighting the role of ethylene oxide units in enhancing solubility. Among the lignin types, H-HW produced a lignin polyol with the highest total hydroxyl value (163 mg KOH/g) and aliphatic hydroxyl content (89%), compared to O-HW and K-SW, as seen in **Figure 3.5e**. This difference is attributed to variations in lignin hydroxyl content and the distribution of syringyl (S), guaiacyl (G), and p-hydroxyphenyl (H) units in each lignin.

The O-HW lignin, with a lower hydroxyl value (3.9 mmol/g) than H-HW lignin (5.43 mmol/g), resulted in the lignin polyol with the lowest hydroxyl value (131 mg KOH/g). However, despite having a hydroxyl value similar to H-HW, K-SW produced a lignin polyol with the lowest aliphatic hydroxyl content (66%). This can be attributed to the absence of S unit in K-SW, compared to the high S unit content (1.46 mmol/g) in H-HW. Kuhnel et al.[91] also investigated the impact of lignin hydroxyl moieties on the oxyalkylation reaction and reported that S units are the most reactive towards cyclic carbonates, followed by G units, with H units being the least reactive. They attributed the high reactivity of S units to the presence of electron-donating methoxy groups, which enhance the nucleophilicity of phenolate ions and facilitate the reaction with PC.[91] Additionally, the differences in reactivity of lignin's hydroxyl moieties toward PC were found to also influence the viscosity of the resulting lignin polyols, as seen in **Figure 3.5f**. Due to the higher reactivity of S units, H-HW consumed more PC, leading to a lignin polyol with the highest viscosity compared to those derived from K-SW. Although O-HW also contained a similar proportion of S units as H-

HW (1.47 mmol/g), it exhibited the lowest viscosity, likely attributed to its relatively low average Mw (4066 Da). In polyurethane applications where flexibility is required, high molecular weight and low hydroxyl value polyols are preferred. To assess the impact of lignin type when increasing co-polyol molecular weight, PO/EO-C (1000 Da) was replaced with PO/EO-D (4000 Da), while maintaining a similar ethylene oxide content of approximately 75 % for both. The results showed that all these three lignin types, except O-HW, formed a two-phase solid-liquid mixture, indicating that only the organosolv lignin was compatible with the high molecular weight co-polyol in the oxyalkylation reaction. This behavior can be attributed to the lower average Mw and polydispersity index (PDI) of O-HW lignin (4066 Da, PDI=2.48) compared to H-HW (5480 Da, PDI=4.9) and K-SW (7650 Da, PDI=4.6) lignin. This implies that selecting a high EO co-polyol with a lower molecular weight than lignin is essential to achieving a higher degree of compatibility. Apart from molecular weight differences, the high purity and the less modified nature of organosolv lignins also contributed to their solubility. Polymer solubility is primarily governed by chain disentanglement, which is influenced by both average molecular weight and dispersity.[138] According to this principle, lower molecular weight polymers are more likely to dissolve in various solvents due to their greater capacity for disentanglement, thereby enhancing solubility. Increasing the co-polyol molecular weight from 1000 to 4000 g/mol led to a 38% reduction in the hydroxyl value of O-HW-based oxyalkylated lignin polyol, while the aliphatic hydroxyl content decreased from 69% to 49%. Additionally, viscosity nearly doubled due to the incorporation of the high-molecular-weight (4000 Da) co-polyol (PO/EO-D), which increased intermolecular friction and restricted polyol mobility.

3.3.2.3 PLS Modelling

Partial least-square (PLS) regression modeling was used to find correlations between co-polyol properties and their compatibility with the lignin oxyalkylation reaction. The secondary objective was to identify the correlation between the oxyalkylation reaction parameters and co-polyol compatibility. The PLS model was developed with two PLS components, which had 86% fitting accuracy (R2Y=the explained variation), and 67% prediction ability (Q2Y=the predicted variation) based on a cross-validation method. Two PLS components were shown to be optimal for the model. **Figure 3.6** plots the components' contributions, showing R2 as an indicator of how well the model fits the experimental data (green bars) and Q2 as an indicator of how well the model can predict any new co-polyol's compatibility (blue bars).

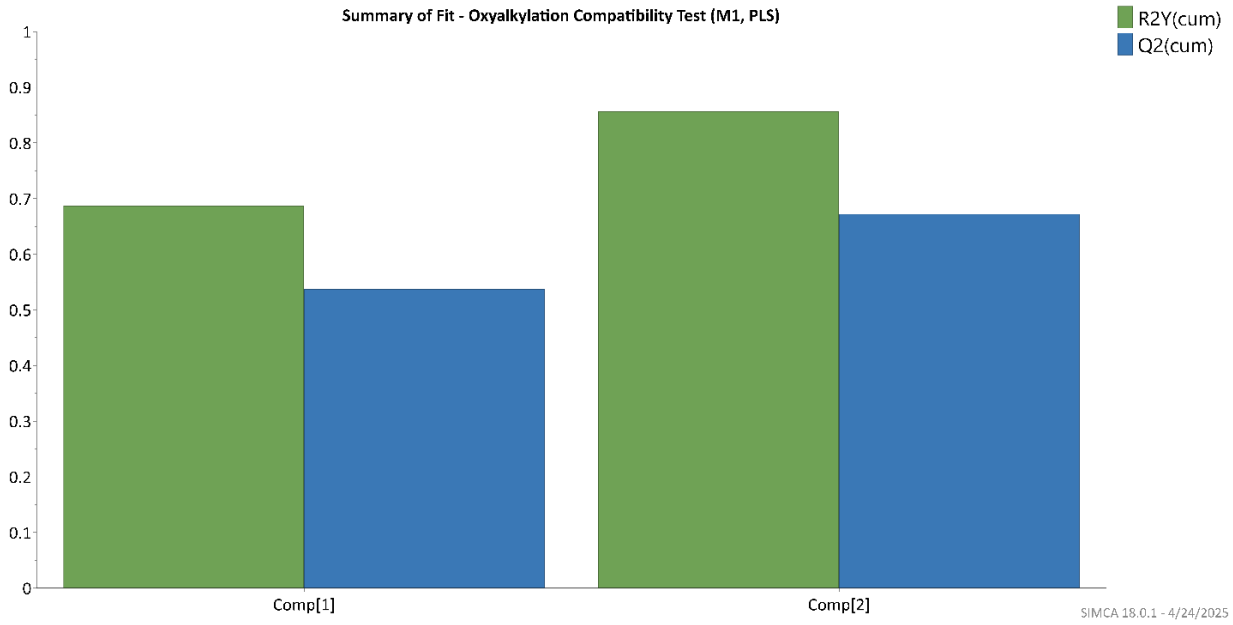

Figure 3.6: Component contribution of the response variable (co-polyol compatibility).

According to the loading plot **(Figure 3.7)**, co-polyol structure (PO, ester, and novolac) and Mw have strong negative (opposite side) correlations with compatibility. In contrast, EO content has strong positive correlation (same side) with co-polyol's compatibility. In other words, co-polyols with higher amounts of PO, ester, or novolac structural units and Mw are incompatible, whereas

co-polyols with higher EO content are more compatible with the oxyalkylation reaction process. Reaction parameters such as catalyst type and ratio, time, in addition to the lignin type were found to have a weaker impact on the model (lower effect on determining co-polyol compatibility).

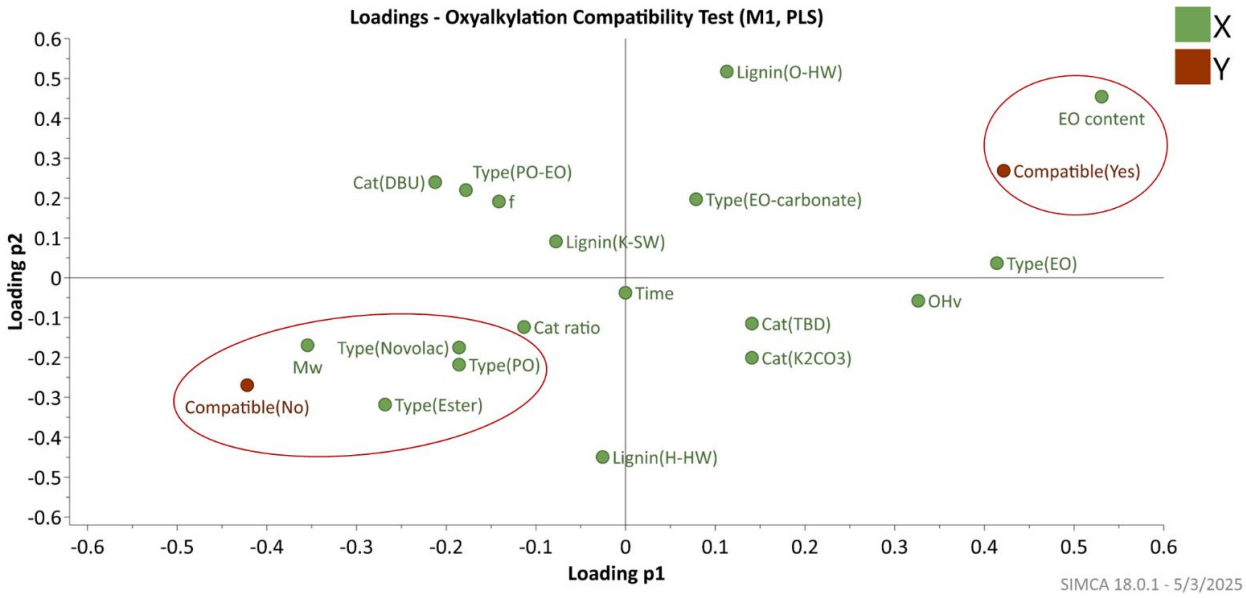

Figure 3.7: Loading plot of PLS modeling of compatibility based on co-polyol properties and oxyalkylation reaction parameters.

3.3.2.4 Reaction Optimization for Polyurethane Flexible Foam

For the development of lignin-based polyols suitable for flexible foam formulation, PEG 1000 was selected over PO/EO-C and PO/EO-D due to its lower functionality (f = 2) and remarkable ability to dissolve lignin, resulting in a homogeneous oxyalkylated lignin polyol. Although PO/EO-C and PO/EO-D produced lignin polyols with lower hydroxyl values, their higher functionality (f = 3) would likely increase the crosslinking density of flexible polyurethane foams, making them more rigid. However, the use of PEG 1000 as a co-polyol in the oxyalkylation reaction resulted in a highly viscous lignin polyol (31,440 mPa.s), necessitating further optimization of reaction parameters. To address this, the DBU catalyst loading was reduced from 0.05 to 0.023 eq, and the

reaction time was shortened from 1.5 hours to 1 hour. These modifications significantly lowered the polyol's (Ligol 2) viscosity to 8,450 mPa.s. Further reducing the reaction time to 30 minutes led to an additional 43% decrease in viscosity (Ligol 1). These findings highlight that adjusting catalyst loading and reaction time can effectively tailor lignin polyol properties to meet specific application requirements. Although these adjustments were necessary to reduce polyol viscosity, not all phenolic hydroxyl groups reacted, as shown in **Figure B3 (**Appendix B). **Table 3.3** presents the summarized results of the oxyalkylation reaction optimization. Ligol 1 and Ligol 2 were selected for flexible polyurethane (PU) formulation. Additionally, Ligol 3, synthesized with 5eq. of PC and without a co-polyol, was produced to directly assess the impact of co-polyol on foam properties. Unlike Ligol 1 (2 eq.) and Ligol 2 (2eq.), Ligol 3 (5eq). exhibited almost complete conversion of phenolic hydroxyl groups (see **Figure B3** in Appendix B for ^{31}P NMR spectrum) due to the high concentration of PC used in the reaction. FTIR analysis of the synthesized polyols revealed that Ligol 3, produced without a co-polyol, contained more unreacted PC compared to Ligol 1 and Ligol 2, as expected and indicated by the lower intensity of the PC carbonyl peak around 1786 cm^{-1} in **Figure 3.8**. Additionally, the low viscosity of Ligol 3 (900 mPa.s) further confirms its high unreacted PC content. This indicates that the inclusion of a co-polyol helps reduce the amount of unreacted propylene carbonate in the reaction product following the oxyalkylation reaction.

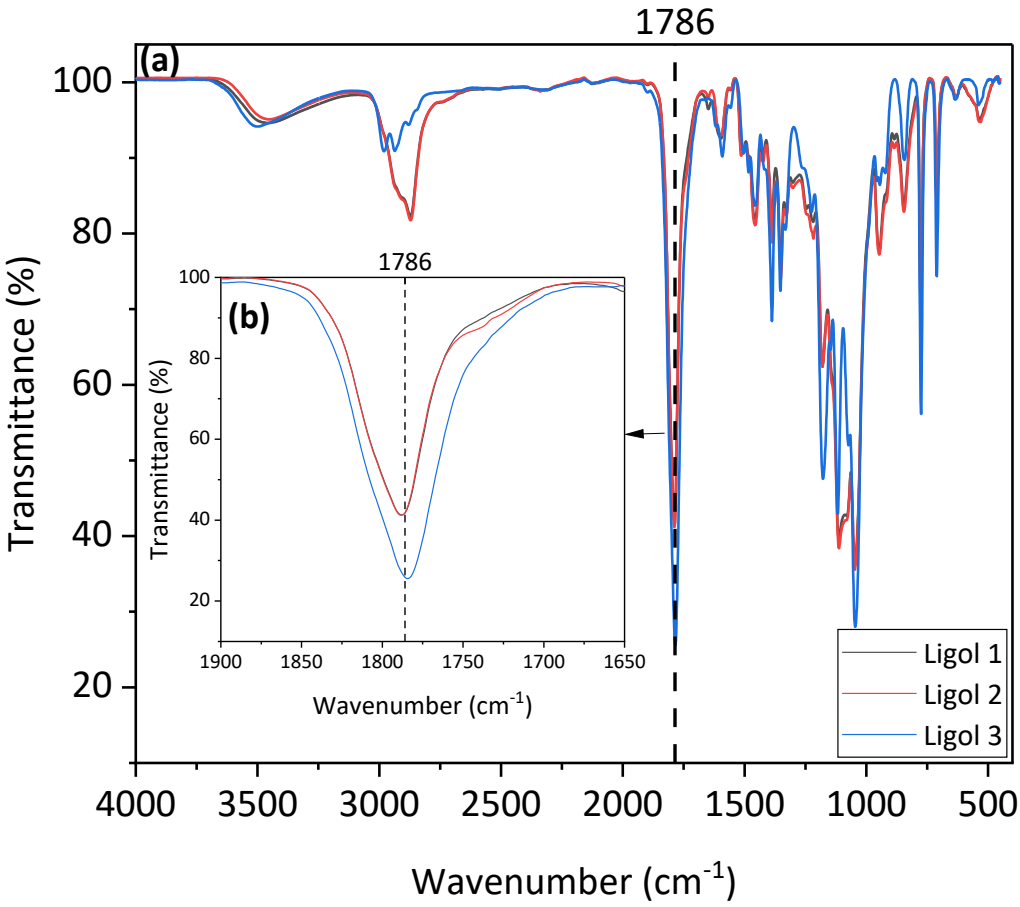

Figure 3.8: FTIR-ATR spectra of synthesized lignin (H-HW) polyols: (a) full spectral range and (b) expanded view of the carbonyl (C=O) region attributed to propylene carbonate. Ligol 1 and Ligol 2 were synthesized using PEG 1000 as a co-polyol, while Ligol 3 was synthesized without a co-polyol.

Table 3.3: Hydroxyl value (OHv), aliphatic hydroxyl content, and viscosity of synthesized oxyalkylated lignin (H-HW) polyols. Ligol 1 and Ligol 2 were synthesized with PEG 1000 as a co-polyol, whereas Ligol 3 was synthesized without a co-polyol. **H-HW**-Hydrolysis Hardwood.

Polyol ID	PC molar ratio (eq.)	OHV (mg KOH/g)	Aliphatic OH content (%)	Viscosity (mPa.s)	Resulting Flexible PU foams
Ligol 1	2	149	65	4,840 ± 70	A
Ligol 2	2	145	70	8,450 ± 110	B
Ligol 3	5	163	99	900 ± 20	C

3.3.3 Flexible Foam Mechanical Properties

The mechanical properties of the foams were measured and are presented in **Figures 3.9** and **3.10.** All formulated foams had densities within the range of 30 to 50 kg/m³. The compressive properties of the foams demonstrated that lignin polyol imparted superior load-bearing performance, evident in the lignin-based foam's (A, B, and C) higher compression force deflection (CFD) as seen in **Figure 3.9a**. However, there was no significant difference in the support factor of lignin-based foams compared to the control, with all foams falling within the range of 3 to 4, which is acceptable for seating applications. Support factor is an empirical parameter related to the compression modulus that is widely used in the industry to evaluate foam cushioning performance. A foam with a higher support factor is less prone to "bottoming out" under compressive stress. Hysteresis loss, which is an indication of foam recovery rate under compressive stress, for lignin-based foams were found to be higher than that of the control foam. This implies that lignin-based foam recovers much slower than the control foam when compressed, dissipating energy as heat, making them less

resilient. This presents a great opportunity for shock absorption, and sound-damping applications. Also, the addition of optimized lignin polyols (Ligol 1 and 2) significantly enhanced the tensile strength but led to a reduction in foam's ultimate elongation at break compared to the control foam. This behavior can be explained by the higher hydroxyl value (OHV) of the lignin polyols (145 to 149 mg KOH/g) compared to OHV of the long-chain polyether polyol (28 mg KOH/g) used as a co-polyol in the foam formulation, resulting in a greater proportion of hard segments in the foam. This, in turn, restricts the elastomeric activity of the soft segments (polyols) due to the presence of the Ligols, which increases the foam's crosslinking density.

Among the lignin-based foams (A, B, and C), significant differences in mechanical properties were observed depending on whether their respective Ligols were synthesized with or without an oxyalkylation co-polyol (PEG 1000). Foams A and B, which were formulated with Ligols synthesized in the presence of oxyalkylation co-polyol, showed superior mechanical properties compared to Foam C. Notably, Foam B (produced using Ligol 2) demonstrated the highest tensile and tear strength, outperforming foam A (made with Ligol 1). This can be attributed to Ligol 2's lower total phenolic and carboxylic OH content (30%) relative to Ligol 1 (35%), making Ligol 2 more reactive towards isocyanate. Phenolic and carboxylic OH groups have reduced reactivity towards isocyanate due to their acidity, making them less nucleophilic.[139] Additionally, steric hindrance from the aromatic ring in phenolic OH further impedes the interactions with isocyanate, significantly slowing the reaction rate. Somes studies have also shown that the presence of methoxy groups on lignin's phenolic moieties adds further steric hindrance, [79,140] further limiting reactivity. Ligol 3, despite its high aliphatic hydroxyl content (99%), produced a PU (Foam C) with relatively poor tensile and tear strength. A similar outcome was observed by Kevin et al.,[73] who incorporated PC oxyalkylated lignin polyol (lignin-to-PC molar ratio of 1:5, no co-polyol)

into flexible PU foam. This outcome can be attributed to the plasticizing effect of unreacted PC in the lignin polyol. Moreover, the excessively high unreacted PC in Ligol 3 likely contributed to Foam C's high hysteresis loss (66%), an undesirable characteristic for high-resilience seating applications. This further confirms the importance of oxyalkylation co-polyols in the Ligol synthesis step to minimize the amount of unreacted PC. Foam A fulfilled all the standard criteria for automotive seating applications, whereas Foam B met all requirements except for the ultimate elongation at break.

Based on the mechanical property results, Foam B was optimized by reducing the isocyanate (NCO) index from 100 to 85. This adjustment aimed to lower the crosslinking density caused by lignin's high functionality and aromatic structure, thereby improving elongation at break. As shown in **Figure 3.10b**, this modification increased the elongation at break of the optimized foam (B-opt) from 55% to 68%, meeting the standard requirement for seating applications. Building on this improvement, a new foam formulation containing 20 pphp Ligol 2 and 30 pphp soy polyol (at an NCO index of 85) was developed to further increase the biobased content. The resulting flexible PU foam met all standard requirements for automotive seating applications except for elongation at break (46%). Future studies could focus on optimizing foam performance to achieve the desired elongation while exploring ways to incorporate soy polyol beyond 30 pphp.

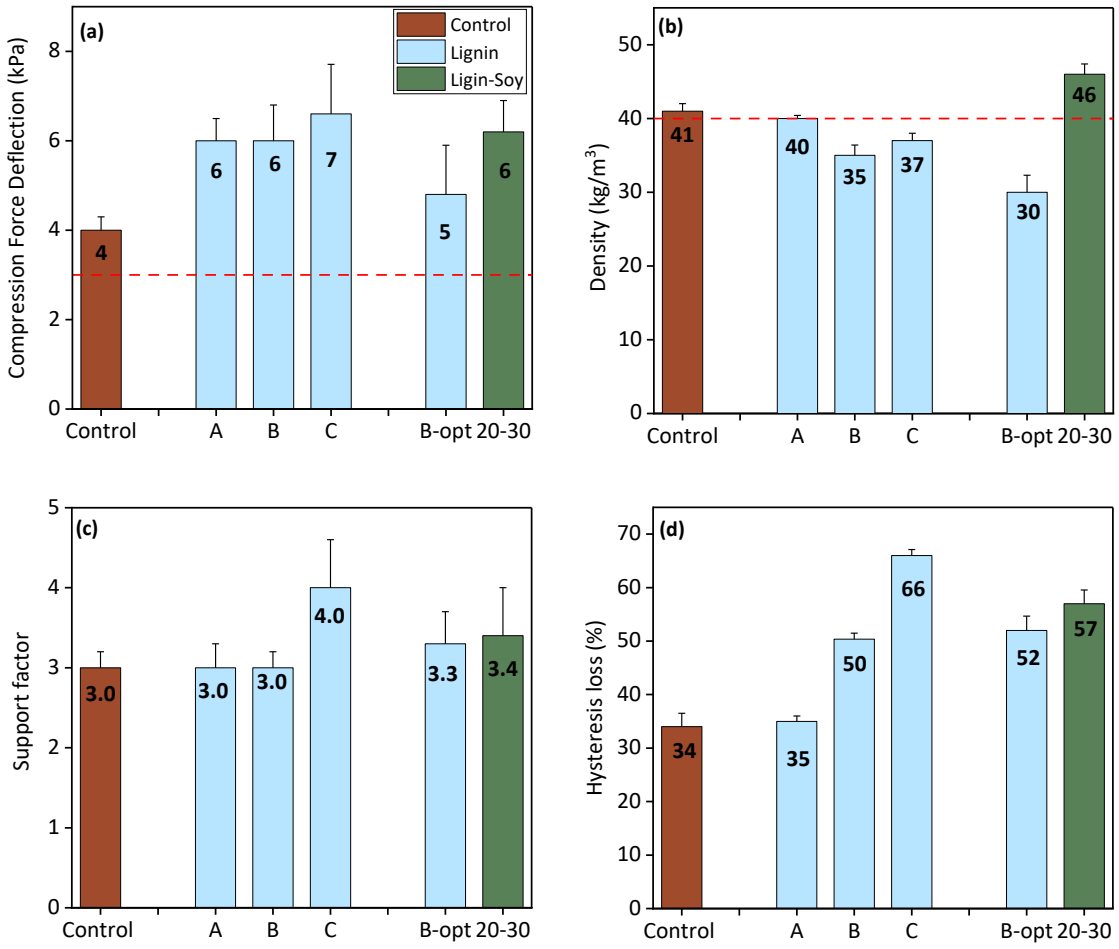

Figure 3.9: Mechanical properties of flexible polyurethane (PU) foams formulated with 20 pphp lignin polyols and lignin-soy polyol blends (20 pphp lignin polyol and 30 pphp soy polyol), as measured by ASTM D3574: (a) compression force deflection at 50% strain, (b) density, (c) support factor, and (d) hysteresis loss. Foams A, B, and C were formulated with Ligol 1, Ligol 2, and Ligol 3, respectively at isocyanate (NCO) index of 100. B-opt represents an optimized version of Foam B developed using a lower NCO index of 85. The lignin-soy foam (20-30) was formulated with Ligol 2 at an NCO index of 85. **Pphp**-part per hundred polyol.

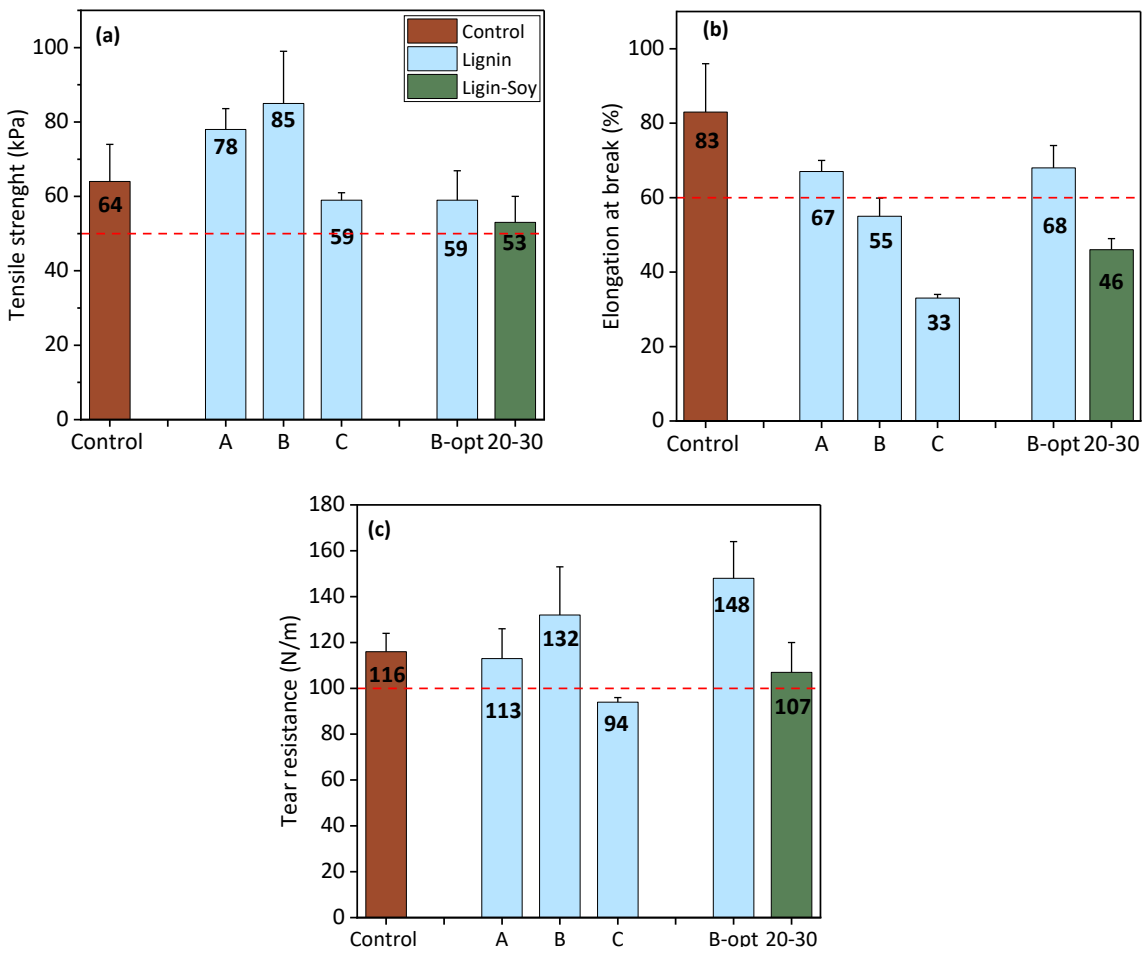

Figure 3.10: ASTM D3574 measured (a) tensile strength, (b) ultimate elongation at break, and (c) tear strength of flexible polyurethane (PU) foams formulated with 20 pphp lignin polyols and lignin-soy polyol blends (20 pphp lignin polyol and 30 pphp soy polyol). Foams A, B, and C were formulated with Ligol 1, Ligol 2, and Ligol 3, respectively at isocyanate (NCO) index of 100. B-opt represents an optimized version of Foam B developed using a lower NCO index of 85. The lignin-soy foam (20-30) was formulated with Ligol 2 at an NCO index of 85. **Pphp**-part per hundred polyol.

3.4 Conclusion

This study successfully demonstrated the potential of using co-polyols to optimize the oxyalkylation of lignin with propylene carbonate (PC), addressing the challenges associated with unreacted PC and enabling the direct use of lignin-based polyols in flexible polyurethane (PU) foam formulations for high end applications such as automotive seating. The findings highlighted the importance of co-polyol selection, with high ethylene oxide (EO)-based polyols proving to be the most effective in solubilizing lignin and enhancing its reactivity towards propylene carbonate. In contrast, propylene oxide (PO)-based, and bio-based polyols (castor oil, soy polyol, and cashew nut shell liquid-based polyol) exhibited poor compatibility due to steric hindrance and weak hydrogen bonding. The study also revealed that lignin type significantly influences oxyalkylation process, with hydrolysis hardwood lignin (H-HW) exhibiting the highest reactivity due to its high syringyl hydroxyl content. Reaction optimization, including adjusting catalyst loading and reaction time, was crucial in achieving lignin polyols with desirable properties, such as reduced viscosity and appropriate hydroxyl values. The formulated PU flexible foam, produced by replacing 20% of petroleum-based polyols with optimized lignin polyol (Ligol), met all standard requirements for automotive seating applications. In contrast, foams developed using a combination of lignin polyol (20%) and soy polyol (30%) met all criteria except elongation at break, demonstrating superior compression force deflection compared to control foams. Therefore, incorporating lignin polyol offers a promising pathway to increase soy polyol content in flexible PU foams. However, further optimization is required to ensure the elongation at break meets seating application standards.

Chapter 4: Synthesis and Characterization of Lignin-Based Polycarbonate Polyols for Flexible Polyurethane Foam Application

Abstract

With the increasing demand for sustainable materials, lignin-based polyols offer a promising renewable alternative to traditional petroleum-based polyols in flexible polyurethane (PU) foams. This study focuses on synthesizing novel high-performance lignin-based polycarbonate polyols, via dimethyl carbonate transesterification chemistry. The resulting lignin polyols exhibited hydroxyl values ranging from 111 to 179 mg KOH/g and viscosities between 11,660 and 25,950 mPa·s, making them suitable for flexible foam formulation. An in-depth structural analysis using Nuclear Magnetic Resonance (NMR) confirmed the grafting of long polyether chains and the introduction of multiple carbonate linkages onto the lignin structure. Foams were formulated by replacing up to 60% of petroleum-based polyols with either synthesized lignin polyol or a mixture of lignin and soy polyols. Formulated foams demonstrated superior mechanical properties, including enhanced tensile strength and load-bearing properties, compared to petroleum-based foams. Additionally, the foams exhibited improved thermal stability, shock absorption, and biodegradability.

4.1 Introduction

Polyurethane (PU) flexible foams are widely used in various industries due to their versatility, lightweight nature, and excellent mechanical properties.[3] The performance of PU flexible foams is heavily influenced by the type of polyol used in their synthesis, with polycarbonate polyols emerging as a superior alternative to traditional polyester and polyether polyols.[4] Polycarbonate polyols offer enhanced mechanical strength,[141–143] superior resistance to hydrolysis,[144] improved thermal stability,[141,145,146] and impact resistance[147] making them particularly suitable for higher-end applications such as automotive seating, where durability and performance under varying environmental conditions are critical. In contrast, polyester polyols, though mechanically strong and resistant to oxidation, are prone to hydrolysis, while polyether polyols, despite their hydrolytic stability, often lack the mechanical strength and thermal resistance provided by polycarbonate polyols.[4] Consequently, polycarbonate polyols have received considerable attention as a high-performance alternative for flexible PU foam formulations.

Traditionally, the synthesis of polycarbonate polyols relied on phosgene-based processes that, while effective, raised significant safety and environmental concerns due to phosgene's toxicity.[4] Developing safer and more sustainable alternatives, such as dimethyl carbonate (DMC), has revolutionized polycarbonate polyols production.[148] DMC is a non-toxic, biodegradable reagent that can be derived from renewable resources, including carbon dioxide captured from the atmosphere and methanol, making it a more sustainable option.[149] Unlike phosgene, DMC does not require stringent safety measures during handling and enables cleaner and more efficient polycarbonate synthesis. Additionally, DMC promotes the introduction of carbonate linkages into polymer chains, enhancing the mechanical and thermal properties of the resulting polyols while maintaining processability.[150] This transition from phosgene to DMC aligns with the principles of

green chemistry and sustainable manufacturing, making DMC a preferred reagent for polycarbonate polyol synthesis.

Several studies have demonstrated the effectiveness of DMC in polycarbonate polyol production using 1,4 butanediol,[151,152] 1,6 hexanediol,[151,152] and isosorbide.[153] Foy et al.[154] synthesized linear aliphatic polycarbonate macro glycols using DMC and diols, showing that DMC could produce well-defined polyols with tailored molecular weights and functional properties suitable for PU applications. Similarly, Song et al.[151] prepared polycarbonate diols (PCDLs) through the reaction of DMC with diols using a $KNO_3/\gamma\text{-}Al_2O_3$ catalyst, demonstrating precise control over molecular weight and polymer architecture, which is critical for optimizing PU flexible foam properties. Further advancements in DMC-based polycarbonate synthesis were made by Kim et al.,[141] who developed carbonate-type macrodiols via base-catalyzed polycondensation of DMC with co-diols. Their study demonstrated an environmentally friendly approach to macrodiol synthesis leading to transparent, self-healing thermoplastic polyurethanes. Organo catalysts such as guanidines and amidines have also been explored in the synthesis of polycarbonate polyols due to their great catalytic activity and, in some cases, their bifunctional ability to activate both diol and diethyl carbonate making them an ideal catalyst.[152] Collectively, these studies establish DMC-based synthesis as a promising route for producing high-performance polyols with tunable properties for polyurethane applications. [141,151,154]

Despite these advancements, limited effort has been made to incorporate biobased components in polycarbonate polyols. To date, the few reported biobased polycarbonate diols in literature have primarily been derived from isosorbide,[153,155] highlighting a significant opportunity for further development. Notably, the integration of lignin, a renewable and aromatic biopolymer, into polycarbonate polyol synthesis remains unexplored. Lignin's rich hydroxyl functionality and rigid

structure offer a unique opportunity to enhance the sustainability and performance of polycarbonate polyols. Research on the application of lignin in flexible polyurethane (PU) foams is still relatively limited, with only about 17 studies published to date. However, these studies demonstrate that lignin can significantly improve the thermomechanical properties of PU foams.[57–73] Therefore, incorporating lignin in polycarbonate polyol synthesis could provide an avenue to leverage the unique structural and functional properties of lignin, while reducing the reliance on petroleum-based raw materials such as 1,4 butanediol and 1,6 hexanediol which are commonly used in polycarbonate polyol production. The objective of this study is to synthesize and characterize lignin-based polycarbonate polyols and evaluate, for the first time, their suitability for flexible PU foam formulations.

4.2 Materials and Method

4.2.1 Materials

Huntsman Corporation generously supplied polyether polyol (MW 6000 Da, hydroxyl value 28 mg KOH/g), propylene carbonate, polymeric MDI (Rubinate M), gelation catalyst, and blow catalyst. Momentive Performance Materials provided siloxane surfactants, while Cargill supplied soy polyol (BIOH 2828). Analytical reagents, including cyclohexanol (99% purity), pyridine (HPLC grade), and 2-chloro-4,4,5,5-tetramethyl-1,3,2-dioxaphospholane (TMDP), were purchased from Sigma-Aldrich. Additionally, chromium (III) acetylacetonate, deuterated chloroform, HPLC-grade tetrahydrofuran, dimethyl carbonate (99% purity), potassium carbonate, polyethylene glycol, and acetic anhydride were obtained from Fisher Scientific. Tokyo Chemical Industry (TCI) supplied 1,8-Diazabicyclo [5.4.0] undec-7-ene (DBU). Acid hydrolysis hardwood lignin sample was obtained from Sweetwater Energy, with its properties detailed in **Tables C1** and **C2** (Appendix C).

4.2.2 Lignin Characterization

Various analytical techniques were employed to characterize lignin and assess its composition and properties. The ash content was measured following the TAPPI T 212 om-93 standard method, where lignin samples were heated at 525 °C for 4 hours, and the residual mass was recorded. Elemental composition was analyzed using Inductively Coupled Plasma Atomic Emission Spectroscopy (ICP-AES). The hydroxyl group content was determined via Phosphorus-31 Nuclear Magnetic Resonance (^{31}P NMR) spectroscopy, following established protocols. [126–129] Molecular weight distribution was evaluated using gel permeation chromatography (GPC), with prior acetylation to improve solubility in tetrahydrofuran (THF). All analyses were performed in triplicate, and the average values were reported.

4.2.3 Polyol Synthesis

Step 1: Propylene carbonate (PC) oxyalkylation

Oven-dried acid hydrolysis hardwood lignin was mixed with 2 equivalent molar ratio of propylene carbonate (with respect to the total hydroxyl value of lignin) in a Model 4524 Parr Reactor (0.6L capacity). Polyethylene glycol (molecular weight 200 Da) was added to the mixture to obtain 30% lignin content. 1,8-Diazabicyclo [5.4.0] undec-7-ene (0.05 molar equivalent of total hydroxyl value of lignin) was added to the mixture. The reactor was purged with nitrogen for 5 minutes to completely remove air trapped in the reactor. The mixture was heated at 150 °C for 1.5 hours, mixing at 400 rpm. Gas outlet valve was opened occasionally to vent carbon dioxide produced from the reaction to avoid pressure build-up in the reactor. The reaction mixture was allowed to cool to room temperature before the transesterification step was carried out.

Step 2: Dimethyl Carbonate (DMC) Transesterification

The mixture obtained from the oxyalkylation step was heated with 0.5 eq. of dimethyl carbonate (with respect to the total hydroxyl value of polyol mixture in step 1) at 150 °C under reflux for 30 minutes. At the end of the reaction, methanol and unreacted DMC were removed completely at 90 ^{o}C under reduced pressure using a vacuum pump. The process of polyol synthesis was repeated for polyethylene glycol with molecular weight 400, 600 and 1000 Da.

4.2.4 Polyol Characterization

4.2.4.1 Hydroxyl Value (OHV)

The hydroxy contents of the polyol were measured using ^{31}P-NMR spectroscopy, using a method similar to that used for lignin characterization. The hydroxyl value (OHV), measured in mg KOH/g, of the polyol was computed by multiplying the total hydroxyl content (mmol/g) by 56.1.

4.2.4.2 Viscosity

The lignin viscosity of developed polyols was assessed at ambient temperature employing a Discovery HR-1 hybrid rheometer manufactured by TA Instruments. A 40 mm stainless steel Peltier plate geometry with a 1 mm gap was utilized, with samples sandwiched between the plates and trimmed before analysis. Viscosity measurements were conducted under a constant shear rate of 50 s^{-1}, with the recorded viscosity representing the average value over 60 seconds.

4.2.4.3 Modified lignin content

The quantification of modified lignin content in the polyol at the end of PC oxyalkylation reaction was conducted gravimetrically. Initially, the mass of a dry 50 mL beaker and a ceramic filtration device, with a pore size of 10-15 µm, was determined. Subsequently, 1 g of each polyol was combined in a beaker with 20 mL of acidified water (pH 2) and vigorously agitated until the modified lignin precipitated entirely. Following precipitation, the mixture was subjected to vacuum filtration using ceramic filters. The resulting samples were left to dry overnight in a vacuum oven at 85 °C and subsequently cooled in a desiccator. The mass of the dry-modified lignin was computed by subtracting the mass of the dry ceramic filter from the combined dry mass of the lignin and filter. Consequently, the modified lignin content was calculated using equation (4.1).

$$Modified\ lignin\ content\ (\%) = \frac{modified\ lignin\ mass}{lignin\ polyol\ mass} \times 100 \qquad [4.1]$$

4.2.4.4 Chemical Structural Analysis

The oxyalkylation and transesterification reaction were confirmed using FTIR, ^{1}H, ^{13}C, HSQC, and HMBC NMR experiments. Samples for NMR analysis were prepared using the following protocol: 50 mg of 1,3,5 trioxane was dissolved in 1 mL of the solvent (deuterated dimethyl sulfoxide (DMSO-d_6)) to prepare an internal standard solution. Approximately 40 mg of the synthesized lignin polyol was dissolved in 0.6 mL of the solvent, and the mixture was mixed for 30s in a vortex at 3000 rpm. Finally, 100 μL of the internal standard solution was then added, and vortexed for 30s at 3000 rpm to produce a uniform solution. 650 μL of the final mixture was then transferred to a 5mm Wilmad NMR tube. The NMR solution was analyzed in an Agilent DDR2 500 MHz NMR spectrometer equipped with 7600AS autosampler, running VnmrJ 3.2 A. For lignin polyol samples, the following parameters were used: ^{1}H NMR (1s relaxation delay and 16 scans), ^{13}C NMR (2 s relaxation delay and 5000 scans), HSQC (1.5 s relaxation delay and 8 scans), and HMBC (2 s relaxation delay and 16 scans). For precipitated lignin samples, the following parameters were used: ^{1}H NMR (4 s relaxation delay and 128 s scans), ^{13}C NMR (2 s relaxation delay and 8000 scans), HSQC (1.5 s relaxation delay and 64 scans), and HMBC (2 s relaxation delay and 40 scans). The infrared spectra of synthesized lignin polyols were measured with a PerkinElmer Spectrum Two FT-IR Spectrometer, in Attenuated Total Reflectance (ATR) mode. Few drops of lignin polyols were placed on the ATR crystal and data was collected using 32 scans. Spectrum was processed with a baseline correction and noise-reduction algorithm after data collection.

4.2.4.5 Glass Transition Temperature (Tg)

Differential Scanning Calorimetry (DSC) of precipitated lignin samples were conducted using a standard aluminum pan and lid. Approximately 8 mg of each sample was weighed and analyzed using a TA DSC instrument under nitrogen. The testing protocol involved equilibrating the sample at 25°C, ramping the temperature at 20 °C/min to 200 °C, cooling at 20 °C/min back to 25 °C, holding isothermal for 10 minutes, and then ramping again at 20°C/min to 230°C.

4.2.5 Foam Formulation

Foams with varying amounts of lignin polyol were formulated for characterization. 10, 20, 30, and 40 part per hundred polyols (pphp) of the petroleum-based polyols were replaced with the lignin polyol to synthesize flexible polyurethane foams. Foams containing both synthesized lignin polyol and soy polyol were also formulated to increase the biobased content. The Isocyanate index was set at 100 for all foams. In a 12-ounce paper cup, 100 g of polyol blend, water (3 pphp), gelation catalyst (0.65 pphp), blow catalyst (0.32 pphp), and surfactants (1.5 pphp) were mixed at 3000 rpm using a high-speed mixer for two minutes. Finally, the calculated amount of isocyanate was added using a disposable plastic syringe and mixed at 3000 rpm for 3-5 seconds. The mixture was then quickly poured into a silicone mold conditioned at 65 °C and left to cure at room temperature for about 30 minutes before demolding. After removing the foams from the mold, they were left to post-cure for 2 days at room temperature. Samples were cut into various sizes required for mechanical testing **(Figure C5,** Appendix C**)** devoid of skin.

4.2.6 Foam Characterization

4.2.6.1 Mechanical Properties

The foam samples were cut into mechanical testing specimens without any skin present. These samples were then subjected to property characterization using an Instron Universal Testing

machine based on the ASTM D3574 test standard [131] to assess their physical and mechanical properties, including density, compression force deflection (CFD), support factor, tensile strength, ultimate elongation at break, and tear strength. The values obtained were then compared to the control foams made without lignin polyol and the Original Equipment Manufacturer (OEM) standard requirements for automotive seating applications. Six replicates of each foam sample were tested, and the average and standard deviations were reported.

4.2.6.2 Scanning Electron Microscopy

The morphology of foam samples was investigated using scanning electron microscopy (SEM). Samples were cut perpendicular to the foam rise direction. Then, the samples were mounted using carbon tape and made conductive by sputter coating with gold nanoparticles in an argon atmosphere. Images were collected on a JEOL 6610LV SEM with an accelerating voltage of 10 kV and a spot size set to 30. Images were collected at 50x, 100x, and 1000x magnification. Open cell diameters of foams were then measured using ImageJ. The cell diameter of several positions on the foam was determined and the average reported.

4.2.6.3 Impact Test

The dynamic characteristics of foams are essential information in comfort designs and shock absorption of automobile seats. Cushion curves show the deceleration level in g's (e.g. 9.81 m/s^2) versus static stresses. A drop test machine was used to perform the required drop tests for generating cushion curves according to ASTM D1596-14. Foam samples measuring 2 by 4 inches with a thickness of 1 inch, giving a top area of 8 square inches, were used. An accelerometer attached to the drop platen was used to record the shock pulse during each drop scenario. The static stress, σ_s, for this impact event was expressed as equation (4.2):

$$\sigma_s = \frac{W}{A} \qquad [4.2]$$

where W is the weight of the platen, and A is the area. Then, the weight of the platen was increased from 3.5 lbs to 5 lbs in 0.5 lb increments, and each weight was dropped from a height of 6 inches. Since the samples were relatively small, a 6-inch height was opted to avoid excessively fast impacts. The peaks of these pulses were connected to generate a cushion curve, which represents the shock absorption capacity of the foam. Typically, a new sample is used for each test, and tests are repeated five times according to ASTM D1596. This would require a large number of samples, especially when varying both weight and height. However, due to the limited number of samples, foams were reused multiple times.

4.2.6.3.1 Impact Tester Design

The platens of the drop tester model (Lansmont Model 23) were too heavy for testing small foam samples. A smaller drop tester was designed using machine design principles and techniques. Several design drawings were created using SolidWorks software and were analyzed for optimization. The natural frequency of the platen was estimated using Finite Element Method software, ABAQUS, to ensure the platen remains relatively flat during the impact. Two flanges with internal ball bearings were used to facilitate the drop and minimize friction between the parts. **Figures C6 and C7** (Appendix C) show the designed drop tester used in this study.

4.2.6.3.2 Limitations

Due to limited resources in foam creation, the recommended specifications in ASTM D1596 (e.g., a minimum top foam area of 4 by 4 inches) were not fully adhered to. Additional testing with unused samples is necessary, including trials at different drop heights, to accurately assess the full shock absorption capacity of the developed lignin-based foams.

4.2.6.4 Biodegradation Study

The aerobic biodegradation of control, LP40, and LP30-SP30 foams was evaluated in a compost under controlled composting conditions (58 ± 2 ºC and 50 ± 5% relative humidity (RH)) by analysis of evolved CO_2 using an in-house built direct measurement respirometer (DMR), equipped with a non-dispersive infrared gas analyzer (NDIR) following ASTM and ISO standards. [156–159]

Compost (manure straw) was acquired from the Michigan State University (MSU) Composting Facility (East Lansing, MI, U.S.) and its physiochemical properties are summarized in **Table C3** (Appendix C). The compost was sieved through a 10-mm screen to remove inert and large materials and conditioned at approximately 58 ºC until use. Deionized water was added to increase the moisture content of the compost (up to 50%). Additionally, the physiochemical parameters (see **Table C4** in Appendix C) of the compost were determined.

Each bioreactor (1.9 L) was filled with 400 g of compost, then, 8 g of the foam sample, cut into small equal pieces, was added to each bioreactor for testing. To maintain the optimal conditions for the biodegradation process, deionized water was injected into each bioreactor twice a week, and after each water injection, the bioreactor was shaken to distribute the water and avoid clustering. During the operation of the test, air at 50 ± 5% RH flowed to each bioreactor, and the CO_2 evolved was collected and measured by the near-infrared sensor at regular intervals. The CO_2 evolved from the blank bioreactor (without foam) was considered as the background signal. This value was subtracted from the amount of CO_2 produced by each sample bioreactor to calculate the biodegradation of each sample, where the % biodegradation is the total amount of carbon molecules converted to CO_2. It is calculated according to the equation (4.3) below. [160]

$$\%\, Mineralization = \frac{(CO_2)_t - (CO_2)_b}{M_t \times C_t \times \frac{44}{12}} \times 100 \qquad [4.3]$$

where the numerator is the difference between the average of the three bioreactors' cumulative mass of CO_2 evolved for the sample $(CO_2)_t$, and the average CO_2 evolved from the three blank bioreactors $(CO_2)_b$. The denominator represents the theoretical amount of CO_2 able to be produced by the sample. M_t is the total mass of the sample, C_t is the proportion of carbon present in that sample as determined by CHNS/O Analyzer, and 44 and 12 are the molecular mass of CO_2 and the atomic mass of the carbon, respectively. **Figures C8** and **C9** (see Appendix C) present an illustration of the biodegradation study.

4.2.6.4.1 Elemental Analysis

The carbon content of the different test materials was determined by elemental analysis using a PerkinElmer 2400 Series II CHNS/O Elemental Analyzer (Shelton, CT, USA). The test used about 2 milligrams of each sample weighed in small capsules. A blank, and standard values to establish the k-factors were measured before assessing the samples. Results of elemental analysis can be found in **Table S3** (Appendix C).

4.3 Results and Discussion

4.3.1 Chemical Structural Analysis

A comprehensive structural analysis was performed on the synthesized lignin polyol during both the propylene carbonate (PC) oxyalkylation and dimethyl carbonate (DMC) transesterification steps (**Figure 4.1**). This analysis offered deeper insights into the reaction mechanisms and confirmed the configuration of repeating units in the resulting polycarbonate polyol. NMR analysis of the crude lignin polyol after the oxyalkylation reaction indicated that it was composed of oxyalkylated lignin, polyethylene glycol (PEG) and its adduct (formed from the reaction between PEG and PC), unreacted PC, and some propylene glycol (PG). It also verified the reaction between PEG and DMC, demonstrating the successful introduction of carbonate linkages and a significant

reduction in total hydroxyl content. Detailed information on the NMR analysis of the lignin polyol (unprecipitated) is provided in the Appendix C. Although the NMR provided detailed information about the structural changes in PEG, its resolution was insufficient to reliably assess modifications in the lignin backbone due to the complex mixture in the crude material. As a result, lignin precipitation was necessary to isolate and further investigate the structural changes.

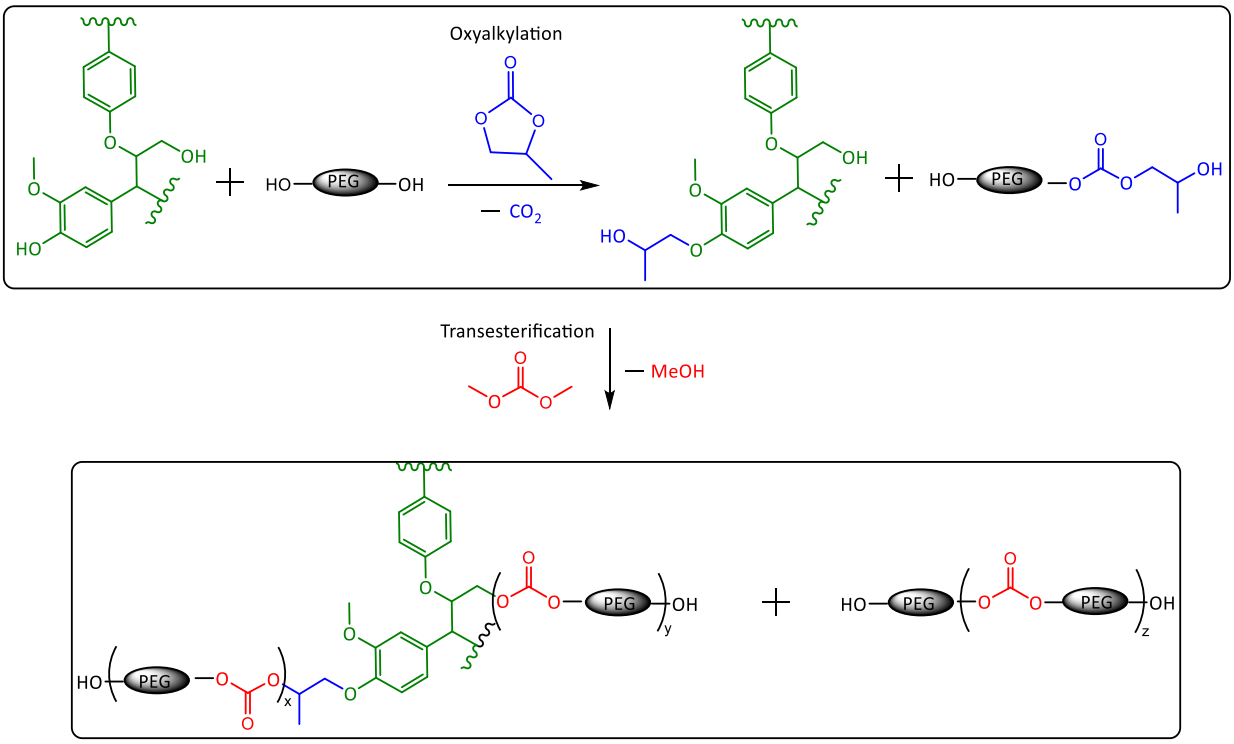

Figure 4.1: Synthesis of lignin-based polycarbonate polyol via propylene carbonate oxyalkylation and dimethyl carbonate transesterification reaction.

The precipitation of modified lignin fractions (oxyalkylated lignin (OL) and transesterified lignin (TL)) was crucial for gaining clearer insight into the structural changes lignin undergoes during propylene carbonate oxyalkylation and dimethyl carbonate transesterification reactions. ^{31}P NMR analysis of precipitated OL, as shown in **Figure 4.2**, revealed a significant reduction in phenolic (137 to 144.6 ppm) and carboxylic (134 to 135.9 ppm) hydroxyl groups. This was expected, as these groups reacted with propylene carbonate (PC). Interestingly, a primary aliphatic hydroxyl

group from PEG was also detected around 147 ppm, suggesting a possible PEG grafting onto lignin. This peak further intensified after the transesterification reaction indicating additional incorporation of PEG on the lignin structure.

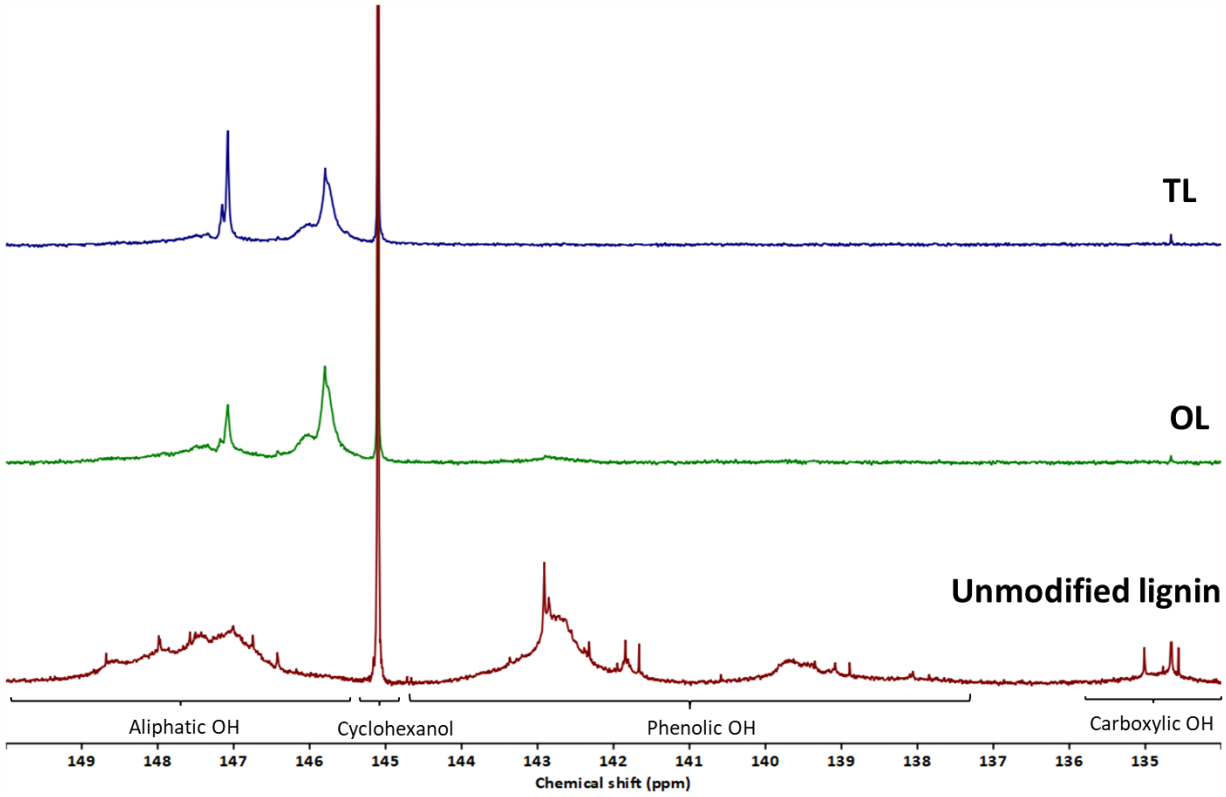

Figure 4.2: Expansion of a ^{31}P NMR spectra of unmodified, precipitated propylene carbonate oxyalkylated (OL), and dimethyl carbonate transesterified (TL) lignin. OL and TL were precipitated from Ligol A. Samples were phosphitylated prior to analysis.

Notably, a small amount of phenolic hydroxyl groups remained in OL but was undetectable after transesterification. Their absence in TL indicates that the lignin-PC reaction may have continued during the transesterification step. Even though the phenoxide ion favors the reaction with PC, it's reaction with DMC is also possible. Overall, the total hydroxyl content decreased from 5.43 mmol/g in unmodified lignin to 3.61 mmol/g in OL and further to 2.88 mmol/g in TL,

demonstrating the progressive modification of lignin's hydroxyl functionalities, making it more suitable for PU flexible foam and some coating applications.

^{1}H NMR analysis of OL, as presented in **Figure 4.3**, showed a new broad methyl proton signal at 1.13 ppm, which was absent in unmodified lignin. This signal is attributed to methyl protons from the hydroxypropyl units grafted onto lignin (peak 1), formed through the reaction of lignin's hydroxyl groups with PC. Additionally, a terminal methylene proton signal was detected in OL around 3.5 ppm (peak 5) which may have originated from grafted PEG during the oxyalkylation reaction.

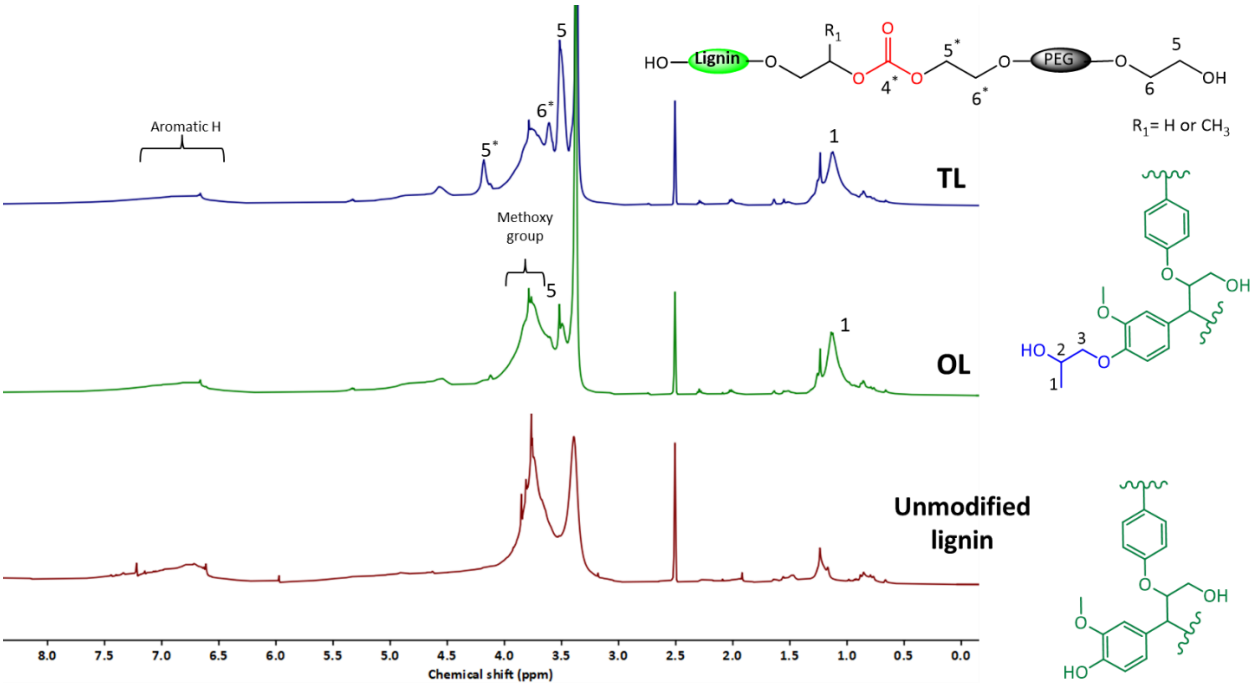

Figure 4.3: Expansions of ^{1}H NMR spectra of unmodified, precipitated propylene carbonate oxyalkylated (OL), and dimethyl carbonate transesterified (TL) lignin. OL and TL were precipitated from Ligol A.

The success of the oxyalkylation reaction was further confirmed by the appearance of hydroxypropyl carbon signals in the ^{13}C NMR spectrum of OL at 20.46 ppm, 65.23 ppm, and 78.75 ppm (**Figure 4.4**). The absence of the carbonyl carbon signal around 154 ppm in OL indicates that the aliphatic hydroxyl groups in lignin did not participate in the reaction with PC as they tend to react with the carbonyl carbon over that of the alkylene carbon. Instead, the reaction selectively targeted more acidic functional groups, such as carboxylic and phenolic hydroxyl groups, consistent with similar findings in the literature.[124] Kuhnel et al.[93] also reported that the reaction between lignin's aliphatic hydroxyl groups and PC to form carbonate linkages can be achieved to some extent under high propylene carbonate concentrations, prolonged reaction times, and the presence of a potassium carbonate catalyst.

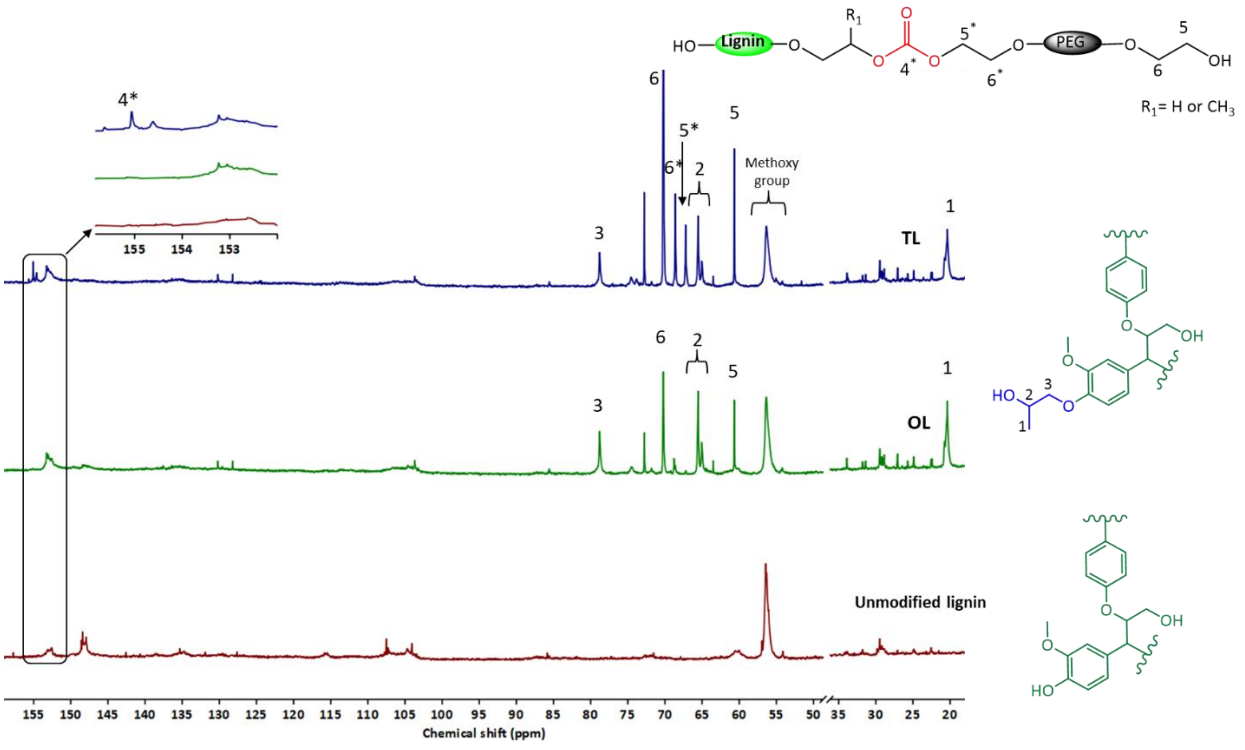

Figure 4.4: Expansion of ^{13}C NMR spectra of unmodified, precipitated propylene carbonate oxyalkylated (OL), and dimethyl carbonate transesterified (TL) lignin. OL and TL were precipitated from Ligol A.

Three new methylene carbon signals at 60.6 ppm (peak 5), 70.2 ppm (peak 6), and 72.8 ppm, consistent with a long polyether PEG-like chain, were detected in the ^{13}C NMR spectrum of OL, aligning with observation from the ^{31}P NMR spectrum. These signals persisted even after multiple washings of OL with distilled water. Since this reaction was performed in the presence of PEG, it's likely that PEG was incorporated into OL. Indeed, when the oxyalkylation reaction was repeated without PEG, these methylene carbon signals were absent, as seen in **Figure C1** (Appendix C), confirming that their presence was directly linked to the inclusion of PEG in the reaction.

Figure 4.5 shows a schematic representation of the proposed reaction mechanism responsible for PEG grafting onto lignin during the oxyalkylation step. In summary, the formation of this structure likely involves the following steps: (i) PEG reacts with PC, resulting in a PEG adduct with a carbonate linkage, terminated by a hydroxyl group. (ii) Lignin hydroxyl groups react with the PEG adduct, either at the carbonyl site or the alkyl site. A carbonyl attack, likely initiated by aliphatic hydroxyl groups, leads to the formation of a carbonate linkage, with PG as the leaving group. An alkyl attack, likely involving phenolic hydroxyl groups, produces an ether linkage, with PG and carbon dioxide as byproducts. The high intensity of the methylene carbon signal around 70 ppm and the absence of carbonyl carbon around 155 ppm in OL in **Figure 4.4** suggests that the alkyl attack was the predominant reaction pathway, resulting in the grafting of PEG onto lignin during the oxyalkylation step. Additionally, the presence of PG in the oxyalkylation reaction mixture further substantiates the proposed reaction mechanism.

The inclusion of PEG provides an additional reactant for PC, enhancing its consumption beyond what occurs through lignin oxyalkylation reaction and reducing the amount of unreacted PC in the lignin polyol. PEG was chosen as the co-polyol due to its capacity to solubilize lignin, and the fact

that its biobased alternative is commercially available. Furthermore, the incorporation of PEG into lignin's structure during oxyalkylation presents a great opportunity to reduce lignin's inherent rigidity. The linear polyether chains in PEG impart flexibility, which is essential for formulating flexible PU foam. Also, due to the primary aliphatic hydroxyl group present in the grafted PEG, it further helps facilitate lignin's reaction with DMC.

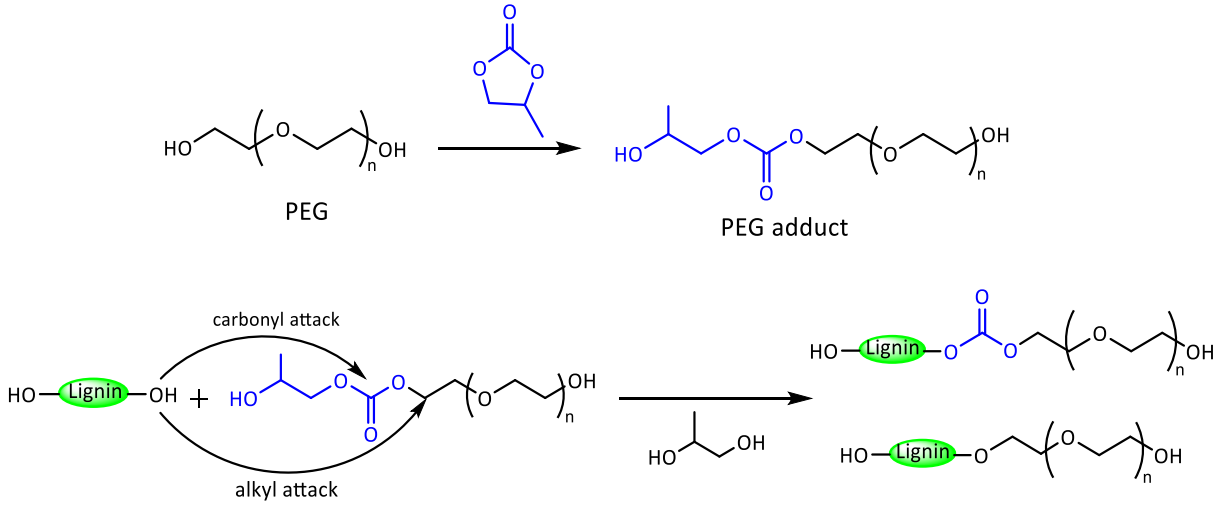

Figure 4.5: Schematic representation of the possible reaction mechanism leading to the grafting of PEG on lignin in the propylene carbonate oxyalkylation reaction step.

Analysis of TL revealed the emergence of two distinct methylene proton peaks at 3.61 ppm (peak 6*) and 4.18 ppm (peak 5*) in the ^{1}H NMR spectra **(Figure 4.3)**, which are directly bonded to carbons at 68.70 ppm and 67.1 ppm, respectively, as identified in the HSQC spectra **(Figure 4.6a)**. ^{13}C NMR analysis **(Figure 4.4)** showed a new carbonyl carbon peak at 155.1 ppm (peak 4*). This peak has a cross-peak with methylene protons at 4.18 ppm (peak 5*), as seen in the HMBC spectra **(Figure 4.6b)**, thereby confirming incorporation of carbonate linkages in TL. The methylene proton at 4.18 (peak 5*) ppm also has a cross-peak with a methylene carbon at 68.70 ppm, indicating that a PEG chain has been grafted onto the lignin macromolecule via a carbonate linkage. Additionally, the increased intensity of the methylene carbon signal at 60.6 ppm (peak 5),

associated with the terminal CH_2 group adjacent to a primary hydroxyl group, and the methylene carbon at 70.2 ppm (peak 6) further supports the successful grafting of PEG via the transesterification reaction. Notably, there was no cross-peak between the methine proton of OL at 3.79 ppm and the carbonate carbonyl at 155.1 ppm, indicating that the hydroxypropyl units in OL did not participate in the transesterification reaction. This implies that secondary aliphatic hydroxyl groups were less reactive towards dimethyl carbonate under current reaction conditions.

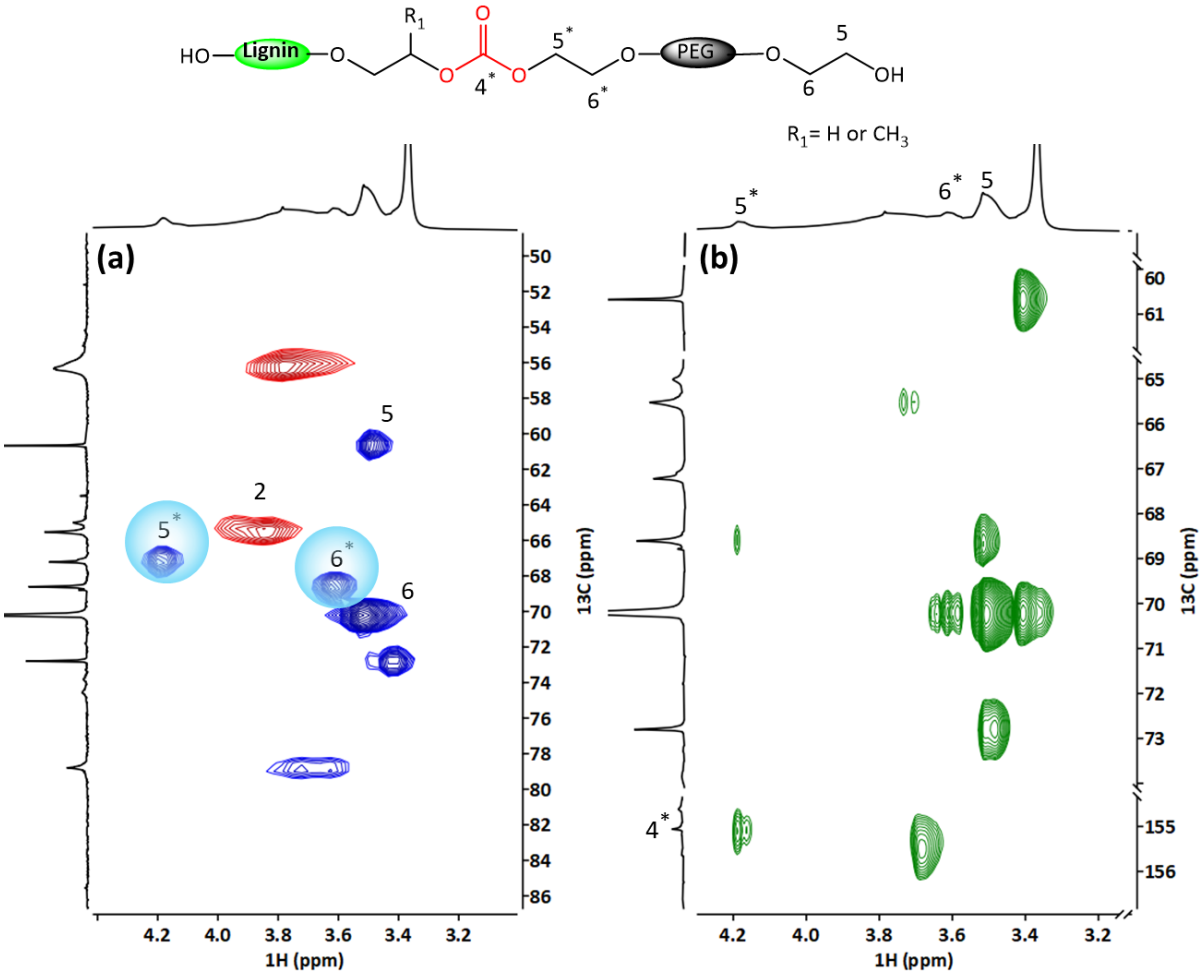

Figure 4.6: Expansion from (a) HSQC and (b) HMBC NMR spectra of precipitated dimethyl carbonate transesterified (TL) lignin.

Differential Scanning Calorimetry (DSC) analysis, summarized in **Table 4.1**, provided additional evidence of structural modifications. The glass transition temperature (*Tg*) of lignin decreased from 156 °C to 109 °C after oxyalkylation, representing a 30% reduction. This reduction is attributed to grafting hydroxypropyl units and PEG onto the lignin structure. The *Tg* further decreased significantly to 62 °C after the transesterification step due to the incorporation of additional long, flexible polyether PEG chains. Depending on the molecular weight of the PEG used, the *Tg* of OL ranged from 88 to 109 °C, while the *Tg* of TL ranged from 60 to 65 °C. Notably, the PEG molecular weight had the greatest impact during the oxyalkylation step, with higher molecular weights resulting in lower *Tg* values. These findings highlight the potential for tailoring lignin's thermal properties for applications requiring lower *Tg* values, such as PU coatings and flexible foams.

Table 4.1: Glass transition temperature (*Tg*) of precipitated propylene carbonate oxyalkylated (OL) and dimethyl carbonate transesterified (TL) lignin based on the molecular weight (MW) of polyethylene glycol (PEG) employed in the polyol synthesis. $TL_{PEG1000}$ resulted in a gelled polymer. *Tg (unmodified lignin) = 160 ± 5.5 °C.*

PEG MW (Da)	**OL (**°C)	**TL (**°C)
200	106 ± 3.8[a]	62 ± 2[a]
400	109 ± 6.0[a]	60 ± 2[a]
600	89 ± 0.9[b]	65 ± 4[a]
1000	96 ± 1.1[b]	-

Within a column, values with different letters are significantly different at P ≤ 0.05 (Tukey's test).

4.3.2 Lignin Polyol Properties

The transesterification process involving oxyalkylation derivatives and DMC was observed to be significantly influenced by both reaction time and the quantity of DMC used. Initial experiments utilizing 1 equivalent of DMC at 150 °C for 1 hour yielded a highly viscous gel-like polymer that could not be used in foam formulations. This outcome was anticipated due to lignin's high functionality, which could lead to crosslinking with PEG or another lignin chain, resulting in the formation of high molecular weight polycarbonate polyols. Even when the reaction time was reduced to 0.5 hours while keeping the temperature and DMC quantity constant, the resulting materials exhibited significantly high viscosities. However, by decreasing the amount of DMC to 0.5 equivalent and maintaining a reaction time of 0.5 hours, a product with a workable viscosity (11,660 to 25,950 mPa.s) was obtained, suitable for further characterization and foam formulation. This indicated that the transesterification reaction was sensitive to both reaction time and the amount of DMC used in the reaction.

PEG with various molecular weights (200, 400, 600, and 1000 $gmol^{-1}$) was used further to achieve a polycarbonate polyol with lower hydroxyl value. The properties of synthesized lignin polyols are summarized in **Table 4.2**. It was observed that an increase in the molecular weight of PEG led to a reduction in the total hydroxyl value. This result was expected as longer chains, such as PEG 1000 (112.2 mg KOH/g), tend to have a much lower hydroxyl value than PEG 200 (561 mg KOH/g). Although PEG 1000 yielded a polyol with a hydroxyl value within the acceptable flexible foam polyol range (157 mg KOH/g) following the oxyalkylation process, it exhibited excessively high viscosity and incomplete phenolic OH conversion. This might be attributed to the elevated viscosity of the medium, which may have restricted the reaction rate. The presence of phenolic hydroxyl groups in modified lignin is undesirable due to their poor reactivity towards isocyanate.[79]

Hence, PEGs with lower molecular weights (≤ 600 Da) are more suitable for this reaction, as they yielded a polyol with a moderately low hydroxyl value (111 to 179 mg KOH/g) and workable viscosities (≤ 25,000 mPa.s), ideal for PU flexible foam formulation. This presents an advantage as these low molecular weight PEGs (200, 400, and 600 Da) are the only biobased options available commercially.

Table 4.2: Modified lignin content (MLc), hydroxyl value (OHV, mgKOH/g), and viscosity after propylene carbonate oxyalkylation and hydroxyl value, hydroxyl value reduction (OHVr) and viscosity of lignin polyol after dimethyl carbonate transesterification reaction based on PEG molecular weight employed.

Polyol ID	PEG Mw	Oxyalkylation			Transesterification		
		MLc (%)	OHV	Viscosity (mPa.s)	OHV	OHVr (%)	Viscosity (mPa.s)
Ligol A	200	39 ± 2.1[a]	365	2,600 ± 30[a]	179	50.96	11660 ± 450[a]
Ligol B	400	35 ± 1.8[a]	266	7,550 ± 10[b]	151	43.23	16880 ± 750[b]
Ligol C	600	38 ± 2.0[a]	205	13,790 ± 430[c]	111	45.85	25950 ± 930[c]
Ligol D	1000	36 ± 1.1[a]	157	30,890 ± 500[d]	-	-	-

Within a column, values with different letters are significantly different at P ≤ 0.05 (Tukey's test).

Note:

1. Ligol D yielded a gelled lignin polyol after transesterification reaction.

2. Ligol A, B and C, after the transesterification step, were incorporated directly into the foam formulation.

4.3.3 Foam Properties

4.3.3.1 Mechanical Properties

A comparative study on the impact of lignin polyol on flexible PU foam properties was performed by formulating foams with Ligol A (179 mg KOH/g) due to its relatively lower viscosity. **Figure 4.7** shows the flexible PU foams produced by partially replacing petroleum-based polyols with synthesized lignin polyols. Foam mechanical properties, presented in **Figures 4.8 and 4.9**, were measured according to ASTM D3574 standard testing method and compared to the standard requirement for automotive seating applications *(red border lines)*. [61,161] As the lignin polyol content (in parts per hundred-gram polyol (pphp)) in the foams increases from 10% to 30%, there was no noticeable change in the density values; however, foams containing 40% lignin polyol exhibited the highest density. This result can be attributed to the higher concentration of lignin polyol in the polyol blend, which consequently necessitates a larger amount of isocyanate to react owing to its high hydroxyl value, thus resulting in a foam with a higher density. Additionally, the higher level of DBU, which catalyzes the gelation reaction may have prevented the foams from blowing enough,[73] thus resulting in denser foam. The densities of all foam samples fell within the range of 39 to 47 kg/m^3.

The compressive force deflection (CFD), indicating the foam's resistance to deformation under load, varied with the percentage of lignin polyol used, as seen in **Figure 4.8a**. Lignin-based foams generally exhibited higher compressive force deflection values compared to control foams, particularly as the lignin content increased. This suggests that lignin imparts greater rigidity and load-bearing capacity to the foams owing to its aromatic structure. The support factor, which is an indication of foam’s cushioning performance, was within 2.6 to 3.0, thus making it suitable for use in automotive seating applications.

Tensile strength, a measure of the foam's ability to withstand tension, varied depending on the lignin polyol content, as presented in **Figure 4.9a**. Foams with higher lignin content demonstrated higher tensile strength due to the robust aromatic structure of lignin and the relatively high hydroxyl value of lignin polyol. Elongation at break, representing the foam's flexibility, also varied with polyol composition. The lignin-based foams exhibited lower elongation at break values due to their inherent rigidity (aromatic structure) compared to the long aliphatic polyether chain of commercial polyol, which provides more flexibility.

Tear strength, indicative of the foam's resistance to propagating cracks, was also influenced by the lignin polyol concentration (see **Figure 4.9c**). Tear strength of lignin polyol foams remained the same as lignin content increased up to 20%, after which it increased slightly. The maximum tear strength (125 N/m) was recorded at 30% lignin polyol substitution. Beyond 30% replacement, the tear resistance of the foams dropped significantly. The dip in this property was expected due to lignin's crosslinked nature. The decrease in tear values of 40% lignin incorporation could also be attributed to an increased residual propylene carbonate content in the foam which may have plasticized it.

Hysteresis loss, related to energy dissipation during cyclic loading, varied with foam composition. Foams with higher lignin polyol content exhibited greater hysteresis loss and thus lower resiliency. This is due to the high rigidity provided by the aromatic structure of lignin and the relatively high hydroxyl value of the lignin polyol (179 mg KOH/g) compared to the petroleum-based polyol (28 mg KOH/g). The high energy dissipation rate of lignin polyol-based foams could benefit for sound and shock absorption applications where low resilient foams are required. This comparative analysis provides valuable insights for optimizing foam formulations for specific applications, balancing rigidity, flexibility, strength, and energy dissipation.

Building upon the mechanical performance of lignin-based foams, an additional strategy was explored to enhance the biobased content and further optimize foam properties by incorporating soy polyol. Soy polyol, derived from epoxidized and ring-opened soybean oil,[81] is a well-established biobased alternative with desirable reactivity and sustainability benefits. By blending lignin polyol with soy polyol, lignin-soy foams were formulated to achieve an improved balance between mechanical performance and renewable content (increasing the amount of soy-polyol in automotive seating foams beyond 10%). The LP20-SP20 and LP30-SP30 foams were designed to systematically evaluate the effect of soy polyol incorporation on foam's mechanical properties. The goal was to determine whether the inclusion of soy polyol could compensate for any mechanical drawbacks associated with the rigidity of lignin-based foams while maintaining the advantages of higher biobased carbon content.

As shown in **Figures 4.8** and **4.9**, the mechanical performance of lignin-soy foams was highly dependent on the soy polyol loading within the foam. At low soy polyol content, as in LP20-SP20, most mechanical properties remained unchanged compared to the pure lignin polyol-based foam (LP20). At higher soy polyol content, as in LP30-SP30, slight reductions were observed in CFD and tensile strength, however, these properties still met the standard requirement for seating application. Hysteresis loss remained unchanged, but tear strength fell below the standard range ($\geq$ 100 N/m) necessitating the need for further optimization. The decline in tear strength can be attributed to the structural differences between the soy polyol employed and the conventional polyether polyols they replace. Due to its secondary aliphatic hydroxyl groups, soy polyol exhibits lower reactivity towards isocyanates than the primary hydroxyl groups in petrochemical polyether polyols. Additionally, the mid-chain hydroxyl positioning introduces steric hindrance, limiting its ability to react with isocyanates effectively. Another contributing factor is soy polyol's relatively

low molecular weight, which reduced elongation at break. The decrease in tear strength observed in soy-based flexible PU foams have also been reported by Sonnenschein et al.,[113] supporting these findings. While the combination of lignin polyol and soy polyol helps increase the soy content to 30%, the adoption of soy-polyols with primary hydroxyl groups could offer a promising pathway to further improve foam properties and increase the biobased content in the final foam. **Figure 4.9d** presents the calculated biobased content of the developed flexible PU foams. The LP 40 foams exhibited a biobased content of 9%, primarily originating from lignin, while the LP30-SP30 foams showed a higher content of 25% due to the incorporation of soy polyol. These values could be increased to 20% (LP40) and 35% (LP30-SP30) by using biobased PEG in the polyol synthesis and selecting lignin polyol with the lowest hydroxyl value (Ligol C) for the foam formulation.

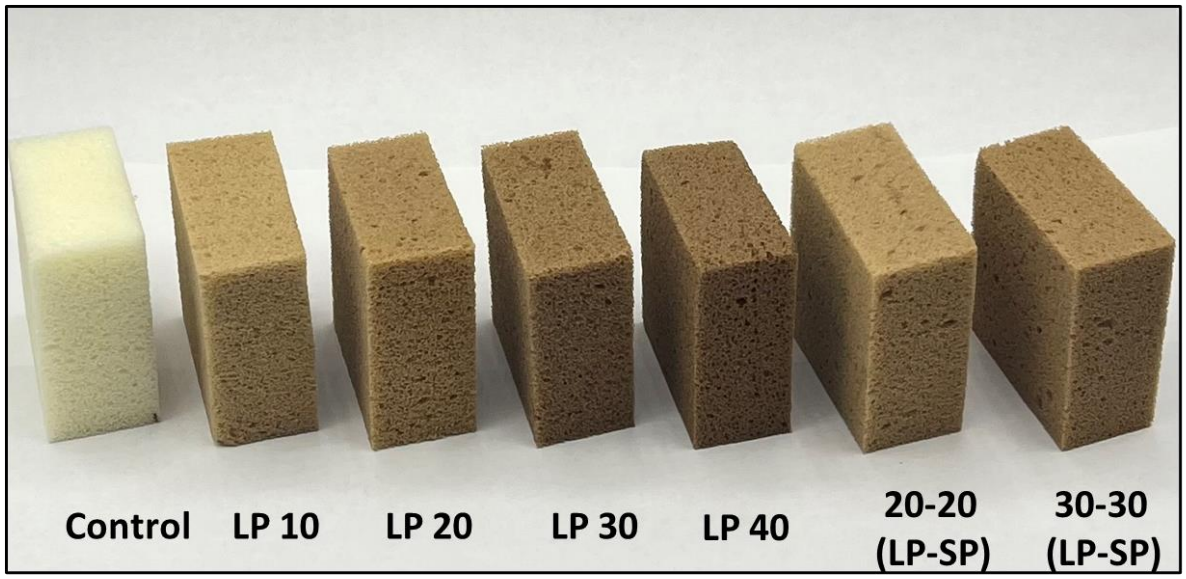

Figure 4.7: Flexible PU foams produced by replacing up to 40% of petroleum-based polyols with synthesized lignin polyol (LP) and up to 60% with a combination of LP and soy polyol (SP).

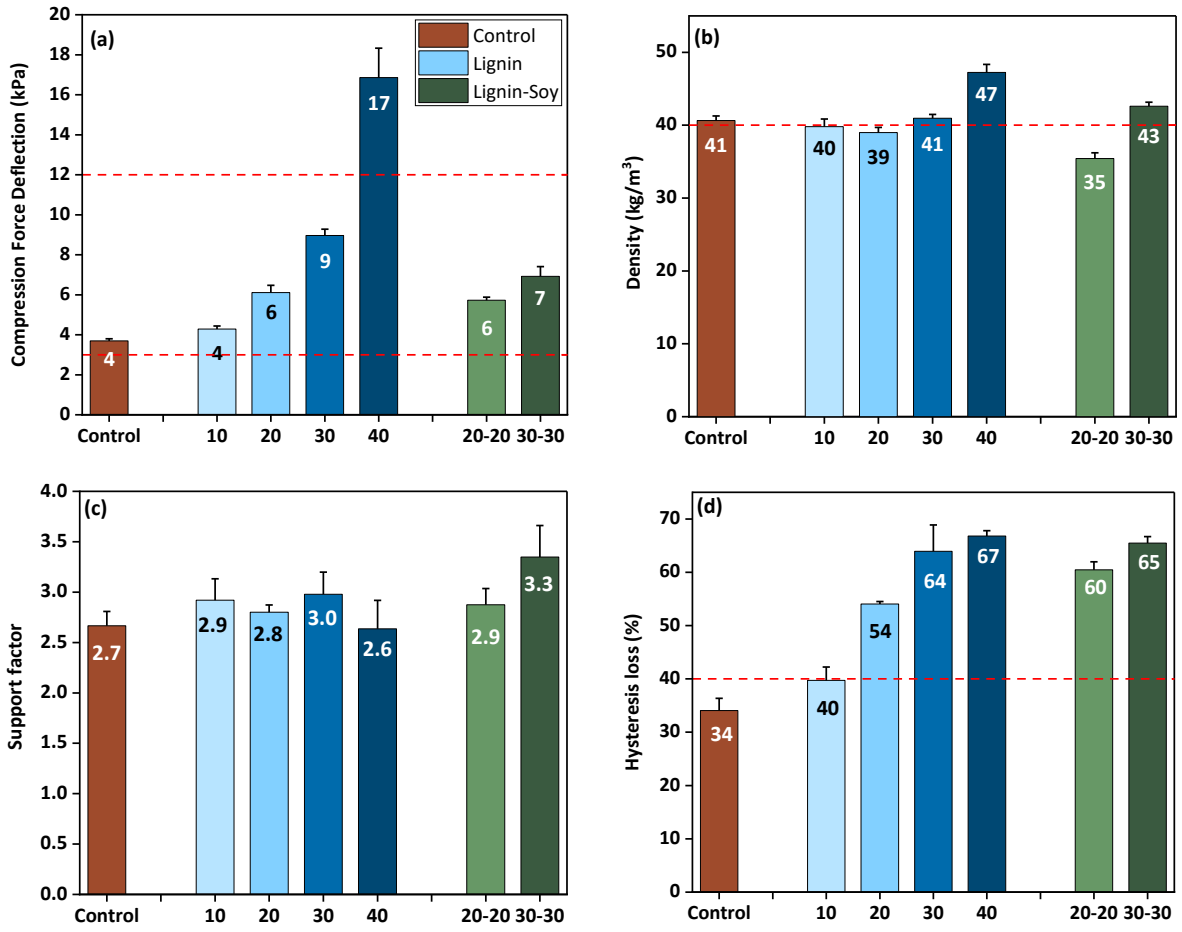

Figure 4.8: Mechanical properties of lignin polyol (LP)-based PU flexible foams (up to 40% petroleum-based polyol replacement) and lignin-soy polyol (LP-SP) foams as measured by ASTM D3574 test method: (a) compression force deflection at 50% strain (b) density (c) support factor and (d) hysteresis loss. All lignin-based foams were formulated with Ligol A.

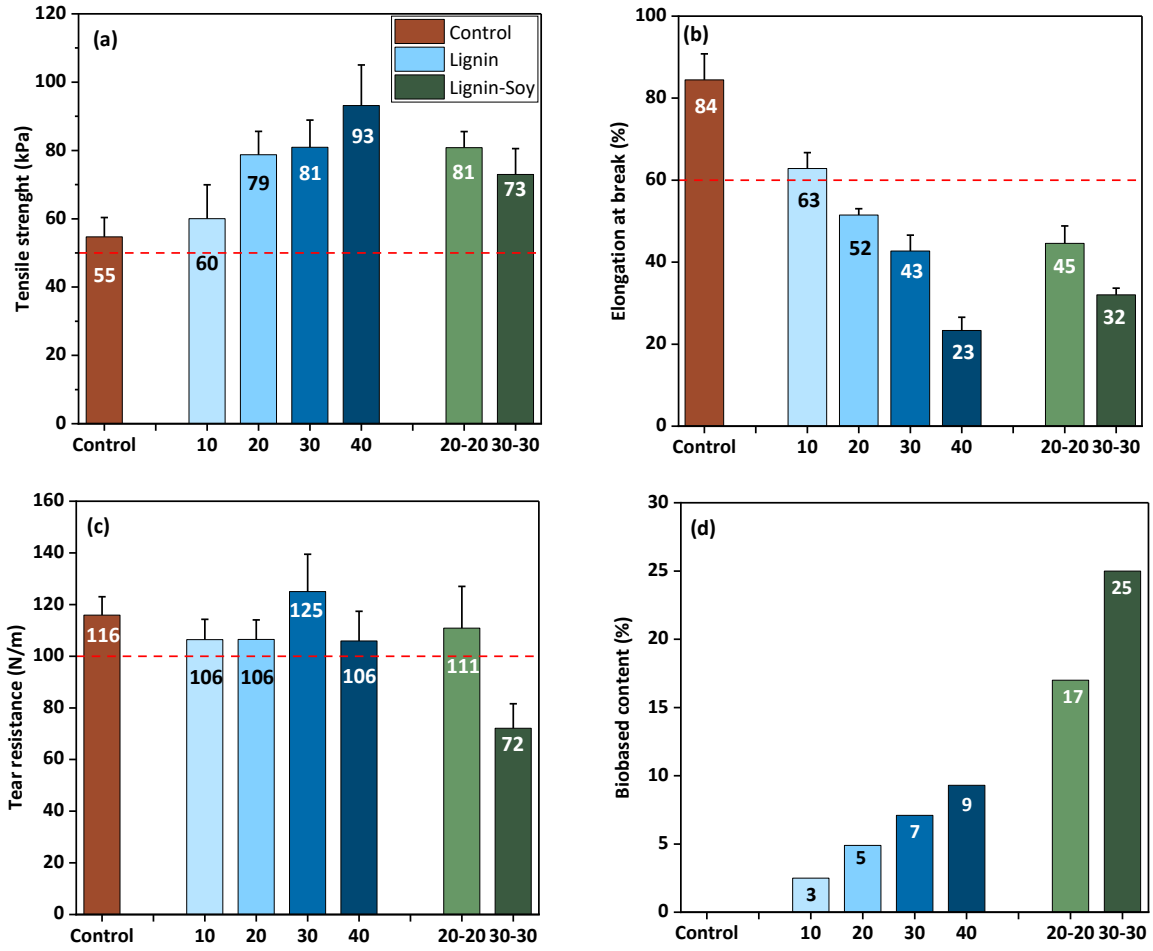

Figure 4.9: ASTM D3574 measured (a) tensile strength, (b) ultimate elongation at break, (c) tear strength, and (d) calculated biobased content of developed lignin polyol (LP)-based PU flexible foams (up to 40% petroleum-based polyol replacement) and lignin-soy polyol (LP-SP) foams. All lignin-based foams were formulated with Ligol A.

Different synthesized lignin polyols (Ligol A, B and C), each with varying lengths of PEG chains, were assessed by formulating foams containing 30 parts per hundred polyol (pphp) lignin polyols to examine their impact on foam mechanical properties. As shown in **Table 4.3**, there was no change in tear strength, but a reduction in CFD as the chain length increased, yet they were still within the standard requirement for seating applications. In addition, it was generally noted that longer PEG chain lengths led to an increase in the support factor, an empirical measure related to the compression modulus that is widely utilized in the industry to gauge foam cushioning. For example, foams with higher support factors are less prone to "sinking in" when subjected to prolonged stress.[73] There was a reduction in foam's tensile strength as the chain length of PEG increased from 200 to 600 Da in the developed lignin polyols. However, the foam's ultimate elongation remained almost the same with an increase in PEG chain length. This outcome was unexpected since low hydroxyl value polyols typically result in reduced crosslinking density, increasing the foam's strain at break. The high functionality of lignin may have also contributed to foam's restricted flexibility. Notably, there was a significant reduction in hysteresis loss with increasing chain length of polyethylene glycol, indicating a potential enhancement in foam resilience, which is pertinent for seating applications.

Table 4.3: Mechanical properties of lignin polyol-based (Ligol A, B, and C) flexible polyurethane foam (30% petroleum-based polyol substitution) measured according to ASTM D3574 test standard. Ligols A, B, and C were synthesized with PEG 200, 400, and 600 respectively.

Mechanical Property	**Desired range**	**Unit**	**Ligol A**	**Ligol B**	**Ligol C**
Density	40-65	kg/m^3	41 ± 0.5^a	47 ± 0.4^b	49 ± 0.2^c
Tear strength	100	N/m	125 ± 14^a	112 ± 9^a	113 ± 14^a
CFD	3-12	kPa	9 ± 0.3^a	8 ± 0.4^b	6 ± 0.1^c
Support factor	Higher is better-	-	3 ± 0.2^a	4 ± 0.2^b	5 ± 1.0^b
Tensile strength	≥ 50	kPa	81 ± 8.0^a	89 ± 8.7^a	71 ± 3.0^b
Elongation	≥ 60	% strain	43 ± 3.9^a	45 ± 4.6^a	41 ± 2.0^a
Hysteresis loss	Lower is better	%	64 ± 4.9^a	53 ± 1.0^b	53 ± 2.0^b

Within a row, values with different letters are significantly different at P ≤ 0.05 (Tukey's test).

4.3.3.2 Impact Test

Impact tests were conducted to study the mechanical response of the developed foams. **Figure 4.10** presents all tested cases' acceleration (*G*) versus static stress. The peak of each pulse was marked by a dot on the line plots, forming what is known as a cushion curve.[162] Almost all cases exhibit a general increasing trend as the drop weight, which is converted to stress, increases. This suggests that heavier impacts led to higher rebound acceleration responses from the foam. The acceleration response of the foams was also dependent on the composition, with lignin-based foams demonstrating a lower acceleration value compared to control foams without lignin polyol. This indicates that the lignin-based foams effectively dissipated the energy impact over a longer

period, making it a better shock absorption material. In automotive seating applications, flexible polyurethane foams with low acceleration values are critical, particularly for headrests and cushioning areas. Lower acceleration responses help mitigate the risk of head, neck, and spinal injuries in the event of an impact or accident, making lignin-based foams a promising alternative for improving passenger safety.

Among the lignin-based foams, as the amount of lignin polyol increases, the acceleration response decreases, as seen in **Figure 4.10a**. Additionally, the combination of soy polyol and synthesized lignin polyol reduced the *G* value, as seen in **Figure 4.10b**. For LP30 foams, as the molecular weight of PEG used in the lignin polyol synthesis increases, the foam's acceleration response decreases (see **Figure C2**, Appendix C). Depending on the application, a cushion designer can determine the appropriate shock response range and decide the required cushion material and dimensions. For instance, if the acceleration response limit for an application is 40 gs, a 0.5 psi static stress (from a 4 lb weight drop on an 8 sq-in foam's top area) that produces about 42 gs on a control foam might fail as the 42 gs is larger than 40 gs limit. In such a case, a lower acceleration value option like LP20, which responds to 30 gs, should be considered.

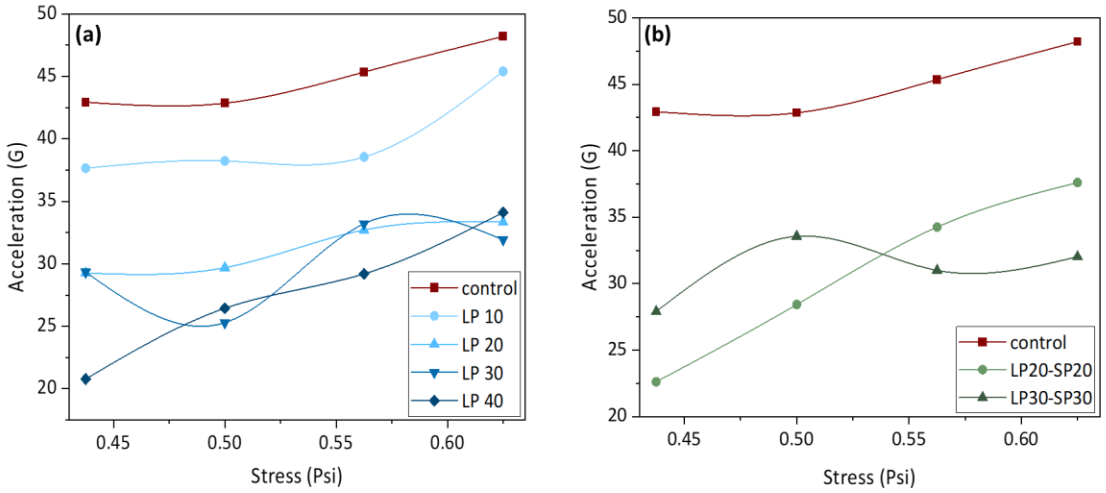

Figure 4.10: Cushion curves of (a) lignin polyol (LP)-based PU flexible foams (0, 10, 20, 30, and 40% petroleum-based polyol substitution) and (b) lignin-soy polyol (LP-SP)-based PU flexible foams. All lignin-based foams were formulated with Ligol A.

4.3.3.3 Foam Morphology

Figure 4.11 shows the SEM images of the developed lignin-based flexible foams, revealing an open-cell structure consistent with that of the petroleum-derived control foam. Unlike flexible polyurethane foams produced using unmodified or solid lignin, no visible lignin particles were observed in the synthesized foams at higher resolution (see **Figure C3**, Appendix C). This absence suggests that the lignin served as a reactive component, integrating into the foam's polymer matrix. This incorporation likely contributed to the superior compressive force deflection and tensile properties of the lignin-based foams compared to the control.

Additionally, the open-cell sizes of the foams varied with the lignin polyol concentration. The cell diameter decreased as the lignin polyol content increased, a phenomenon attributed to the relatively high hydroxyl value of the synthesized lignin polyols, which enhanced the foam's crosslinking density. Another contributing factor could be the residual DBU (1,8-diazabicyclo

[5.4.0] undec-7-ene) present in the synthesized lignin polyol. DBU is known to catalyze gelation reactions, [163] and as the lignin polyol concentration rises, so does the level of residual DBU, accelerating the gelation rate and further reducing cell diameter. This interplay between lignin polyol concentration, hydroxyl value, and residual DBU highlights the intricate relationship between foam formulation and microstructural properties.

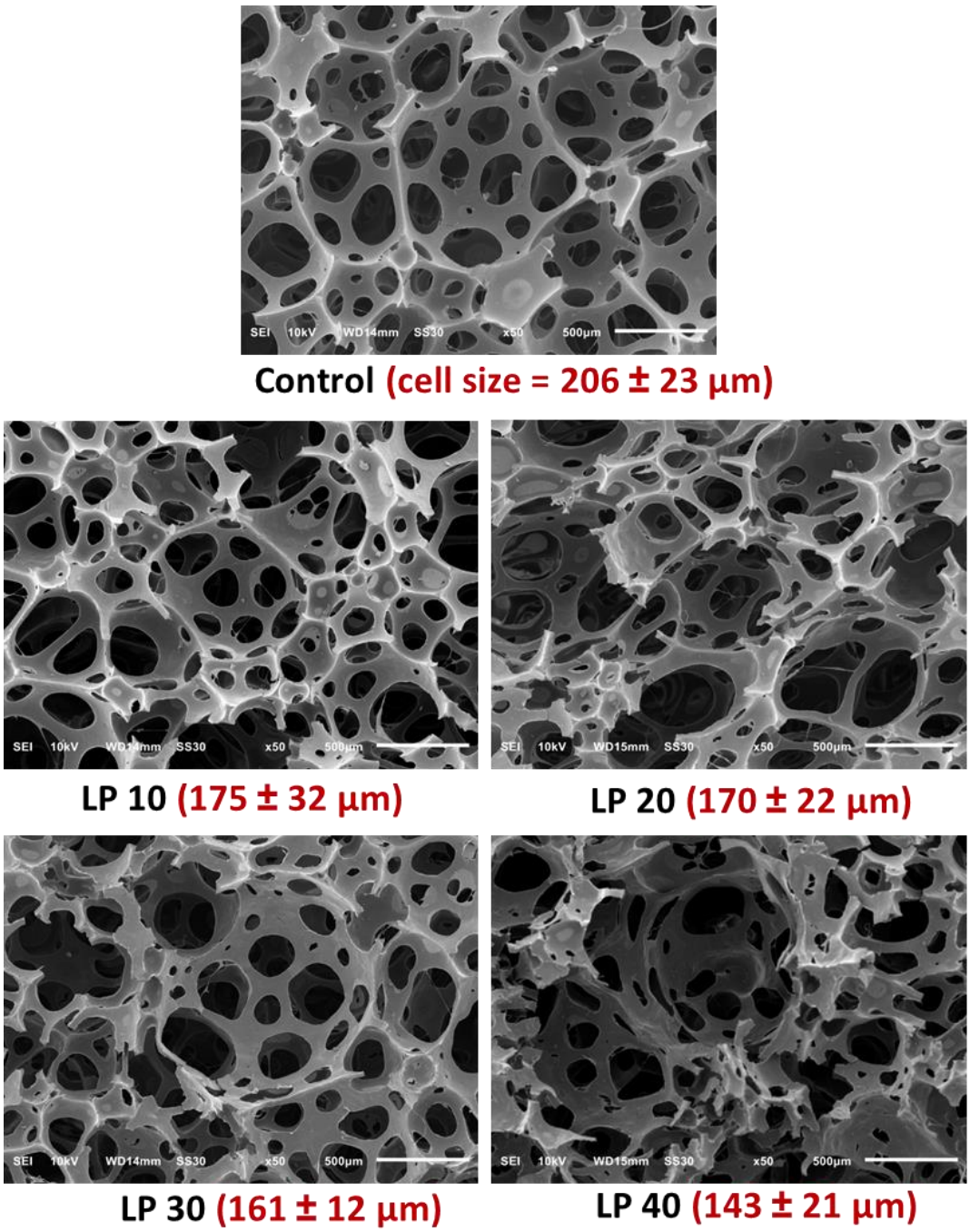

Figure 4.11: Scanning Electron Micrographs (SEM) of developed PU flexible foams at 50x magnification, formed by replacing 0, 10, 20, 30, and 40% of the petroleum-based polyols with synthesized lignin polyol, LP (Ligol A). Average cell-diameter and its standard deviations, µm, are enclosed in parenthesis.

4.3.3.4 Thermal Properties

Figures 4.12a and 4.12b display the weight loss-temperature and differential thermogravimetric analysis (DTG) curves of the foams. Both control and lignin polyol-based foams exhibited similar thermal weight loss characteristics. All foams showed a minor weight loss at temperatures below 150 °C, peaking around 105 °C, likely due to evaporation of small molecules such as water and propylene carbonate. [164] As lignin polyol content increases, the percentage of weight loss from small molecule evaporation rises, with LP40 showing the highest weight change at 2.31%. The first major thermal degradation around 296 to 315 °C can be associated with weight loss from urethane bond breakage resulting in amines, olefins, and CO_2 formation.[116] The subsequent weight loss between 354 and 379 °C is linked to soft segment degradation.[117] The soft segment degradation temperature (*Tmax*) decreases with increasing lignin polyol. As seen in **Figure C4** (Appendix C), the temperature at onset (*Tonset*) and the temperature at 10% degradation ($T_{10\%}$) also decreased with an increase in lignin polyol content, possibly due to residual propylene carbonate and its oligomers in the lignin polyols. In the derivative weight change curve (**Figure 4.12b**), the incorporation of lignin polyol significantly reduced the degradation rate of foams, enhancing their thermal stability. This stability can be attributed to lignin's complex aromatic structure and the lignin polyol's strong carbonate linkage. Additionally, the residue content of the foams at 800 °C was highest in the lignin-based foams, ranging from 12% to 15.26%, compared to 9.74% in the control foams. This increased residue content is attributed to lignin's robust and complex structure, which is more resistant to thermal degradation. Foams containing both synthesized lignin polyol and soy polyol (LP30-SP30) also exhibited high thermal stability. This is evident from the low DTG peak intensity around 370 °C and the higher residue content (13.74%), which can be attributed to the presence of lignin.

4.3.3.5 Biodegradation

The aerobic biodegradation of control foam (made entirely with petrochemical polyols), LP30-SP30, and LP40 PU foams under composting conditions at 58 ± 2 °C and 50 ± 5% relative humidity was assessed. The extent of mineralization was evaluated by carbon dioxide evolution over 120 days.

Biodegradation generally occurs in three main stages. The first stage, the lag phase, is characterized by slow degradation as microbes adapt to the substrate material. This is followed by the active phase, during which the microbial population increases rapidly, leading to the secretion of enzymes that accelerate degradation. Finally, the plateau phase is reached, where microbial activity declines due to diminishing carbon sources, and biodegradation stabilizes.[165] The type of secreted enzyme depends on the chemical structure of the polymeric substrate and the surrounding environment.[166]

In PU degradation, both bacteria and fungi play roles, but fungi are the primary agents.[167] The mode of PU degradation occurs through either hydrolysis or oxidation, depending on the chemical composition of the polyol. Polyester polyol-based PU primarily undergoes hydrolytic degradation,[168] whereas polyether polyol-based PU degrades through oxidation.[169] Ester linkages are more susceptible to microbial attack than ether linkages.[170] During biodegradation, fungi produce extracellular hydrolytic enzymes such as esterases and proteases, which break down ester and urethane bonds.[168] Additionally, oxidative enzymes such as peroxidases and laccases are responsible for degrading ether bonds.[171,172]

As shown in **Figure 4.12c**, lignin-based PU foams (LP40) and lignin-soy foams (LP30-SP30) exhibited higher carbon dioxide evolution than the foams made with 100% petroleum-based foams (control). The higher biodegradation rate of LP40 (39.8% at 120 days), as presented in **Figure**

4.12d, can be attributed to the presence of hydrolyzable carbonate linkages in the synthesized lignin polyol, in contrast to the non-hydrolyzable polyether chains in the petroleum-based polyol used for the control foam (35.2% at 120 days). However, LP30-SP30 demonstrated even higher mineralization than LP40. The increased biodegradation of LP30-SP30 foams (42.6%) can be attributed to the hydrolytic effect of ester linkages in the soft segment of the PU foam due to the presence of soy-polyol.

Ester linkages, predominantly found in soy polyol, are more susceptible to hydrolysis than carbonate linkages due to the generation of carboxylic acids during hydrolysis, which further catalyzes their breakdown.[4] Another factor contributing to the slightly lower mineralization of LP40 compared to LP30-SP30 is the higher concentration of lignin in LP40. While some studies have shown that white-rot fungi can effectively biodegrade lignin,[173–175]compost environment is not the most favorable degradable environment for lignin. Also, the main lignin degradation product is humic acid, [176] which is not detected in the employed method which relies on carbon dioxide released.

Figure 4.12e highlights the lag phase duration of the developed foams. The results indicate that control foams took approximately 40 days for biodegradation to initiate, whereas LP40 and LP30-SP30 foams began degrading within 25 and 5 days, respectively. This further confirms the susceptibility of ester linkages to biodegradation compared to the carbonate and ether bonds. Additionally, the more extended lag phase of LP40 suggests that its high lignin concentration (9% wt) may have contributed to slower degradation, owing to lignin's complex aromatic structure and its high functionality, which increases foam's crosslinking density. In the case of the control foam, it was surprising to see biodegradation, but the present or production of ester due to oxidation may be responsible for the partial biodegradation.

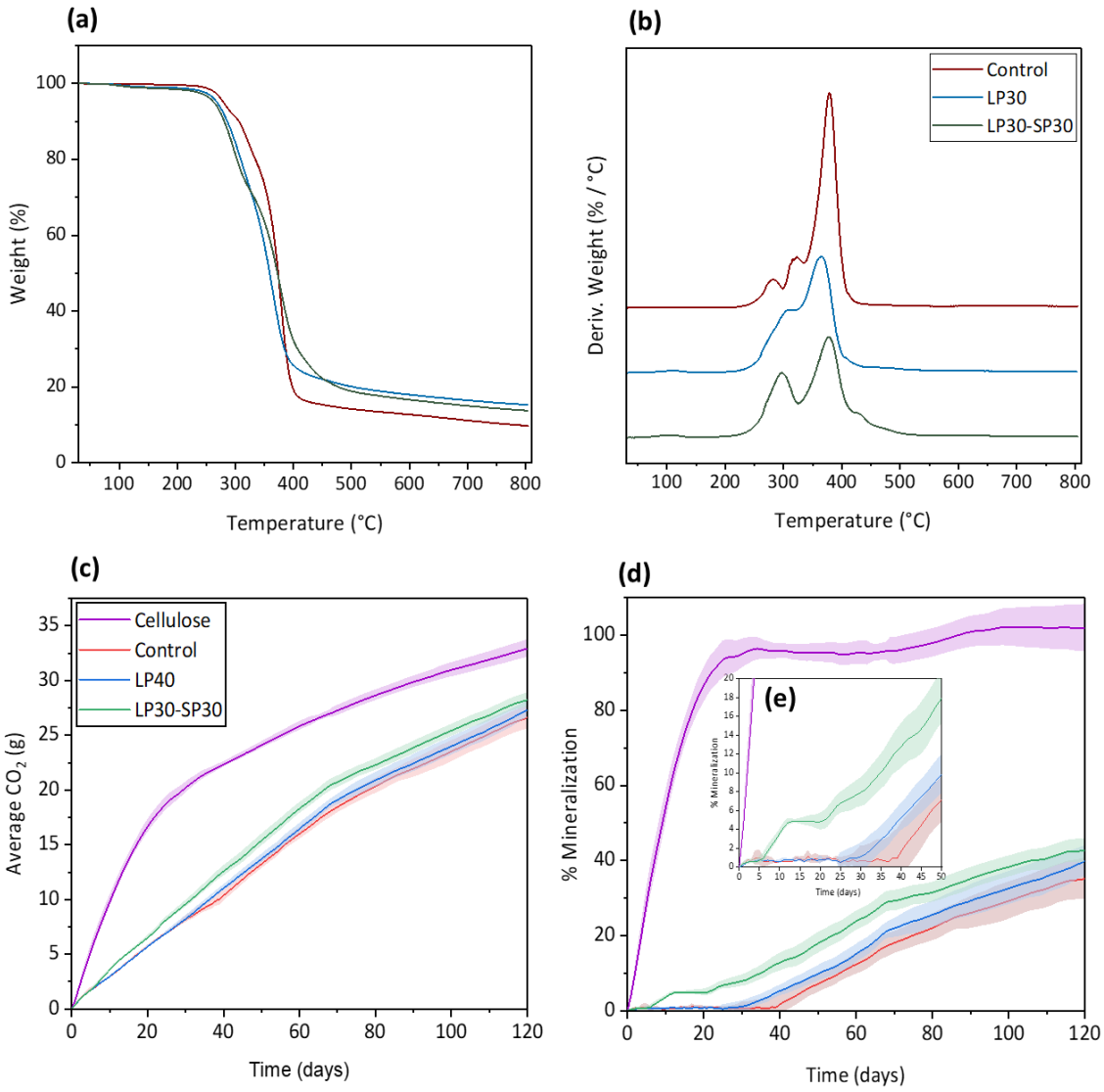

Figure 4.12: Thermogravimetric analysis (TGA) (a) thermogram, and (b) differential thermogravimetric (DTG) curve. Thermophilic anaerobic biodegradation under compost environment (58 ± 2 °C and 50 ± 5% relative humidity) (c) CO_2 evolution until 120 days (d) percentage mineralization until 120 days, and (e) lag phase region of formulated lignin polyol (LP) and soy polyol (SP)-based flexible PU foams.

4.4 Conclusions

This study presents the first successful synthesis and integration of lignin-based polycarbonate polyols into flexible polyurethane foam formulations. By successfully modifying lignin through propylene carbonate oxyalkylation and dimethyl carbonate transesterification, a reactive polyol with favorable hydroxyl values and workable viscosities suited for high-performance foam applications were produced. These findings not only validate the technical feasibility of using lignin as a functional polyol precursor in polycarbonate chemistry but also underscore its potential as a viable substitute for petroleum-based materials such as 1,4-butanediol and 1,6-hexanediol that are commonly used to synthesis traditional polycarbonate polyols. The improved mechanical strength, thermal stability, shock absorption, and biodegradability of the resulting foams not only emphasize lignin's potential as a value-added biopolymer but also address key industry demands for more environmentally friendly and durable materials. These findings are particularly relevant for automotive seating applications, where stringent performance requirements must be balanced with sustainability goals. Moreover, the demonstrated compatibility with soy polyol opens avenues for hybrid bio-based formulations with even greater environmental benefits and higher biobased content. Beyond material performance, this work contributes to the broader effort to valorize lignin, an abundant yet underutilized byproduct of the pulp and paper industry, supporting the transition to a more circular and carbon-conscious materials economy. Future studies should explore scalability, long-term aging performance, and industrial processing adaptability of these polyols to further assess their commercial viability.

Chapter 5: Conclusions and Future Recommendations

5.1 Conclusions

This research explored the development of sustainable flexible polyurethane (PU) foams by replacing petroleum-based polyols with lignin, a renewable and abundant natural polymer, aiming to address environmental concerns while maintaining or enhancing the mechanical and thermal performance of the foams. Lignin, with its rich hydroxyl functionality, was investigated as a viable alternative to petroleum-based polyols, offering a pathway to reduce reliance on fossil fuels and increase the biobased content of PU foams. However, the rigid structure, high hydroxyl value (OHV), poor solubility of lignin in other co-polyols, and low reactivity towards isocyanate posed significant challenges for its direct incorporation into flexible PU formulations. To overcome these limitations, this study systematically explored various modification strategies, including oxyalkylation with propylene carbonate (PC) with and without the use of co-polyols and dimethyl carbonate transesterification, to enhance lignin's application in flexible PU systems.

In the initial phase of the research, lignin was oxyalkylated with propylene carbonate (one-step) to produce liquid lignin polyols with high aliphatic OH content. While this approach successfully increased the biobased carbon content of the foams, the presence of unreacted PC negatively impacted mechanical properties such as tensile strength, tear resistance, and compression force deflection (CFD). This highlighted the need to minimize unreacted PC in the lignin polyols, setting the stage for further optimization. Building on these findings, the study introduced co-polyols into the oxyalkylation reaction to reduce PC loading. High ethylene oxide (EO)-based polyols were found to be the most effective, enhancing lignin solubility and reactivity with PC, while propylene oxide (PO)-based and biobased polyols exhibited poor compatibility. The optimized lignin polyols demonstrated improved mechanical properties, meeting the standard requirements for automotive

seating applications. This highlighted the importance of co-polyol selection and reaction optimization in achieving desirable polyol properties.

To further enhance the performance of lignin-based polyols, a novel two-step process was developed, involving oxyalkylation with PC in the presence of polyethylene glycol (PEG) followed by transesterification with dimethyl carbonate (DMC). This approach not only reduced the OHV and viscosity of the lignin polyols but also introduced carbonate linkages, which significantly improved the mechanical and thermal properties of the resulting foams. The lignin-based polycarbonate polyols exhibited superior tensile strength, load-bearing capacity, and thermal stability compared to conventional petroleum-based foams. Additionally, the foams demonstrated improved shock absorption capacity and biodegradability, making them a more sustainable option for flexible PU applications.

Despite these advances, achieving higher biobased content in lignin polyol remains challenging due to the petroleum origin of EO-based co-polyols employed in the oxyalkylation reaction. One alternative strategy involves blending low OHV biobased polyols with high EO-content polyols (also low OHV) prior to lignin oxyalkylation. While commercially available biobased PEGs are limited to low molecular weights (200–600 Da) and yield high OHV lignin polyols, they can still replace petroleum-derived PEGs in the two-step lignin-based polycarbonate polyol synthesis pathway. Similarly, biobased glycerol carbonate can be used to replace PC. However, glycerol carbonate contains a pendant hydroxyl group that would introduce additional functionality during oxyalkylation, leading to higher OHVs, undesirable in flexible PU foam applications. Furthermore, residual glycerol carbonate in the final polyol may inhibit polymer growth upon reaction with isocyanates due to its monofunctionality (f = 1), which would likely consume isocyanate without contributing to network formation. Though biobased PC is not yet commercially available, its

synthesis from CO_2 partially offsets its fossil origin. In the long term, selective lignin modification at the extraction stage could improve compatibility with biobased polyols, enhancing both economic viability and sustainability.

Overall, the progression from the initial oxyalkylation of lignin to the development of lignin-based polycarbonate polyols represents an incremental advancement in the utilization of lignin for flexible PU foams. Each phase of the research addressed specific challenges identified in the previous one, leading to the successful synthesis of high-performance lignin-based polyols that enabled the replacement of up to 60% of petroleum-based polyols in flexible PU foams. The findings from this research highlights the potential of lignin as a renewable resource for polyol production, offering a viable alternative to petroleum-based materials. In conclusion, this research has demonstrated that lignin, through strategic modification and optimization, can be effectively utilized in flexible PU foam formulations. The integration of lignin-based polyols not only enhances the sustainability of PU flexible foams but also improves their mechanical, thermal, and shock absorption properties.

5.2 Future Recommendations

Based on the findings of this thesis, the following recommendations are proposed for future research:

- Optimization of Lignin-Based Polycarbonate Polyol Chemistry: Further studies should investigate the effect of lignin source and isolation processes on polyol properties to refine reaction parameters and performance. Additionally, the resulting polyols can be potentially evaluated for polyurethane adhesive and coating applications.
- Enhancing Flame Retardancy: Although not a critical performance requirement for automotive, it is worthwhile exploring the feasibility of partially or fully replacing dimethyl carbonate with dimethyl methyl phosphonate (DMMP) to introduce phosphonate linkages into the polyol structure, thereby improving flame retardant properties.
- Technoeconomic and Life Cycle Assessment: It is important to conduct technoeconomic analysis (TEA) and life cycle assessment (LCA) to assess the scalability, cost-effectiveness, and environmental impact of polycarbonate lignin polyol production, ensuring its viability for industrial applications.

REFERENCES

1. Marketsandmarkets. Polyurethane Foam Market. *https://www.marketsandmarkets.com/Market-Reports/polyurethane-foams-market-1251.html* (2023).

2. Ionescu, M. *Chemistry and Technology of Polyols for Polyurethanes. Volume 1*.

3. Szycher, M. *Szycher's Handbook of Polyurethanes: Second Edition*. *Szychers Handbook of Polyurethanes, Second Edition* (2012). doi:10.1201/b12343.

4. Ionescu, Mihail. *Chemistry and Technology of Polyols for Polyurethane Volume 2*. *Rapra Publishing* vol. 2 (2016).

5. Haridevan, H. *et al.* Processing and rheological properties of polyol/cellulose nanofibre dispersions for polyurethanes. *Polymer (Guildf)* **255**, (2022).

6. Li, J. W. *et al.* Synthesis and properties of castor oil-based polyurethane containing short fluorinated segment. *J Appl Polym Sci* **137**, (2020).

7. Michalowski, S. & Prociak, A. Flexible polyurethane foams modified with new bio-polyol based on rapeseed oil. in *Journal of Renewable Materials* vol. 3 (2015).

8. Zhang, M., Zhang, J., Chen, S. & Zhou, Y. Synthesis and fire properties of rigid polyurethane foams made from a polyol derived from melamine and cardanol. *Polym Degrad Stab* **110**, 27–34 (2014).

9. Pawlik, H. & Prociak, A. Influence of Palm Oil-Based Polyol on the Properties of Flexible Polyurethane Foams. *J Polym Environ* **20**, 438–445 (2012).

10. Prociak, A., Malewska, E., Kurańska, M., Bąk, S. & Budny, P. Flexible polyurethane foams synthesized with palm oil-based bio-polyols obtained with the use of different oxirane ring opener. *Ind Crops Prod* **115**, 69–77 (2018).

11. Chan, Y. Y., Ma, C., Zhou, F., Hu, Y. & Schartel, B. Flame retardant flexible polyurethane foams based on phosphorous soybean-oil polyol and expandable graphite. *Polym Degrad Stab* **191**, (2021).

12. John, J., Bhattacharya, M. & Turner, R. B. Characterization of polyurethane foams from soybean oil. *J Appl Polym Sci* **86**, 3097–3107 (2002).

13. Guo, A., Demydov, D., Zhang, W. & Petrovic, Z. S. *Polyols and Polyurethanes from Hydroformylation of Soybean Oil*. *Journal of Polymers and the Environment* vol. 10 (2002).

14. Petrović, Z. S., Yang, L., Zlatanić, A., Zhang, W. & Javni, I. Network structure and properties of polyurethanes from soybean oil. *J Appl Polym Sci* **105**, 2717–2727 (2007).

15. Gu, R., Konar, S. & Sain, M. Preparation and characterization of sustainable polyurethane foams from soybean oils. *JAOCS, Journal of the American Oil Chemists' Society* **89**, 2103–2111 (2012).

16. Gu, R., Konar, S. & Sain, M. Preparation and characterization of sustainable polyurethane foams from soybean oils. *JAOCS, Journal of the American Oil Chemists' Society* **89**, 2103–2111 (2012).

17. Zhang, L., Jeon, H. K., Malsam, J., Herrington, R. & Macosko, C. W. Substituting soybean oil-based polyol into polyurethane flexible foams. *Polymer (Guildf)* **48**, 6656–6667 (2007).

18. Petrovi, Z. S., Guo, A., Javni, I., Cvetković, I. & Hong, D. P. Polyurethane networks from polyols obtained by hydroformylation of soybean oil. *Polym Int* **57**, 275–281 (2008).

19. Latere Dwan'isa, J.-P., Mohanty, A. K., Misra, M., Drzal, L. T. & Kazemizadeh, M. *Novel Biobased Polyurethanes Synthesized from Soybean Phosphate Ester Polyols: Thermomechanical Properties Evaluations*. *Journal of Polymers and the Environment* vol. 11 (2003).

20. Tu, Y. C., Suppes, G. J. & Hsieh, F. H. Water-blown rigid and flexible polyurethane foams containing epoxidized soybean oil triglycerides. *J Appl Polym Sci* **109**, 537–544 (2008).

21. Cifarelli, A. *et al.* Flexible polyurethane foams from epoxidized vegetable oils and a bio-based diisocyanate. *Polymers (Basel)* **13**, 1–21 (2021).

22. Lange, H., Bartzoka, E. D. & Crestini, C. 11. Lignin biorefinery: structure, pretreatment and use. in *Biorefineries* (2015). doi:10.1515/9783110331585-015.

23. Erfani Jazi, M. *et al.* Structure, chemistry and physicochemistry of lignin for material functionalization. *SN Applied Sciences* vol. 1 Preprint at https://doi.org/10.1007/s42452-019-1126-8 (2019).

24. Putra, Z. A. Lignocellulosic biomass pretreatment for biorefinery: A review. *Indonesian Journal of Science and Technology* vol. 3 Preprint at https://doi.org/10.17509/ijost.v3i1.10796 (2018).

25. Marita, J. M. *et al.* NMR characterization of lignins from transgenic poplars with suppressed caffeic acid O-methyltransferase activity. *J Chem Soc Perkin 1* **22**, (2001).

26. Ralph, J., Lapierre, C. & Boerjan, W. Lignin structure and its engineering. *Current Opinion in Biotechnology* vol. 56 Preprint at https://doi.org/10.1016/j.copbio.2019.02.019 (2019).

27. Eswaran, S. cheranma devi, Subramaniam, S., Sanyal, U., Rallo, R. & Zhang, X. Molecular structural dataset of lignin macromolecule elucidating experimental structural compositions. *Sci Data* **9**, (2022).

28. Katahira, R., Elder, T. J. & Beckham, G. T. A Brief Introduction to Lignin Structure. in *Lignin Valorization: Emerging Approaches* (2018).

29. Sipponen, M. H. *et al.* Structural changes of lignin in biorefinery pretreatments and consequences to enzyme-lignin interactions - OPEN ACCESS. *Nord Pulp Paper Res J* **32**, (2017).

30. Ponnusamy, V. K. *et al.* A review on lignin structure, pretreatments, fermentation reactions and biorefinery potential. *Bioresource Technology* vol. 271 Preprint at https://doi.org/10.1016/j.biortech.2018.09.070 (2019).

31. Sadeghifar, H. & Ragauskas, A. Technical Lignin Fractionation: A Powerful Tool for Lignin Structure Homogenization and Its Application. in *Lignin-based Materials* (2023). doi:10.1039/bk9781839167843-00059.

32. Azadfar, M., Gao, A. H., Bule, M. V. & Chen, S. Correlation of lignin structure to its antioxidant activity. in *American Society of Agricultural and Biological Engineers Annual International Meeting 2014, ASABE 2014* vol. 1 (2014).

33. Zhao, H. Y., Wei, J. H. & Song, Y. R. Advances in research on lignin biosynthesis and its genetic engineering. *Zhi wu sheng li yu fen zi sheng wu xue xue bao = Journal of plant physiology and molecular biology* vol. 30 Preprint at (2004).

34. Ralph, J., Lapierre, C. & Boerjan, W. *Lignin Engineering-Special Issue for Lignin Structure and Its Engineering*. *Current Opinion in Biotechnology* (2019).

35. Shoushrah, S. H., Alzagameem, A., Bergrath, J., Tobiasch, E. & Schulze, M. Lignin and Its Composites for Tissue Engineering. in *Lignin-based Materials* (2023). doi:10.1039/bk9781839167843-00161.

36. Sipponen, M. H. *et al.* Structural changes of lignin in biorefinery pretreatments and consequences to enzyme-lignin interactions. *Nord Pulp Paper Res J* **32**, (2017).

37. Narron, R. H., Kim, H., Chang, H. M., Jameel, H. & Park, S. Biomass pretreatments capable of enabling lignin valorization in a biorefinery process. *Current Opinion in Biotechnology* vol. 38 Preprint at https://doi.org/10.1016/j.copbio.2015.12.018 (2016).

38. Narron, R. H., Chang, H. M., Jameel, H. & Park, S. Soluble Lignin Recovered from Biorefinery Pretreatment Hydrolyzate Characterized by Lignin-Carbohydrate Complexes. *ACS Sustain Chem Eng* **5**, (2017).

39. Zhang, K. *et al.* An engineered monolignol 4-O-methyltransferase depresses lignin biosynthesis and confers novel metabolic capability in Arabidopsis. *Plant Cell* **24**, (2012).

40. Katahira, R., Elder, T. J. & Beckham, G. T. Chapter 1: A Brief Introduction to Lignin Structure. in *RSC Energy and Environment Series* vols 2018-January (2018).

41. Kumar, M., Morya, R., Gupta, A., Kumar, V. & Thakur, I. S. Bacterial-Mediated Depolymerization and Degradation of Lignin. in *Environmental Microbiology and Biotechnology* (2021). doi:10.1007/978-981-15-7493-1_4.

42. Amiri, M. T., Bertella, S., Questell-Santiago, Y. M. & Luterbacher, J. S. Establishing lignin structure-upgradeability relationships using quantitative 1H-13C heteronuclear single quantum coherence nuclear magnetic resonance (HSQC-NMR) spectroscopy. *Chem Sci* **10**, (2019).

43. Crestini, C., Lange, H., Sette, M. & Argyropoulos, D. S. On the structure of softwood kraft lignin. *Green Chemistry* **19**, (2017).

44. Meng, X. *et al.* Determination of hydroxyl groups in biorefinery resources via quantitative 31P NMR spectroscopy. *Nat Protoc* **14**, (2019).

45. Vieira, F. R., Magina, S., Evtuguin, D. V. & Barros-Timmons, A. Lignin as a Renewable Building Block for Sustainable Polyurethanes. *Materials* vol. 15 Preprint at https://doi.org/10.3390/ma15176182 (2022).

46. Alam, M. M., Greco, A., Rajabimashhadi, Z. & Esposito Corcione, C. Efficient and environmentally friendly techniques for extracting lignin from lignocellulose biomass and subsequent uses: A review. *Cleaner Materials* vol. 13 Preprint at https://doi.org/10.1016/j.clema.2024.100253 (2024).

47. Saadan, R., Hachimi Alaoui, C., Ihammi, A., Chigr, M. & Fatimi, A. A Brief Overview of Lignin Extraction and Isolation Processes: From Lignocellulosic Biomass to Added-Value Biomaterials. in *IECF 2024* 3 (MDPI, Basel Switzerland, 2024). doi:10.3390/eesp2024031003.

48. Constant, S. *et al.* New insights into the structure and composition of technical lignins: A comparative characterisation study. *Green Chemistry* **18**, (2016).

49. Rodrigues Gurgel da Silva, A., Errico, M. & Rong, B. G. Techno-economic analysis of organosolv pretreatment process from lignocellulosic biomass. *Clean Technol Environ Policy* **20**, (2018).

50. Zhao, X., Cheng, K. & Liu, D. Organosolv pretreatment of lignocellulosic biomass for enzymatic hydrolysis. *Applied Microbiology and Biotechnology* vol. 82 Preprint at https://doi.org/10.1007/s00253-009-1883-1 (2009).

51. Crestini, C., Crucianelli, M., Orlandi, M. & Saladino, R. Oxidative strategies in lignin chemistry: A new environmental friendly approach for the functionalisation of lignin and lignocellulosic fibers. *Catal Today* **156**, (2010).

52. Yearla, S. R. & Padmasree, K. Preparation and characterisation of lignin nanoparticles: evaluation of their potential as antioxidants and UV protectants. *J Exp Nanosci* **11**, (2016).

53. Zhang, D. *et al.* Pristine lignin as a flame retardant in flexible PU foam. *Green Chemistry* **23**, (2021).

54. Lu, W., Ye, J., Zhu, L., Jin, Z. & Matsumoto, Y. Intumescent flame retardant mechanism of lignosulfonate as a char forming agent in rigid polyurethane foam. *Polymers (Basel)* **13**, (2021).

55. Costes, L., Laoutid, F., Brohez, S. & Dubois, P. Bio-based flame retardants: When nature meets fire protection. *Materials Science and Engineering R: Reports* vol. 117 Preprint at https://doi.org/10.1016/j.mser.2017.04.001 (2017).

56. Luo, X., Mohanty, A. & Misra, M. Lignin as a reactive reinforcing filler for water-blown rigid biofoam composites from soy oil-based polyurethane. *Ind Crops Prod* **47**, 13–19 (2013).

57. Gurgel, D., Bresolin, D., Sayer, C., Cardozo Filho, L. & Hermes de Araújo, P. H. Flexible polyurethane foams produced from industrial residues and castor oil. *Ind Crops Prod* **164**, 113377 (2021).

58. Wang, F. *et al.* Flexible, recyclable and sensitive piezoresistive sensors enabled by lignin polyurethane-based conductive foam †. *Cite this: Mater. Adv* **4**, 586 (2023).

59. Quan, P. *et al.* Kraft Lignin with Improved Homogeneity Recovered Directly from Black Liquor and Its Application in Flexible Polyurethane Foams. *ACS Omega* (2022) doi:10.1021/acsomega.2c01206/asset/images/medium/ao2c01206_m002.gif.

60. Ajao, O. *et al.* Multi-product biorefinery system for wood-barks valorization into tannins extracts, lignin-based polyurethane foam and cellulose-based composites: Techno-economic evaluation. *Ind Crops Prod* **167**, 113435 (2021).

61. Gondaliya, A. & Nejad, M. Lignin as a Partial Polyol Replacement in Polyurethane Flexible Foam. *Molecules 2021, Vol. 26, Page 2302* **26**, 2302 (2021).

62. Gondaliya, A. M. *comparative analysis of different lignins as partial polyol replacement in polyurethane flexible foam formulations*. (2020).

63. Maillard, D. *et al.* Influence of lignin's pH on polyurethane flexible foam formation and how to control it. *J Appl Polym Sci* **138**, 50319 (2021).

64. Zieglowski, M. *et al.* Reactivity of Isocyanate-Functionalized Lignins: A Key Factor for the Preparation of Lignin-Based Polyurethanes. *Front Chem* **7**, 562 (2019).

65. Wang, S., Liu, W., Yang, D. & Qiu, X. Highly Resilient Lignin-Containing Polyurethane Foam. *Ind Eng Chem Res* **58**, 496–504 (2019).

66. Gómez-Fernández, S., Günther, M., Schartel, B., Corcuera, M. A. & Eceiza, A. Impact of the combined use of layered double hydroxides, lignin and phosphorous polyol on the fire behavior of flexible polyurethane foams. *Ind Crops Prod* **125**, 346–359 (2018).

67. Gómez-Fernández, S. *et al.* Properties of flexible polyurethane foams containing isocyanate functionalized kraft lignin. *Ind Crops Prod* **100**, 51–64 (2017).

68. Wysocka, K., Szymona, K., Mcdonald, A. G., Mamiński, M. & Maminski, M. Characterization of Thermal and Mechanical Properties of Lignosulfonate-and Hydrolyzed Lignosulfonate-based Polyurethane Foams. *Bioresources* **11**, 7355–7364 (2016).

69. Bernardini, J., Anguillesi, I., Coltelli, M. B., Cinelli, P. & Lazzeri, A. Optimizing the lignin based synthesis of flexible polyurethane foams employing reactive liquefying agents. *Polym Int* **64**, 1235–1244 (2015).

70. Bernardini, J., Cinelli, P., Anguillesi, I., Coltelli, M. B. & Lazzeri, A. Flexible polyurethane foams green production employing lignin or oxypropylated lignin. *Eur Polym J* **64**, 147–156 (2015).

71. Jeong, H., Park, J., Kim, S., Lee, J. & Ahn, N. Compressive viscoelastic properties of softwood kraft lignin-based flexible polyurethane foams. *Fibers and Polymers* **14**, 1301–1310 (2013).

72. Cinelli, P., Anguillesi, I. & Lazzeri, A. Green synthesis of flexible polyurethane foams from liquefied lignin. *Eur Polym J* **49**, 1174–1184 (2013).

73. Dunne, K., Acquah, E. K., Allohverdi, T., Schenck, R. & Nejad, M. Technical lignin-derived liquid polyols for flexible polyurethane foam in automotive seating. *Biofuels, Bioproducts and Biorefining* (2025) doi:10.1002/bbb.2750.

74. Henry, C. & Nejad, M. Lignin-Based Low-Density Rigid Polyurethane/Polyisocyanurate Foams. *Ind Eng Chem Res* **62**, (2023).

75. Henry, C., Gondaliya, A., Thies, M. & Nejad, M. Studying the Suitability of Nineteen Lignins as Partial Polyol Replacement in Rigid Polyurethane/Polyisocyanurate Foam. *Molecules* **27**, (2022).

76. Gondaliya, A. & Nejad, M. Lignin as a partial polyol replacement in polyurethane flexible foam. *Molecules* **26**, (2021).

77. Nikafshar, S., Wang, J., Dunne, K., Sangthonganotai, P. & Nejad, M. Choosing the Right Lignin to Fully Replace Bisphenol A in Epoxy Resin Formulation. *ChemSusChem* **14**, (2021).

78. Baumberger, S. *et al.* Molar mass determination of lignins by size-exclusion chromatography: Towards standardisation of the method. *Holzforschung* **61**, (2007).

79. Antonino, L. D. *et al.* Reactivity of aliphatic and phenolic hydroxyl groups in kraft lignin towards 4,4′ mdi. *Molecules* **26**, (2021).

80. Wu, L. C. -F & Glasser, W. G. Engineering plastics from lignin. I. Synthesis of hydroxypropyl lignin. *J Appl Polym Sci* **29**, (1984).

81. Wang, C. S., Yang, L. T., Ni, B. L. & Shi, G. Polyurethane networks from different soy-based polyols by the ring opening of epoxidized soybean oil with methanol, glycol, and 1,2-propanediol. *J Appl Polym Sci* **114**, (2009).

82. Gandhi, T. S., Patel, M. R. & Dholakiya, B. Z. Synthesis of cashew Mannich polyol via a three step continuous route and development of PU rigid foams with mechanical, thermal and fire studies. *Journal of Polymer Engineering* **35**, (2015).

83. Chaffanjon, P. & Schroter, S. Rigid polyurethane foams comprising modified phenolic resins additives. (2016).

84. Haridevan, H., Evans, D. A. C., Martin, D. J. & Annamalai, P. K. Rational analysis of dispersion and solubility of Kraft lignin in polyols for polyurethanes. *Ind Crops Prod* **185**, (2022).

85. Jin, Y., Ruan, X., Cheng, X. & Lü, Q. Liquefaction of lignin by polyethyleneglycol and glycerol. *Bioresour Technol* **102**, (2011).

86. Jasiukaityte-Grojzdek, E., Kunaver, M. & Crestini, C. Lignin structural changes during liquefaction in acidified ethylene glycol. *Journal of Wood Chemistry and Technology* **32**, (2012).

87. Bernardini, J., Anguillesi, I., Coltelli, M. B., Cinelli, P. & Lazzeri, A. Optimizing the lignin based synthesis of flexible polyurethane foams employing reactive liquefying agents. *Polym Int* **64**, 1235–1244 (2015).

88. Kühnel, I., Podschun, J., Saake, B. & Lehnen, R. Synthesis of lignin polyols via oxyalkylation with propylene carbonate. *Holzforschung* **69**, (2015).

89. Vieira, F. R., Barros-Timmons, A., Evtuguin, D. V. & Pinto, P. C. R. Effect of different catalysts on the oxyalkylation of eucalyptus Lignoboost® kraft lignin. *Holzforschung* **74**, (2020).

90. Vieira, F. R., Barros-Timmons, A., Evtuguin, D. V. & Pinto, P. C. O. R. Oxyalkylation of Lignoboost™ Kraft Lignin with Propylene Carbonate: Design of Experiments towards Synthesis Optimization. *Materials* **15**, (2022).

91. Kühnel, I., Saake, B. & Lehnen, R. Comparison of different cyclic organic carbonates in the oxyalkylation of various types of lignin. *React Funct Polym* **120**, 83–91 (2017).

92. Vieira, F. R., Gama, N. V., Barros-Timmons, A., Evtuguin, D. V. & Pinto, P. C. O. R. Development of Rigid Polyurethane Foams Based on Kraft Lignin Polyol Obtained by Oxyalkylation Using Propylene Carbonate. *ChemEngineering* **6**, (2022).

93. Kühnel, I., Saake, B. & Lehnen, R. Oxyalkylation of lignin with propylene carbonate: Influence of reaction parameters on the ensuing bio-based polyols. *Ind Crops Prod* **101**, (2017).

94. Cinelli, P., Anguillesi, I. & Lazzeri, A. Green synthesis of flexible polyurethane foams from liquefied lignin. in *European Polymer Journal* vol. 49 1174–1184 (2013).

95. Aniceto, J. P. S., Portugal, I. & Silva, C. M. Biomass-based polyols through oxypropylation reaction. *ChemSusChem* vol. 5 1358–1368 Preprint at https://doi.org/10.1002/cssc.201200032 (2012).

96. Pescarmona, P. P. Cyclic carbonates synthesised from CO2: Applications, challenges and recent research trends. *Current Opinion in Green and Sustainable Chemistry* vol. 29 Preprint at https://doi.org/10.1016/j.cogsc.2021.100457 (2021).

97. Lopes, E. J. C., Ribeiro, A. P. C. & Martins, L. M. D. R. S. New trends in the conversion of Co2 to cyclic carbonates. *Catalysts* vol. 10 Preprint at https://doi.org/10.3390/catal10050479 (2020).

98. Clements, J. H. Reactive applications of cyclic alkylene carbonates. *Ind Eng Chem Res* **42**, 663–674 (2003).

99. Zhao, X., Sun, N., Wang, S., Li, F. & Wang, Y. Synthesis of propylene carbonate from carbon dioxide and 1,2-propylene glycol over zinc acetate catalyst. *Ind Eng Chem Res* **47**, (2008).

100. Liu, L. Y., Cho, M., Sathitsuksanoh, N., Chowdhury, S. & Renneckar, S. Uniform Chemical Functionality of Technical Lignin Using Ethylene Carbonate for Hydroxyethylation and Subsequent Greener Esterification. *ACS Sustain Chem Eng* **6**, (2018).

101. Sternberg, J. & Pilla, S. Materials for the biorefinery: High bio-content, shape memory Kraft lignin-derived non-isocyanate polyurethane foams using a non-toxic protocol. *Green Chemistry* **22**, 6922–6935 (2020).

102. Meng, X. *et al.* Determination of hydroxyl groups in biorefinery resources via quantitative 31P NMR spectroscopy. *Nat Protoc* **14**, 2627–2647 (2019).

103. ASTM D3574 - 17 Standard Test Methods for Flexible Cellular Materials—Slab, Bonded, and Molded Urethane Foams. https://www.astm.org/Standards/D3574.htm.

104. Alinejad, M. *et al.* Lignin-based polyurethanes: Opportunities for bio-based foams, elastomers, coatings and adhesives. *Polymers* vol. 11 Preprint at https://doi.org/10.3390/polym11071202 (2019).

105. Szycher, M. *Szycher's Handbook of Polyurethanes*. *Szycher's Handbook of Polyurethanes* (CRC Press, 1999). doi:10.1201/9781482273984.

106. Kairytė, A., Vaitkus, S., Pundienė, I. & Balčiūnas, G. Effect of propylene glycol, rapeseed glycerine, and corn starch modified polyol blends parameters on the properties of thermal insulating polyurethane foams. *Journal of Cellular Plastics* **55**, 365–384 (2019).

107. Li, W., Ryan, A. J. & Meier, I. K. Effect of chain extenders on the morphology development in flexible polyurethane foam. *Macromolecules* **35**, 6306–6312 (2002).

108. Aneja, A. & Wilkes, G. L. Exploring macro- and microlevel connectivity of the urea phase in slabstock flexible polyurethane foam formulations using lithium chloride as a probe. *Polymer (Guildf)* **43**, (2002).

109. Aneja, A., Wilkes, G. L. & Rightor, E. G. Study of slabstock flexible polyurethane foams based on varied toluene diisocyanate isomer ratios. *J Polym Sci B Polym Phys* **41**, (2003).

110. Neff, R. A. & Macosko, C. W. Simultaneous measurement of viscoelastic changes and cell opening during processing of flexible polyurethane foam. *Rheol Acta* **35**, (1996).

111. Aneja, A. & Wilkes, G. L. On the issue of urea phase connectivity in formulations based on molded flexible polyurethane foams. *J Appl Polym Sci* **85**, (2002).

112. Armistead, J. P., Wilkes, G. L. & Turner, R. B. Morphology of water-blown flexible polyurethane foams. *J Appl Polym Sci* **35**, (1988).

113. Sonnenschein, M. F. & Wendt, B. L. Design and formulation of soybean oil derived flexible polyurethane foams and their underlying polymer structure/property relationships. *Polymer (Guildf)* **54**, 2511–2520 (2013).

114. Zhang, L., Jeon, H. K., Malsam, J., Herrington, R. & Macosko, C. W. Substituting soybean oil-based polyol into polyurethane flexible foams. *Polymer (Guildf)* **48**, 6656–6667 (2007).

115. Li, W., Ryan, A. J. & Meier, I. K. Effect of chain extenders on the morphology development in flexible polyurethane foam. *Macromolecules* **35**, (2002).

116. Hablot, E., Zheng, D., Bouquey, M. & Avérous, L. Polyurethanes based on castor oil: Kinetics, chemical, mechanical and thermal properties. *Macromol Mater Eng* **293**, 922–929 (2008).

117. Liang, J. *et al.* Fabrication of Bio-Based Flexible Polyurethane Foam with Biodegradation by Etherification of Kraft Lignin. *ACS Appl Polym Mater* **6**, 4441–4448 (2024).

118. Dai, H., Yang, L., Lin, B., Wang, C. & Shi, G. Synthesis and characterization of the different soy-based polyols by ring opening of epoxidized soybean oil with methanol, 1,2-ethanediol and 1,2-propanediol. *JAOCS, Journal of the American Oil Chemists' Society* **86**, (2009).

119. Usman, M. *et al.* Synthesis of cyclic carbonates from CO2 cycloaddition to bio-based epoxides and glycerol: an overview of recent development. *RSC Advances* vol. 13 Preprint at https://doi.org/10.1039/d3ra03028h (2023).

120. Chen, Y., Yu, J., Yang, Y., Huo, F. & Li, C. A continuous process for cyclic carbonate synthesis from CO2 catalyzed by the ionic liquid in a microreactor system: Reaction kinetics, mass transfer, and process optimization. *Chemical Engineering Journal* **455**, (2023).

121. Nejad, M. & Nikafshar, S. Lignin-based polyurethane prepolymers, polymers, related compositions, and related methods. (2019) doi:WO2019241607A1.

122. Abdul-Karim, R., Hameed, A. & Malik, M. I. Ring-opening polymerization of propylene carbonate: Microstructural analysis of the polymer and selectivity of polymerization by 2D-NMR techniques. *Eur Polym J* **105**, (2018).

123. Clements, J. H. Reactive applications of cyclic alkylene carbonates. *Industrial and Engineering Chemistry Research* vol. 42 663–674 Preprint at https://doi.org/10.1021/ie020678i (2003).

124. Zhang, X. *et al.* Rigid polyurethane foams containing lignin oxyalkylated with ethylene carbonate and polyethylene glycol. *Ind Crops Prod* **141**, (2019).

125. Duval, A., Vidal, D., Sarbu, A., René, W. & Avérous, L. Scalable single-step synthesis of lignin-based liquid polyols with ethylene carbonate for polyurethane foams. *Mater Today Chem* **24**, (2022).

126. Akim, L. G. *et al.* Quantitative 31P NMR spectroscopy of lignins from transgenic poplars. *Holzforschung* **55**, 386–390 (2001).

127. Argyropoulos, D. S. Quantitative phosphorus-31 NMR analysis of six soluble lignins. *Journal of wood chemistry and technology* **14**, 65–82 (1994).

128. Meng, X. *et al.* Determination of hydroxyl groups in biorefinery resources via quantitative 31 P NMR spectroscopy. *Nat Protoc* **14**, 2627–2647 (2019).

129. Argyropoulos, D. S. Quantitative phosphorus-31 nmr analysis of lignins, a new tool for the lignin chemist. *Journal of Wood Chemistry and Technology* **14**, 45–63 (1994).

130. Test Methods of Polyurethane Raw Materials: Determination of the Polymerized Ethylene Oxide Content of Polyether Polyols. Preprint at https://doi.org/10.1520/D4875-11 (2011).

131. Standard Test Method for Dynamic Shock Cushioning Characteristics of Packaging Material 1. doi:10.1520/D1596-14.

132. Patel, V. R., Dumancas, G. G., Viswanath, L. C. K., Maples, R. & Subong, B. J. J. Castor oil: Properties, uses, and optimization of processing parameters in commercial production. *Lipid Insights* vol. 9 Preprint at https://doi.org/10.4137/LPI.S40233 (2016).

133. Aoki, H. *et al.* Influence of the methyl group on the dielectric constant of boron carbon nitride films containing it. *Diam Relat Mater* **19**, (2010).

134. Lam, C. K. & Mak, T. C. W. Carbonate and oxalate dianions as prolific hydrogen-bond acceptors in supramolecular assembly. *Chemical Communications* (2003) doi:10.1039/b306649e.

135. Ponnuchamy, V., Gordobil, O., Diaz, R. H., Sandak, A. & Sandak, J. Fractionation of lignin using organic solvents: A combined experimental and theoretical study. *Int J Biol Macromol* **168**, (2021).

136. Lommerse, J. P. M., Price, S. L. & Taylor, R. Hydrogen bonding of carbonyl, ether, and ester oxygen atoms with alkanol hydroxyl groups. *J Comput Chem* **18**, (1997).

137. Li, R., Wu, Y., Bai, Z., Guo, J. & Chen, X. Effect of molecular weight of polyethylene glycol on crystallization behaviors, thermal properties and tensile performance of polylactic acid stereocomplexes. *RSC Adv* **10**, (2020).

138. Miller-Chou, B. A. & Koenig, J. L. A review of polymer dissolution. *Progress in Polymer Science (Oxford)* vol. 28 Preprint at https://doi.org/10.1016/S0079-6700(03)00045-5 (2003).

139. Rubens, M. *et al.* Exploring the reactivity of aliphatic and phenolic hydroxyl groups in lignin hydrogenolysis oil towards urethane bond formation. *Ind Crops Prod* **180**, (2022).

140. Zieglowski, M. *et al.* Reactivity of Isocyanate-Functionalized Lignins: A Key Factor for the Preparation of Lignin-Based Polyurethanes. *Front Chem* **7**, (2019).

141. Kim, S. M. *et al.* Environmentally-friendly synthesis of carbonate-type macrodiols and preparation of transparent self-healable thermoplastic polyurethanes. *Polymers (Basel)* **9**, (2017).

142. Rogulska, M., Kultys, A. & Pikus, S. The effect of chain extender structure on the properties of new thermoplastic poly(carbonate–urethane)s derived from MDI. *J Therm Anal Calorim* **127**, (2017).

143. Kojio, K., Furukawa, M., Motokucho, S., Shimada, M. & Sakai, M. Structure-mechanical property relationships for polycarbonate urethane elastomers with novel soft segments. *Macromolecules* **42**, 8322–8327 (2009).

144. Eceiza, A. *et al.* Structure-property relationships of thermoplastic polyurethane elastomers based on polycarbonate diols. *J Appl Polym Sci* **108**, (2008).

145. Zhu, R., Wang, Y., Zhang, Z., Ma, D. & Wang, X. Synthesis of polycarbonate urethane elastomers and effects of the chemical structures on their thermal, mechanical and biocompatibility properties. *Heliyon* **2**, (2016).

146. Guo, J., Zhao, M., Ti, Y. & Wang, B. Study on structure and performance of polycarbonate urethane synthesized via different copolymerization methods. *J Mater Sci* **42**, (2007).

147. Kultys, A., Rogulska, M., Pikus, S. & Skrzypiec, K. The synthesis and characterization of new thermoplastic poly(carbonate-urethane) elastomers derived from HDI and aliphatic-aromatic chain extenders. *Eur Polym J* **45**, (2009).

148. Eceiza, A. *et al.* Thermoplastic polyurethane elastomers based on polycarbonate diols with different soft segment molecular weight and chemical structure: Mechanical and thermal properties. *Polym Eng Sci* **48**, (2008).

149. Pyo, S. H., Park, J. H., Chang, T. S. & Hatti-Kaul, R. Dimethyl carbonate as a green chemical. *Current Opinion in Green and Sustainable Chemistry* vol. 5 Preprint at https://doi.org/10.1016/j.cogsc.2017.03.012 (2017).

150. Kojio, K., Nonaka, Y., Masubuchi, T. & Furukawa, M. Effect of the composition ratio of copolymerized poly(carbonate) glycol on the microphase-separated structures and mechanical properties of polyurethane elastomers. *J Polym Sci B Polym Phys* **42**, (2004).

151. Song, M., Yang, X. & Wang, G. Preparation of polycarbonate diols (PCDLs) from dimethyl carbonate (DMC) and diols catalyzed by KNO3/γ-Al2O3. *RSC Adv* **8**, 35014–35022 (2018).

152. Sun, J. & Kuckling, D. Synthesis of high-molecular-weight aliphatic polycarbonates by organo-catalysis. *Polym Chem* **7**, 1642–1649 (2016).

153. Fang, W. *et al.* One-pot synthesis of bio-based polycarbonates from dimethyl carbonate and isosorbide under metal-free condition. *Green Chemistry* **22**, 4550–4560 (2020).

154. Foy, E., Farrell, J. B. & Higginbotham, C. L. Synthesis of linear aliphatic polycarbonate macroglycols using dimethylcarbonate. *J Appl Polym Sci* **111**, 217–227 (2009).

155. Yang, Z. *et al.* Cost-Effective Synthesis of High Molecular Weight Biobased Polycarbonate via Melt Polymerization of Isosorbide and Dimethyl Carbonate. *ACS Sustain Chem Eng* **8**, 9968–9979 (2020).

156. ASTM Standard D5338-15 (2021). *Standard Test Method for Determining Aerobic Biodegradation of Plastic Materials Under Controlled Composting Conditions Incorporating Thermophilic Temperatures*. vol. 15 (2021).

157. International Standard ISO/FDIS 14855-1:2005. *Determination of the Ultimate Aerobic Biodegradability of Plastic Materials under Controlled Composting Conditions - Method by Analysis of Evolved Carbon Dioxide, Part 1: General Method*. (2005).

158. International Standard ISO/FDIS 14855-2:2007. *Determination of the Ultimate Aerobic Biodegradability of Plastic Materials under Controlled Composting Conditions - Method by Analysis of Evolved Carbon Dioxide, Part 2: Gravimetric Measurement of Carbon Dioxide Evolved in a Laboratory-Scale Test*. (2007).

159. ASTM. *ASTM D6400 - Standard Specification for Labeling of Plastics Designed to Be Aerobically Composted in Municipal or Industrial Facilities*. *Astm* (2021) doi:10.1520/D6400-21.

160. Kijchavengkul, T., Auras, R., Rubino, M., Ngouajio, M. & Thomas Fernandez, R. Development of an automatic laboratory-scale respirometric system to measure polymer biodegradability. *Polym Test* **25**, 1006–1016 (2006).

161. Burke, J. S. J. D. S. J. A. Engineering Material Specification: Polyurethane (PUR) Foam, Cast - FORD WSB-M2D456-A. 1–5 Preprint at (2009).

162. Joodaky, A., Batt, G. S. & Gibert, J. M. Prediction of cushion curves of polymer foams using a nonlinear distributed parameter model. *Packaging Technology and Science* **33**, 3–14 (2020).

163. Sardon, H. *et al.* Synthesis of polyurethanes using organocatalysis: A perspective. *Macromolecules* vol. 48 3153–3165 Preprint at https://doi.org/10.1021/acs.macromol.5b00384 (2015).

164. Zhang, M. *et al.* Green co-solvent-assisted one-pot synthesis of high-performance flexible lignin polyurethane foam. *Chemical Engineering Journal* **499**, 156142 (2024).

165. Adeleh, S. *et al.* Radiolabeling for polymers degradation studies: Opportunities and challenges ahead. *Polymer Degradation and Stability* vol. 230 Preprint at https://doi.org/10.1016/j.polymdegradstab.2024.111053 (2024).

166. Huang, S. J. & Roby, M. S. Biodegradable Polymers Poly(amide-urethanes) [1]. *J Bioact Compat Polym* **1**, (1986).

167. Huang, S. J., Roby, M. S. & Macri, C. A. BIODEGRADATION OF POLYURETHANES. in *American Chemical Society, Division of Organic Coatings and Plastics Chemistry, Preprints* vol. 43 (1980).

168. Khan, S. *et al.* Biodegradation of polyester polyurethane by Aspergillus tubingensis. *Environmental Pollution* **225**, (2017).

169. Maestri, C., Plancher, L., Duthoit, A., Hébert, R. L. & Di Martino, P. Fungal Biodegradation of Polyurethanes. *Journal of Fungi* vol. 9 Preprint at https://doi.org/10.3390/jof9070760 (2023).

170. Nakajima-Kambe, T., Shigeno-Akutsu, Y., Nomura, N., Onuma, F. & Nakahara, T. Microbial degradation of polyurethane, polyester polyurethanes and polyether polyurethanes. *Applied Microbiology and Biotechnology* vol. 51 Preprint at https://doi.org/10.1007/s002530051373 (1999).

171. Magnin, A., Entzmann, L., Pollet, E. & Avérous, L. Breakthrough in polyurethane bio-recycling: An efficient laccase-mediated system for the degradation of different types of polyurethanes. *Waste Management* **132**, (2021).

172. Taxeidis, G. *et al.* Triggering and identifying the polyurethane and polyethylene-degrading machinery of filamentous fungi secretomes. *Environmental Pollution* **325**, (2023).

173. Rekik, H. *et al.* Physical and enzymatic properties of a new manganese peroxidase from the white-rot fungus Trametes pubescens strain i8 for lignin biodegradation and textile-dyes biodecolorization. *Int J Biol Macromol* **125**, (2019).

174. Atiwesh, G., Parrish, C. C., Banoub, J. & Le, T. A. T. Lignin degradation by microorganisms: A review. *Biotechnology Progress* vol. 38 Preprint at https://doi.org/10.1002/btpr.3226 (2022).

175. Cui, T. *et al.* Enhanced lignin biodegradation by consortium of white rot fungi: microbial synergistic effects and product mapping. *Biotechnol Biofuels* **14**, (2021).

176. Tuomela, M., Vikman, M., Hatakka, A. & It Avaara, M. *Biodegradation of Lignin in a Compost Environment: A Review*.

177. Kühnel, I., Akil, Y., Lorenz, D., Saake, B. & Lehnen, R. Cyclic organic carbonates as reagents for the functionalization of lignins and hemicelluloses. in *NWBC 2018 - Proceedings of the 8th Nordic Wood Biorefinery Conference* (2018).

178. Shaikh, A.-A. G. & Sivaram, S. *Organic Carbonates †*. https://pubs.acs.org/sharingguidelines (1996).

179. Stokes, K., Mcvenes, R. & Anderson, J. M. Polyurethane elastomer biostability. *J Biomater Appl* **9**, 321–354 (1995).

180. Bian, S., Pagan, C., Andrianovaartemyeva, A. A. & Du, G. Synthesis of Polycarbonates and Poly(ether carbonate)s Directly from Carbon Dioxide and Diols Promoted by a Cs2CO3/CH2Cl2 System. *ACS Omega* **1**, 1049–1057 (2016).

181. Tang, D., Mulder, D. J., Noordover, B. A. J. & Koning, C. E. Well-defined biobased segmented polyureas synthesis via a TBD-catalyzed isocyanate-free route. *Macromol Rapid Commun* **32**, 1379–1385 (2011).

182. Zhu, W. *et al*. High-molecular-weight aliphatic polycarbonates by melt polycondensation of dimethyl carbonate and aliphatic diols: Synthesis and characterization. *Polym Int* **60**, 1060–1067 (2011).

APPENDIX A: CHAPTER 2

Table A1: Measured lignin properties, including lignin source, isolation method, elemental analysis, moisture content, molecular weight, and glass transition temperature.

Lignin Property	**Results**
Isolation Method	Kraft
Source	Softwood
Ash Content (wt.%)	4.43 ± 0.22
Na (wt %)	0.82
Sulfur content (%)	1.96
M_n (Da)	2002
M_w (Da)	7998
Dispersity	3.99
Tg (°C)	130

Table A2: Hydroxy moieties of the lignin used in this study, measured by quantitative ^{31}P-NMR spectroscopy. Samples were phosphitylated prior to analysis.

Hydroxyl Functional Groups	**Hydroxyl Content (mmol/g)**
Aliphatic	2.10
Condensed Phenolic	1.02
Syringyl	-
Guaiacyl	1.83
Hydroxyphenyl	0.26
Carboxylic Acid	0.40
Total Hydroxy Content	5.63

APPENDIX B: CHAPTER 3

Table B1: Measured lignin properties, including lignin source, isolation methods, elemental analysis, moisture content, molecular weight, and glass transition temperature.

Lignin ID	**O-HW**	**K-SW**	**H-HW**
Isolation Method	Organosolv	Kraft	Hydrolysis
Source	Hardwood	Softwood	Hardwood
Ash Content (wt.%)	0.04	0.55	2.3
Moisture Content (wt. %)	1.2 ± 0.3	37.2 ± 2.4	1.2 ± 0.1
Na (wt %)	0.01	0.16	0.56
Sulfur content (%)	-	1.82	0.28
M_n (Da)	1640	1650	1110
M_w (Da)	4066	7650	5480
Dispersity	2.48	4.6	4.9
Tg (°C)	96	162	166

Table B2: Hydroxy moieties of the lignins used in this study were measured by quantitative ^{31}P-NMR spectroscopy. **O-HW**: Organosolv-Hardwood; **K-SW**: Kraft-Softwood; **H-HW**: Hydrolysis-Hardwood.

Hydroxy Moiety Content (mmol/g)	**O-HW**	**K-SW**	**H-HW**
Aliphatic	0.76	1.71	2.66
Condensed Phenolic	0.72	1.20	0.43
Syringyl	1.47	-	1.46
Guaiacyl	0.45	1.92	0.48
Hydroxyphenyl	0.12	0.13	0.12
Carboxylic Acid	0.27	0.41	0.28
Total Hydroxy Content	3.79	5.37	5.43

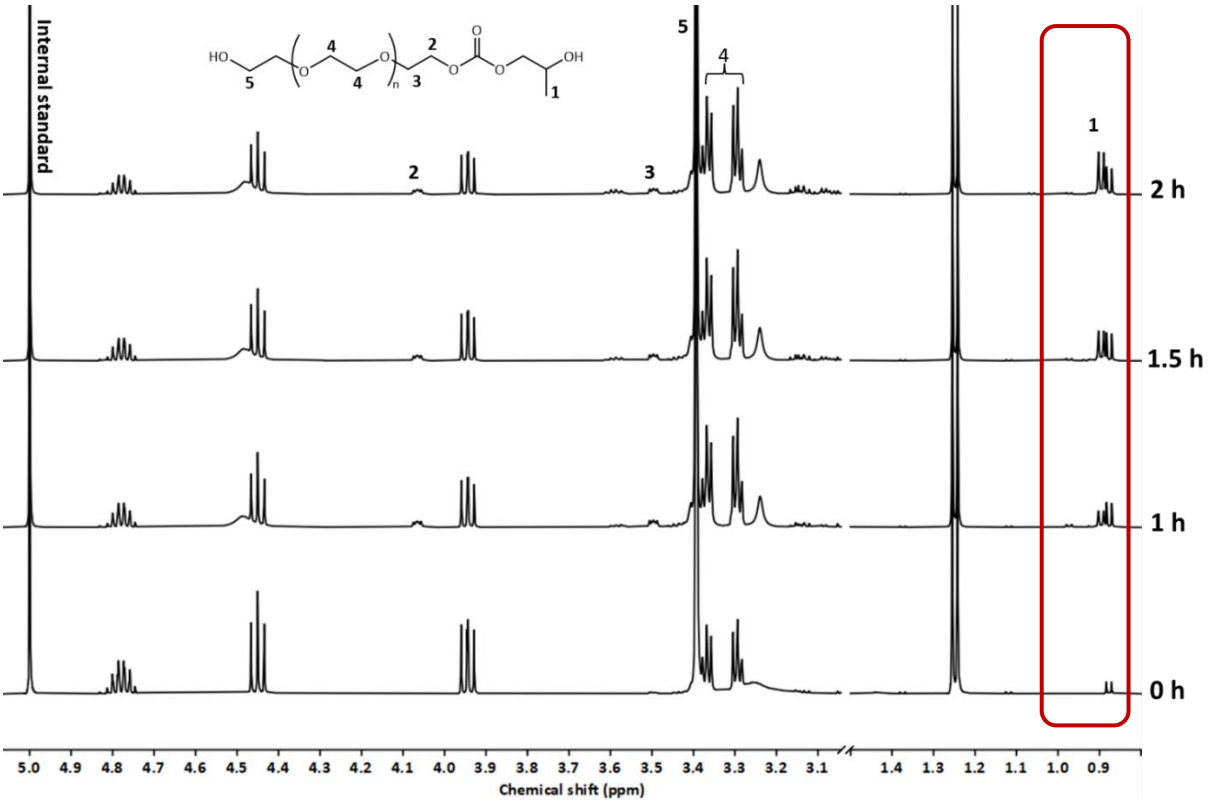

Figure B1: ^{1}H NMR spectra of products obtained from a DBU-catalyzed reaction between polyethylene glycol and propylene carbonate with time.

Table B3: Quantitative result of ^{1}H NMR estimation of percentage (%) propylene carbonate consumed by polyethylene glycol.

Time (h)	% PC Consumed
1.0	19.9
1.5	27.0
2.0	35.5

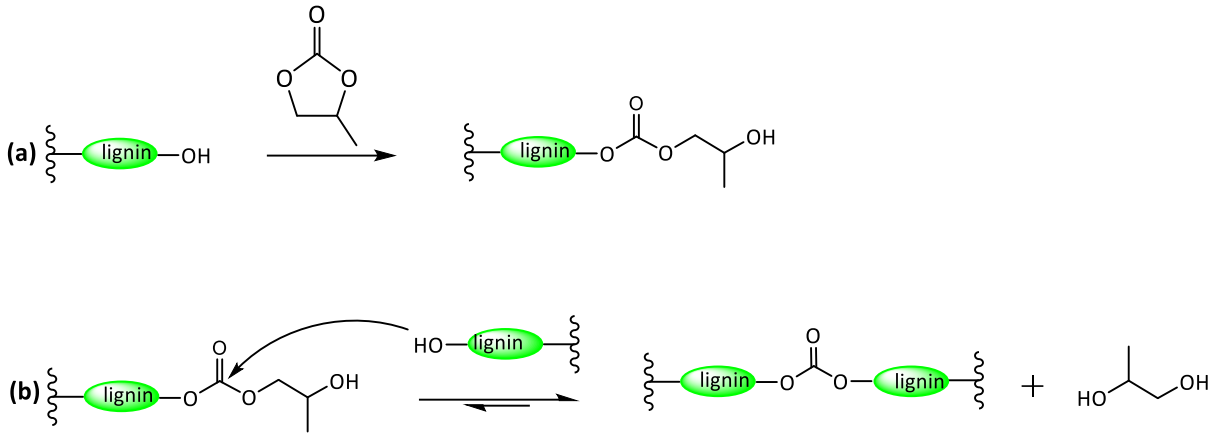

Figure B2: Mechanism for lignin chain coupling reaction.

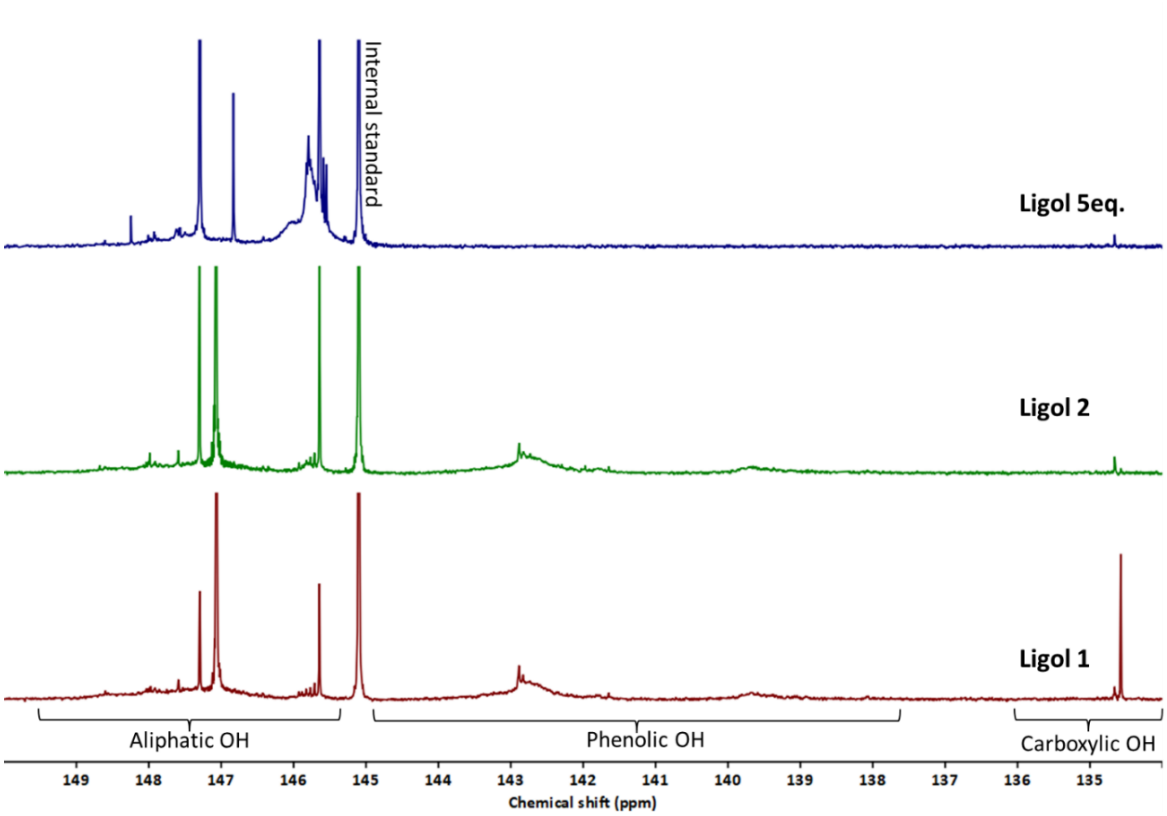

Figure B3: ^{31}P-NMR spectra of synthesized Ligol 1, Ligol 2 and Ligol 5eq.

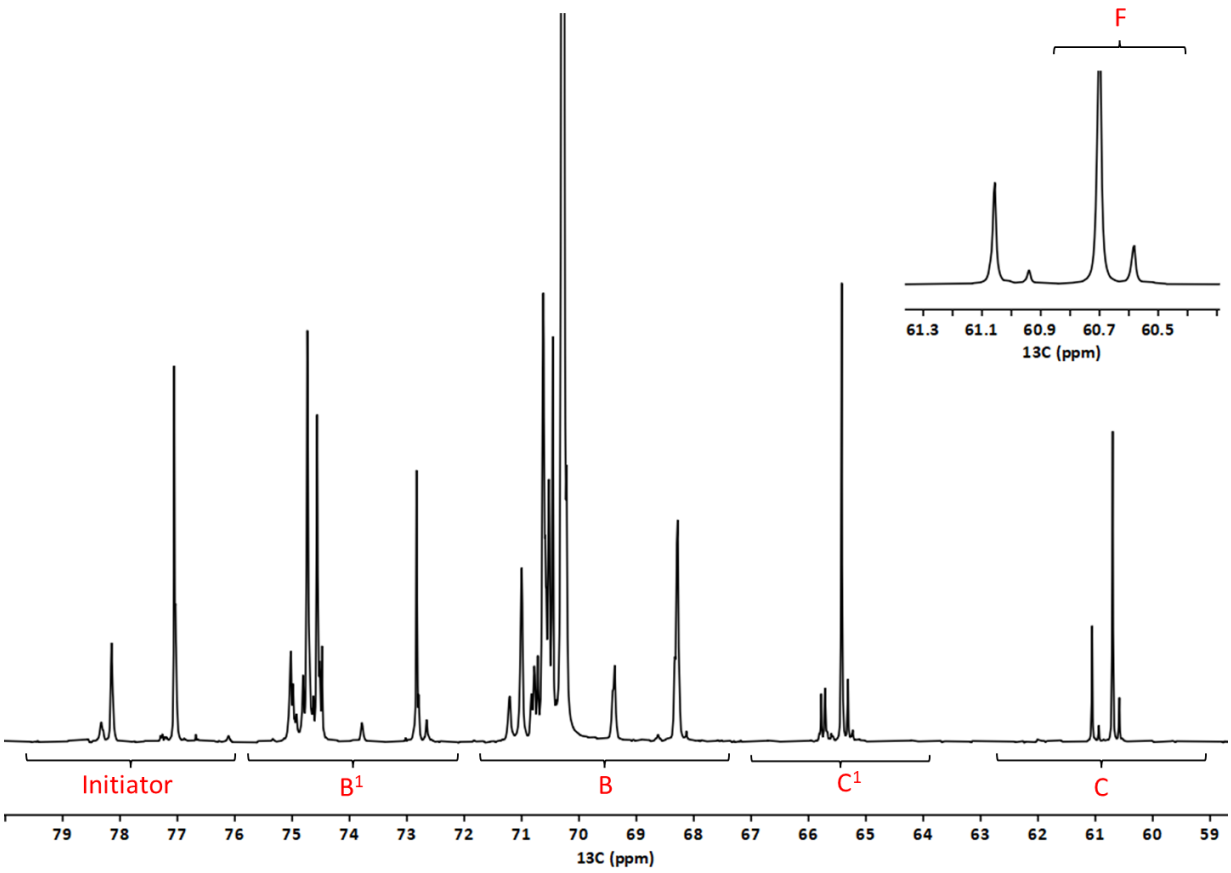

Figure B4: ^{13}C NMR spectrum of propylene oxide/ethylene oxide capped co-polyol (PO/EO-C) showing integrated regions used in the ethylene oxide content estimation.

APPENDIX C: CHAPTER 4

Table C1: Measured lignin properties, including lignin source, isolation method, elemental analysis, moisture content, molecular weight, and glass transition temperature.

Property	**Result**
Isolation Method	Hydrolysis
Source	Hardwood
Ash Content (wt.%)	2.3
Moisture Content (wt. %)	1.2 ± 0.1
Na (wt %)	0.56
Sulfur content (%)	0.28
M_n (Da)	1110
M_w (Da)	5480
Dispersity	4.9
Tg (°C)	160

Table C2: Hydroxy moieties of the lignin used in this study, measured by quantitative ^{31}P-NMR spectroscopy. Samples were phosphitylated prior to analysis.

Hydroxy Moiety Content (mmol/g)	**Result**
Aliphatic	2.66
Condensed Phenolic	0.43
Syringyl	1.46
Guaiacyl	0.48
Hydroxyphenyl	0.12
Carboxylic Acid	0.28
Total Hydroxy Content	5.43

Structural Analysis of Precipitated Oxyalkylated Lignin

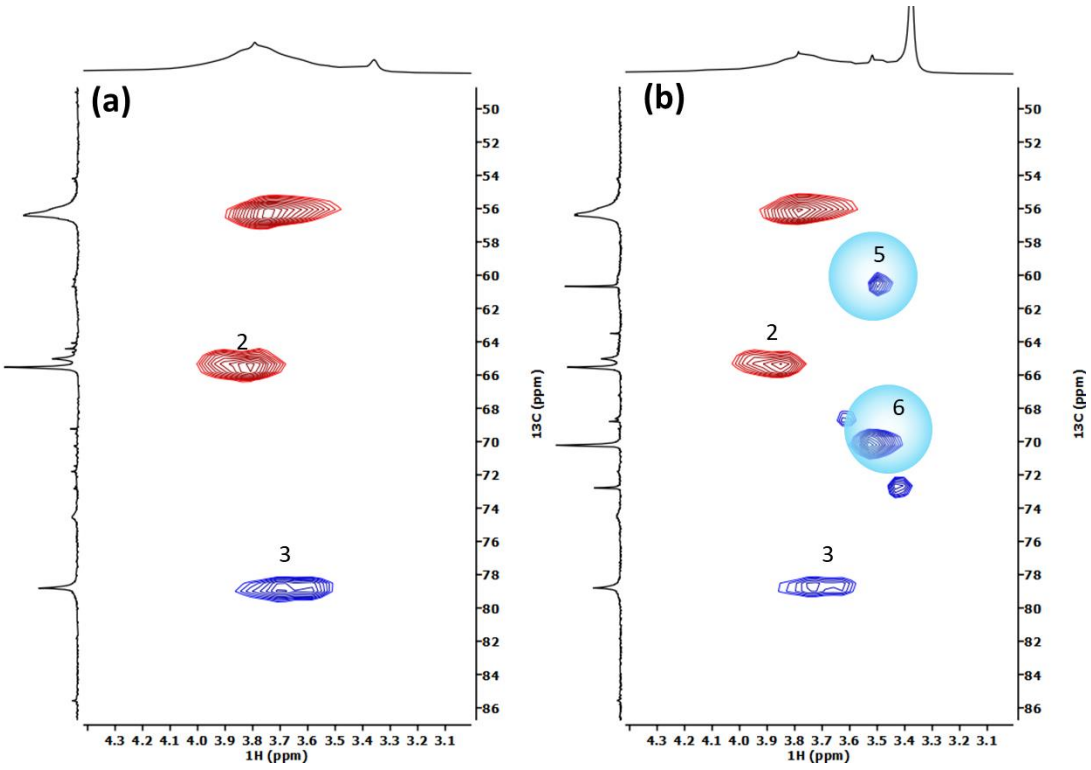

Figure C1: Expansion from HSQC spectra of precipitated propylene carbonate oxyalkylated lignin (OL) from oxyalkylation reaction (a) without PEG and (b) with PEG.

Impact Test

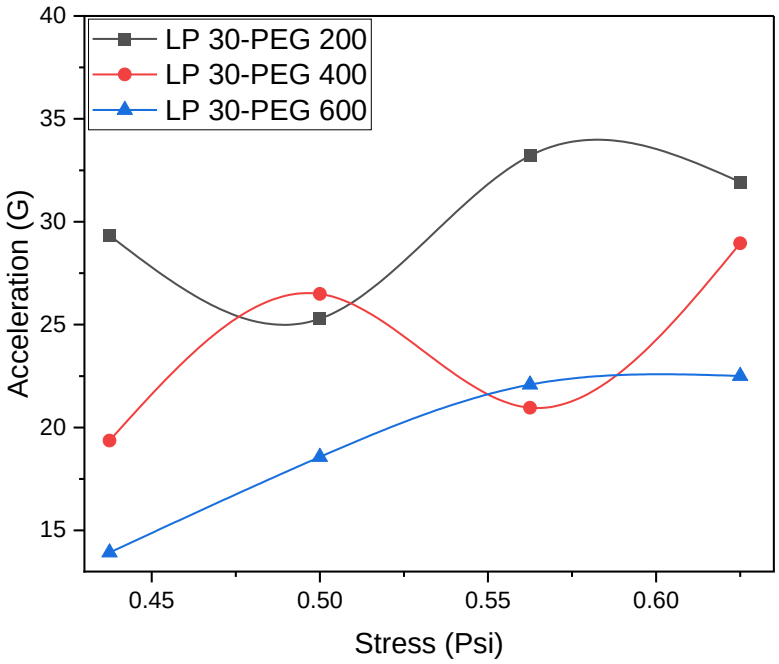

Figure C2: Cushion curve of lignin-based foams (30% petroleum-based polyol substitution). Foams were formulated using Ligols A, B, and C.

Scanning Electron Microscopy (SEM)

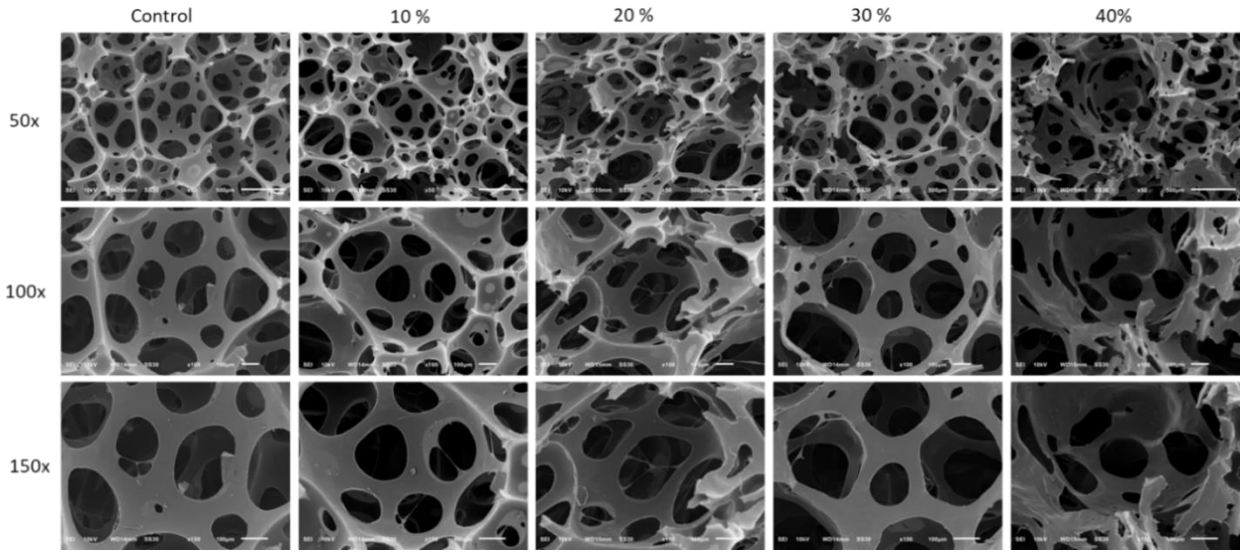

Figure C3: Scanning Electron Microscopy (SEM) of developed control and lignin-based flexible PU foams at 50x, 100x, and 150x magnification. Lignin-based foams were formulated using Ligol A.

Thermogravimetric Analysis (TGA)

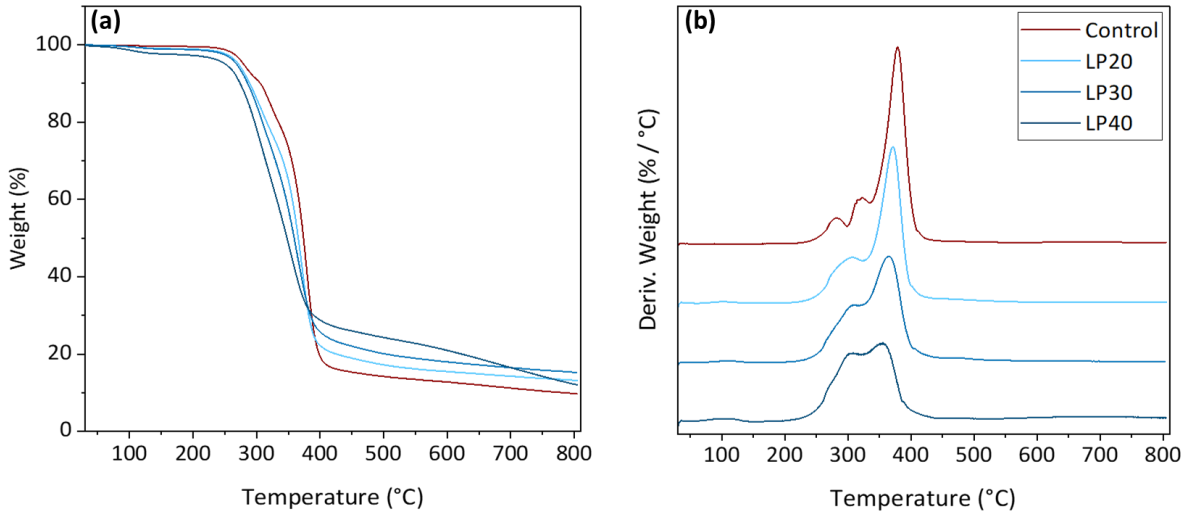

Figure C4: Thermogravimetric analysis (TGA) thermogram (a) and differential thermogravimetric (DTG) curve (b) of control and lignin polyol (LP)-based foams (20, 30 and 40 petroleum-based polyol substitution).

Mechanical Property Test

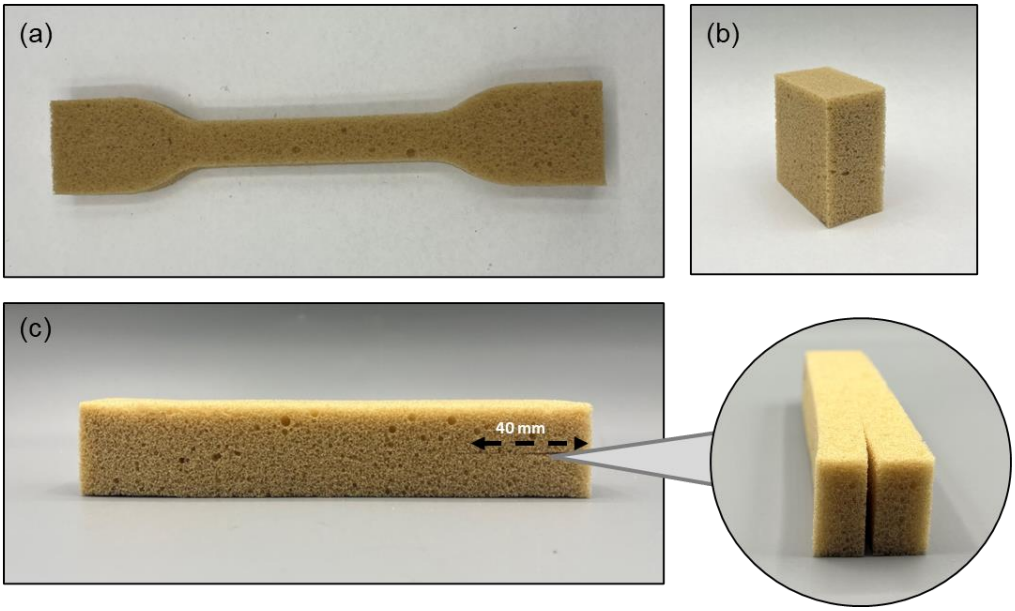

Figure C5: Test specimen geometry according to ASTM D3574 for (a) tensile and elongation at break (b) compressive force deflection, density, and support factor, and (c) tear strength assessments.

Impact Test

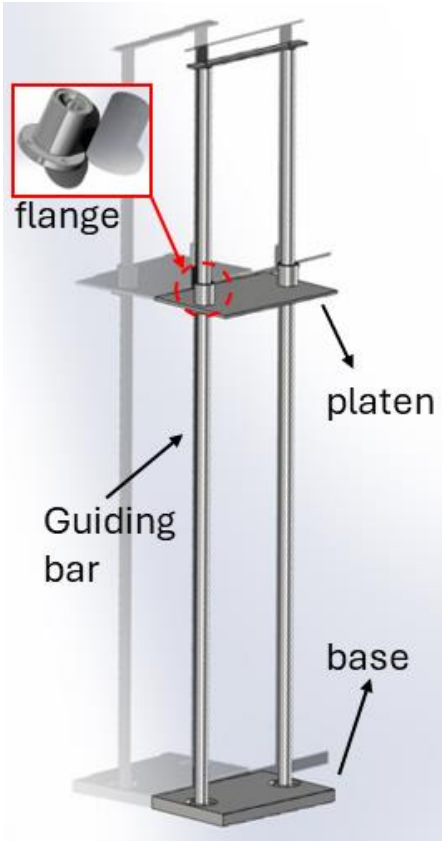

Figure C6: Designed drop tester for measuring shock absorption of developed PU flexible foams.

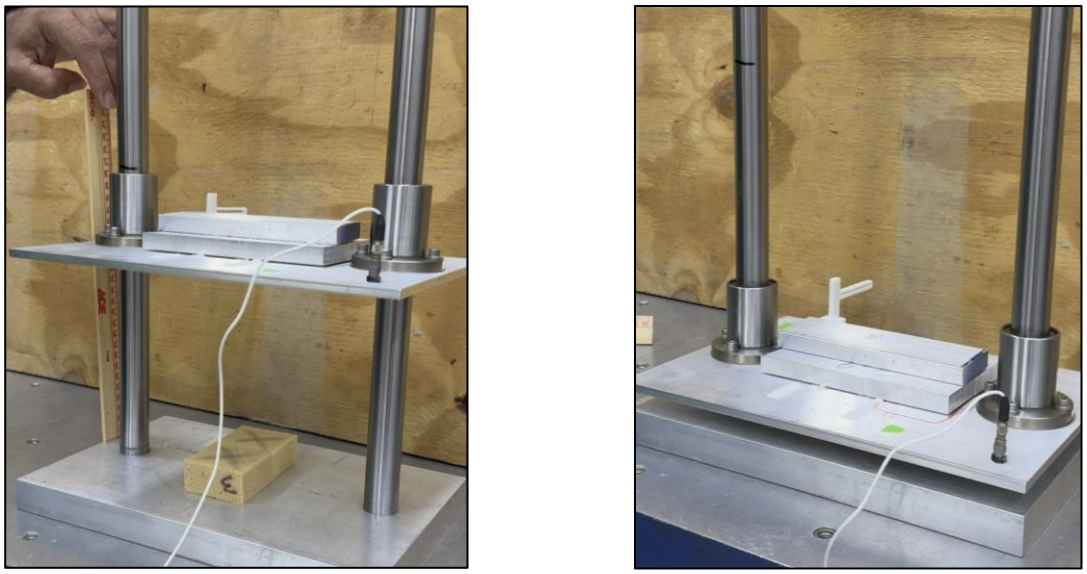

Figure C7: Cushion impact test before (left) and after (right) impact using designed impact tester. The accelerometer and extra weight blocks are installed on the top platen to measure the shock response and increase weight incrementally respectively for generating cushion curves.

Biodegradation

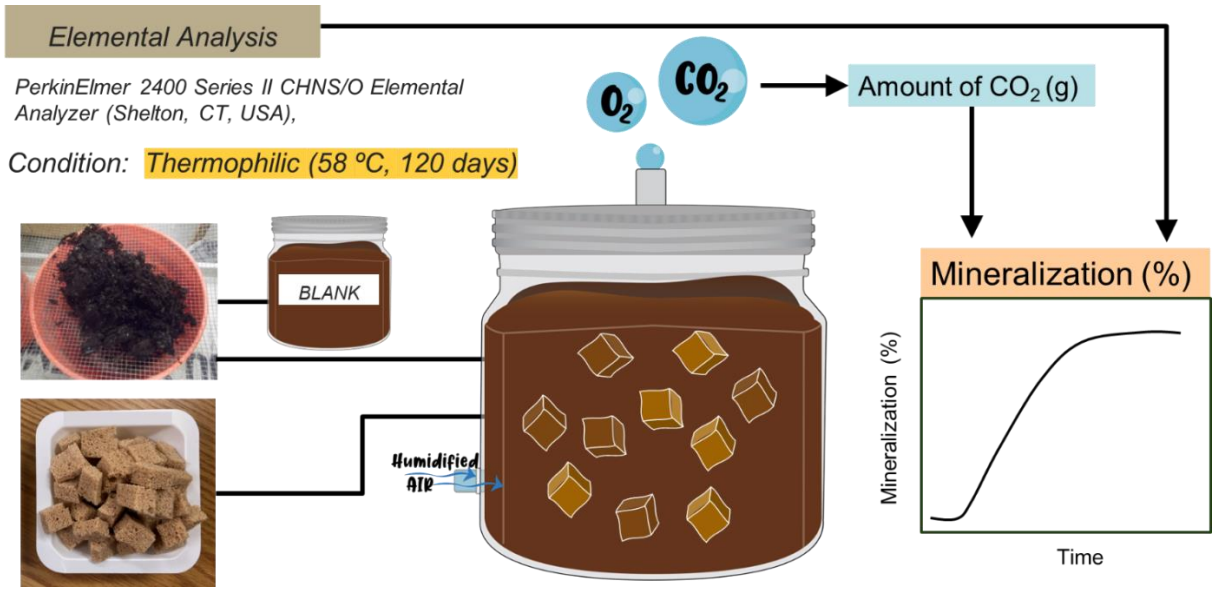

Figure C8: Schematic diagram of thermophilic anaerobic biodegradation study of lignin-based flexible PU foams under compost environment.

Table C3: Physicochemical parameters of compost soil prior to biodegradation test.

Tests	Units	Compost
pH	-	7.22
E. C. - Saturation Paste	mmho/cm	13.8
Total Dry Solid	%	55.7
Total Volatile Solid	%	44.4
C/N Ratio		10.3
Total Nitrogen (N)	%	2.27
Total Phosphorus (P)	%	1.36
Total Potassium (K)	%	1.46
Total Calcium (Ca)	%	6.11
Total Magnesium (Mg)	%	1.57
Total Zinc (Zn)	ppm	380
Total Iron (Fe)	ppm	7033
Total Manganese (Mn)	ppm	294
Total Copper (Cu)	ppm	126
Total Carbon (C)	%	23.3
Total Sodium (Na)	%	0.347
Total Aluminum (Al)	%	0.198
Total Sulfur (S)	%	0.505
Total Boron (B)	ppm	39

Table C4: Carbon content analysis of biodegradation test samples measured using CHNS/O Elemental Analyzer.

Sample	% Carbon (average)
Cellulose	42.5
Control	65.7
Lignin polyol	54.1
Pure lignin	63.2
LP30-SP30	67.1
LP40	64.0

Figure C9: In-house built direct measurement respirometer (DMR) for biodegradation study.

Structural Analysis of Crude (Unprecipitated) Oxyalkylation and Transesterification Lignin Polyol

The propylene carbonate (PC) oxyalkylation was an important step for two reasons. First, it converts sterically hindered phenolic OH functionalities to aliphatic hydroxyl groups, improving lignin's overall reactivity towards isocyanate. Second, to facilitate its subsequent reaction towards dimethyl carbonate (DMC) to produce polycarbonate polyols. It is also important to note that carboxylic hydroxyl groups of lignin also react with propylene carbonate to produce aliphatic OH group terminated derivatives.[93] PC, being a liquid at room temperature, was preferred over ethylene carbonate as the cyclic alkyl carbonate of choice because it yields a polyol mixture with significantly lower viscosity, a crucial factor for foam manufacturing.

^{31}P NMR analysis was performed on the crude lignin polyol (unprecipitated), after phosphitylating, to confirm the success of the oxyalkylation reaction. The absence of both phenolic (137.3 -144.6 ppm) and carboxylic hydroxyl (134 – 135.9 ppm) groups in lignin was evident (**Figure C10**), indicating the conversion of these functional groups to aliphatic hydroxyl groups. During the oxyalkylation of lignin, deprotonated phenolic and carboxylic hydroxyl groups undergo a nucleophilic attack on the alkyl carbon of propylene carbonate, resulting in the generation of carbon dioxide gas.[90,91,93,177] The peaks in the range of 147.2-146.86 ppm in ^{31}P{^{1}H} NMR spectra were identified as derived from PEG's aliphatic hydroxyl groups. Furthermore, the emergence of two distinct peaks at 147.3 and 145.6 ppm suggests the possible formation of propylene glycol (PG) or oligomeric glycols, likely originating from PC-ring opening from residual water molecules or transesterification side reactions.[58] Thus, the oxyalkylation product mainly contains modified lignin, PEG, and oligomeric glycols. The quantitative analysis of the total hydroxyl content of the mixture yielded a value of 6.51 mmol/g (equivalent to 365 mg KOH/g). This value falls beyond

the acceptable range of hydroxyl values (28 to 180 mg KOH/g) for polyols intended for use in flexible polyurethane applications.

After the oxyalkylation step, transesterification with dimethyl carbonate (DMC) was carried out to produce polycarbonate polyols, generating methanol as a byproduct. The $^{31}P\{^{1}H\}$ NMR analysis of the transesterification product, as shown in **Figure C11**, indicates a significant reduction in peaks corresponding to PG at 147.3 and 145.6 ppm. Similarly, the intensity of the peak associated with the aliphatic hydroxyl group of PEG (147.2–146.86 ppm) decreased. In contrast, the aliphatic hydroxyl group of lignin showed a relatively lower reduction, likely due to its bulky structure and the presence of secondary hydroxyl groups formed during oxyalkylation with propylene carbonate. These structural factors may have contributed to lignin's lower reactivity toward DMC. Secondary hydroxyl groups tend to exhibit lower reactivity towards dimethyl carbonate compared to primary aliphatic hydroxyl groups,[178] which are predominantly present in PEG.

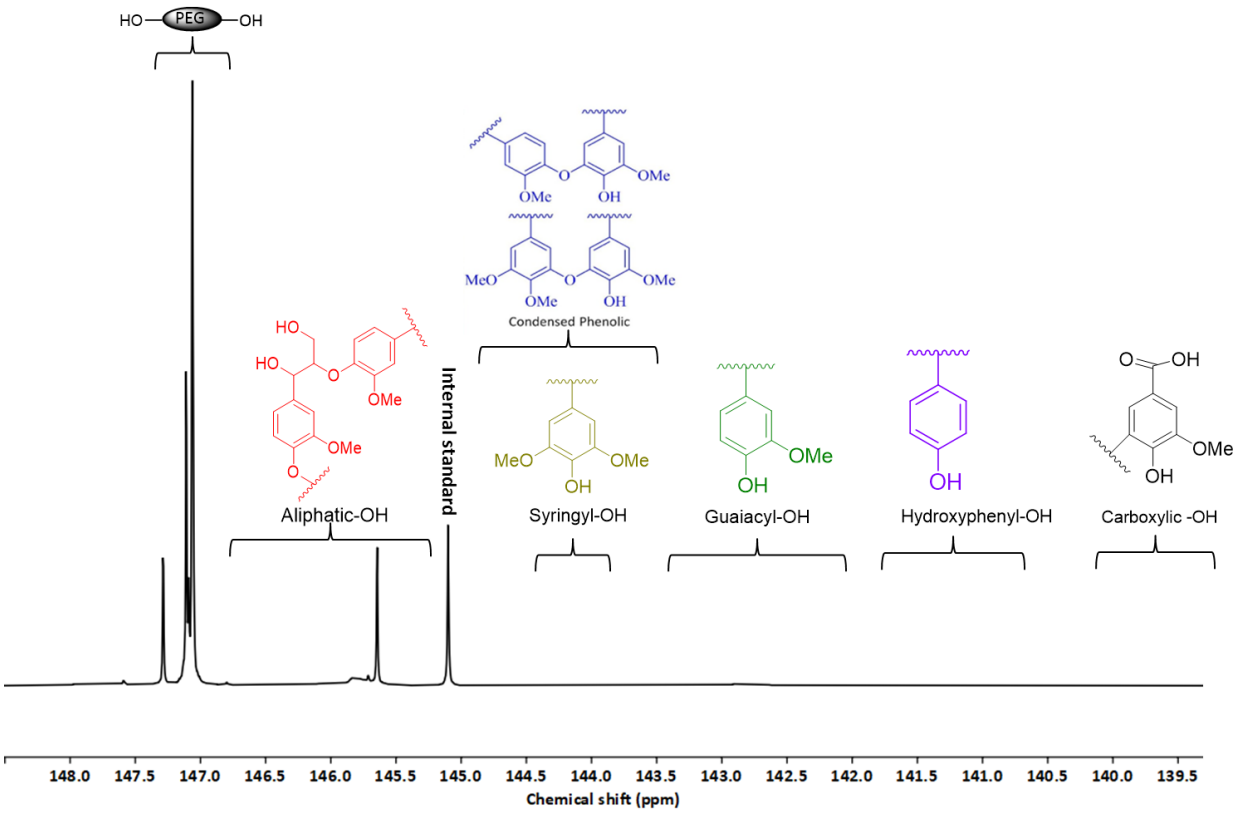

Figure C10: Expansion of a $^{31}P\{^{1}H\}$ NMR spectrum of lignin polyol after propylene carbonate oxyalkylation step. Lignin polyol samples are phosphitylated for ^{31}P quantification and analysis.

Quantitative analysis of polyethylene glycol and oligomeric glycols aliphatic OH group reduction, obtained from integrating their respective $^{31}P\{^{1}H\}$ NMR peaks, after 30 minutes of transesterification was 43.95 and 91.5%, respectively. This further demonstrates that primary hydroxyl groups are more reactive towards dimethyl carbonate. The total hydroxyl content of the reaction mixture after the transesterification reaction yielded a value of 3.19 mmol/g (179 mg KOH/g), making it more suitable for use in flexible PU formulation.

The FTIR spectrum of the transesterification reaction product indicates an increase in the ether linkage at 1260 cm^{-1} and the emergence of a new carbonyl (C=O) peak at 1740 cm^{-1} as seen in **Figure C12**. This new peak is associated with the carbonate linkage formed during the transesterification reaction with dimethyl carbonate. These carbonate linkages have been reported

to improve mechanical properties and resistance to hydrolysis and oxidation of foams. [151,152,154,179–182] The decrease in the OH peak at 3433 cm^{-1} is consistent with the findings observed in the $^{31}P\{^{1}H\}$ NMR analysis. In total, there was a 51% reduction in the hydroxyl groups of oxyalkylation derivatives after the transesterification reaction.

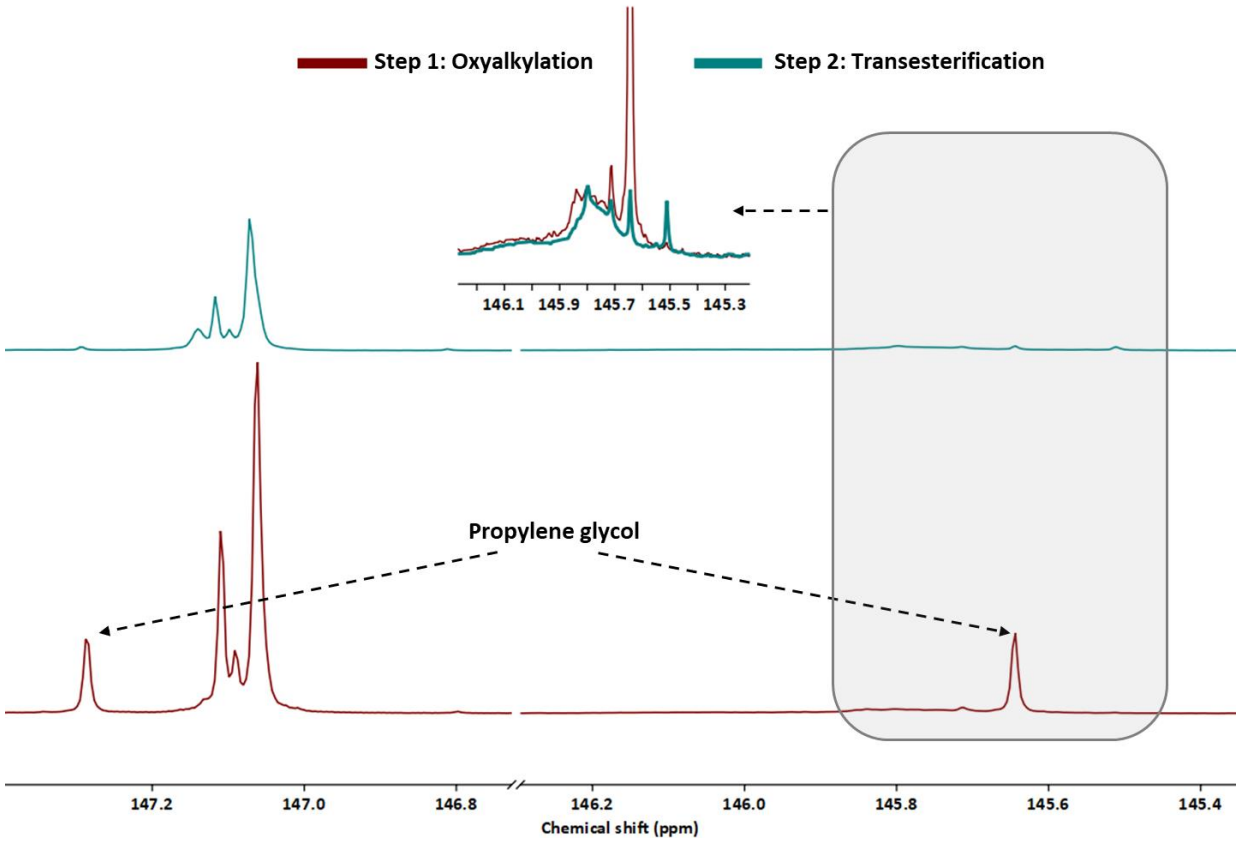

Figure C11: Aliphatic hydroxyl group region of $^{31}P\{^{1}H\}$ NMR spectra of lignin polyols after propylene carbonate oxyalkylation and dimethyl carbonate transesterification reaction steps. Lignin polyol samples were phosphitylated for $^{31}P\{^{1}H\}$ NMR quantification and analysis.

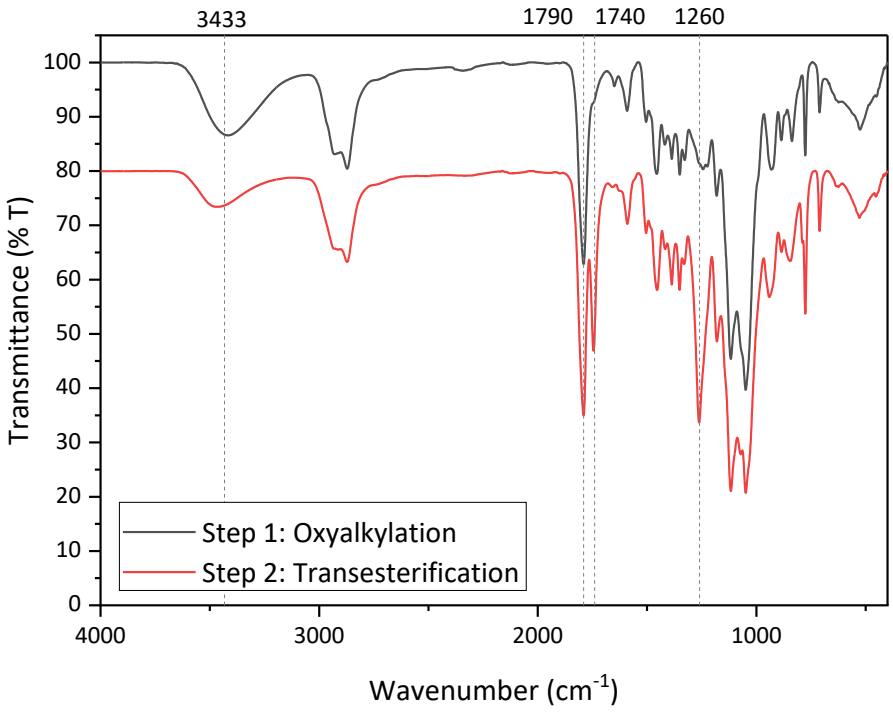

Figure C12: FTIR-ATR spectra of synthesized lignin polyols after (a) Propylene carbonate oxyalkylation (b) dimethyl carbonate transesterification reaction.

^{1}H NMR analysis of the oxyalkylation product displays signals within the 1-1.5 ppm range, as seen in **Figure C13**, which can be attributed to the newly formed methyl group resulting from the reaction of lignin with propylene carbonate.[88] The doublet at 0.98 ppm is associated with the methyl group on propylene glycol generated through side reactions. Further analysis of the transesterification reaction product revealed a decrease in the methyl proton at 0.98 ppm which corresponds to propylene glycol side product. ^{1}H chemical shift signals at 3.41, 3.48 and 3.485 ppm can be attributed to methylene protons in PEG. The reduction in the proton signal intensity at 3.485 ppm, corresponding to PEG's characteristic terminal methylene protons, is consistent with the results from ^{31}P{^{1}H} NMR and FTIR. This can be attributed to the transesterification reaction

between PEG hydroxyl groups and DMC, leading to a decrease in its hydroxyl signals. Subsequently, two new peaks emerged at 3.62, and 4.18 ppm.

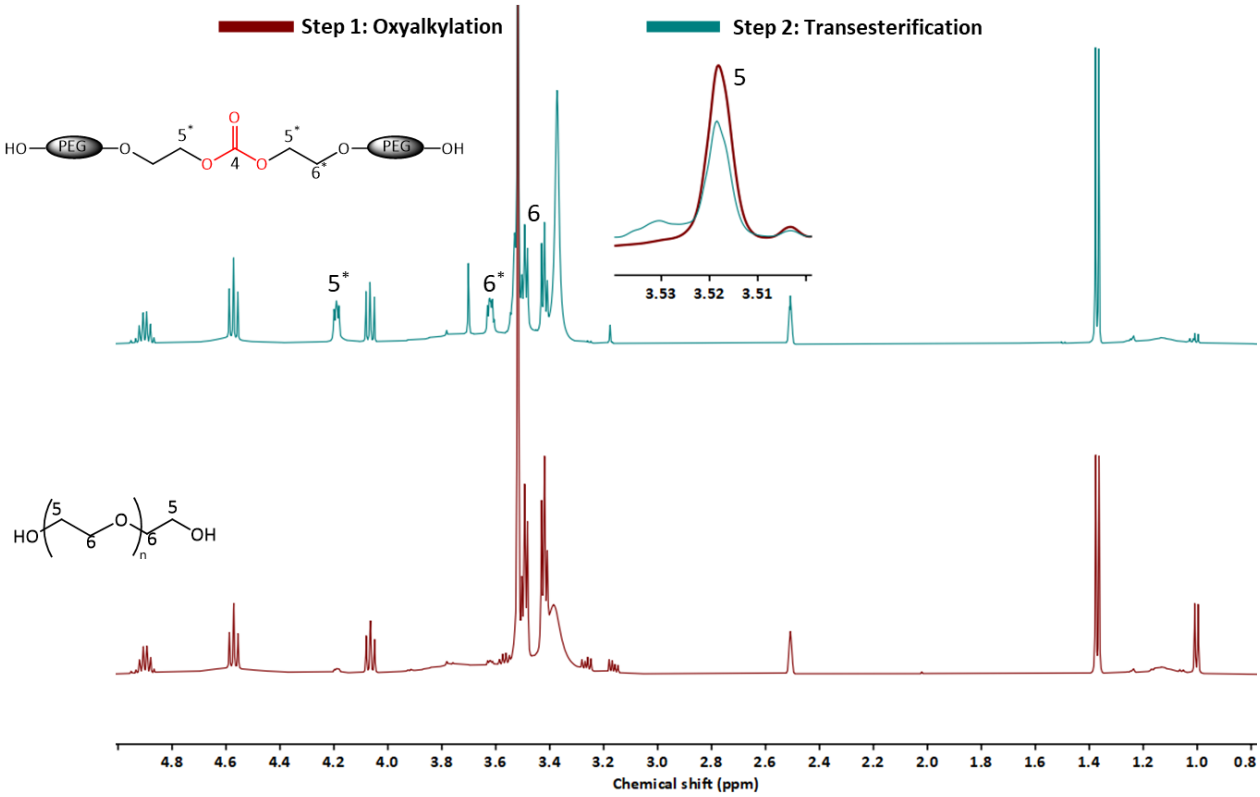

Figure C13: Expansion of ^{1}H NMR spectra of synthesized lignin polyols after propylene carbonate oxyalkylation and dimethyl carbonate transesterification reaction step.

HSQC analysis of these new proton signals confirmed that they are methylene (CH_2) protons as seen in **Figure C15**. The appearance of these protons suggests the potential for random co-polymerization between lignin and polyethylene glycol during the transesterification step. Additionally, a new methyl proton signal was observed at 3.7 ppm. This signal appears as a singlet, which may have originated from either residual DMC or a terminal methyl carbonate group on a PEG molecule.

The confirmation of the formation of polyethylene glycol adducts (resulting from the reaction of PEG with propylene carbonate) was conducted using $^{13}C\{^{1}H\}$ NMR. In addition to the carbonyl

carbon peak (155.4 ppm) of PC, a new minor peak at 155.07 ppm emerged as seen in **Figure C14**, indicating the presence of a PEG adduct in the oxyalkylation products. The intensity of this peak suggests that only a small amount of this product was present. The carbonyl carbon signal at 155.07 ppm increased significantly by the end of the transesterification reaction. This is due to the reaction between PEG hydroxyl groups and DMC leading to the introduction of carbonate linkages. $^{13}C\{^{1}H\}$ NMR spectra also show the emergence of two methylene carbon peaks at 67.46 and 68.97 ppm, thus confirming the reaction of PEG with dimethyl carbonate. Additionally, a new carbonyl carbon emerged at 155.7 ppm.

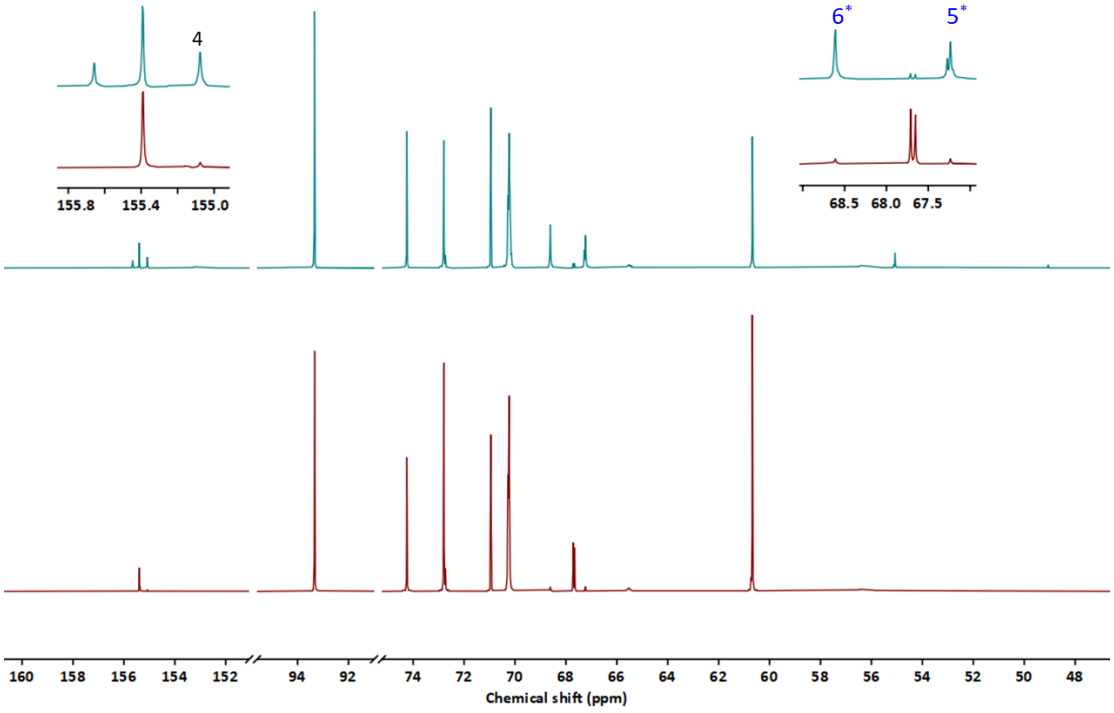

Figure C14: Expansion of $^{13}C\{^{1}H\}$ NMR spectra of synthesized lignin polyols after propylene carbonate oxyalkylation and dimethyl carbonate transesterification reaction step.

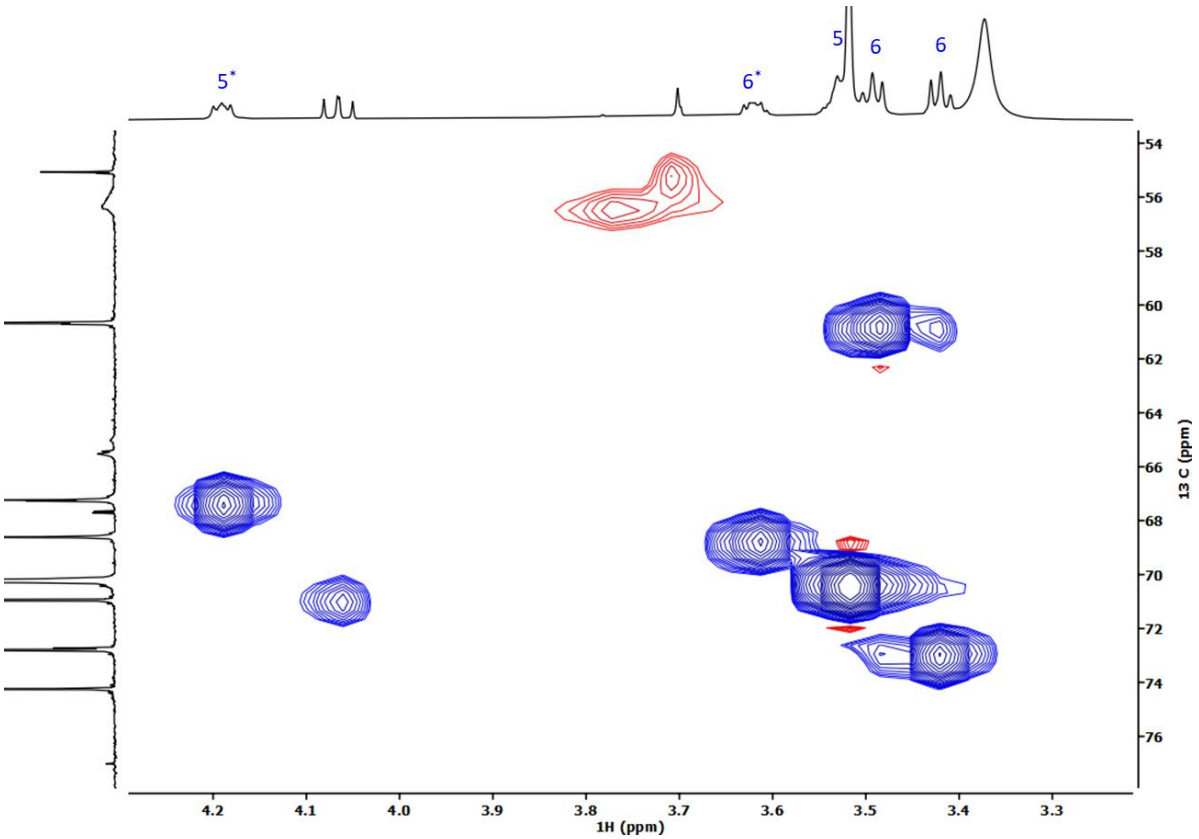

Figure C15: Expansion from HSQC spectrum of lignin polyol after dimethyl carbonate (DMC) transesterification reaction.

To elucidate the structure of the polyol repeating unit predominantly formed after the transesterification reaction, HMBC was conducted. The HMBC spectra, presented in **Figure C16**, shows that the methylene proton at 4.18 ppm has a cross-peak with a carbonyl carbon at 155.07. Methylene carbon at 68.97 ppm also correlates with the proton signal at 4.18 ppm, thus confirming the presence of the PEG-PEG repeating unit in the polymer chain. The carbonyl carbon at 155.7 has a cross-peak with both methylene protons at 4.18 ppm and methyl proton at 3.7 ppm. This cross-peak confirms the presence of a terminal methyl carbonate group on some PEG molecules. The presence of this side product was unexpected considering only 0.5 equivalent of DMC was used in the transesterification reaction indicating the need to extend the reaction time longer to

enable further chain extension. Overall, there was no clear evidence from the NMR analysis to confirm the formation of lignin-PEG and lignin-lignin repeating units. Therefore, an in-depth NMR analysis of precipitated modified lignin (oxyalkylated lignin (OL) and transesterified lignin (TL)) in both reaction steps was performed to further validate the presence of these units.

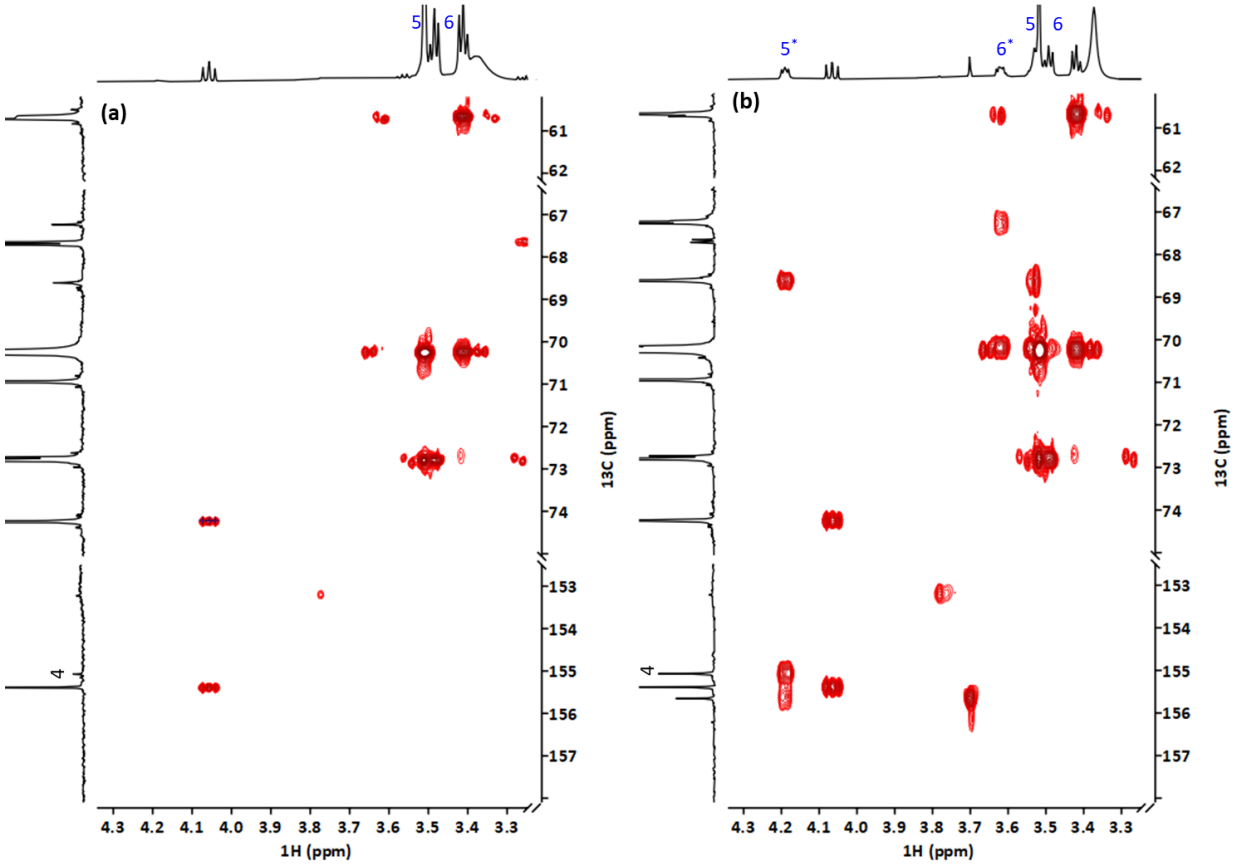

Figure C16: Expansion from HMBC spectra of synthesized lignin polyols in (a) propylene carbonate oxyalkylation and (b) dimethyl carbonate transesterification reaction.

Statistical Analysis

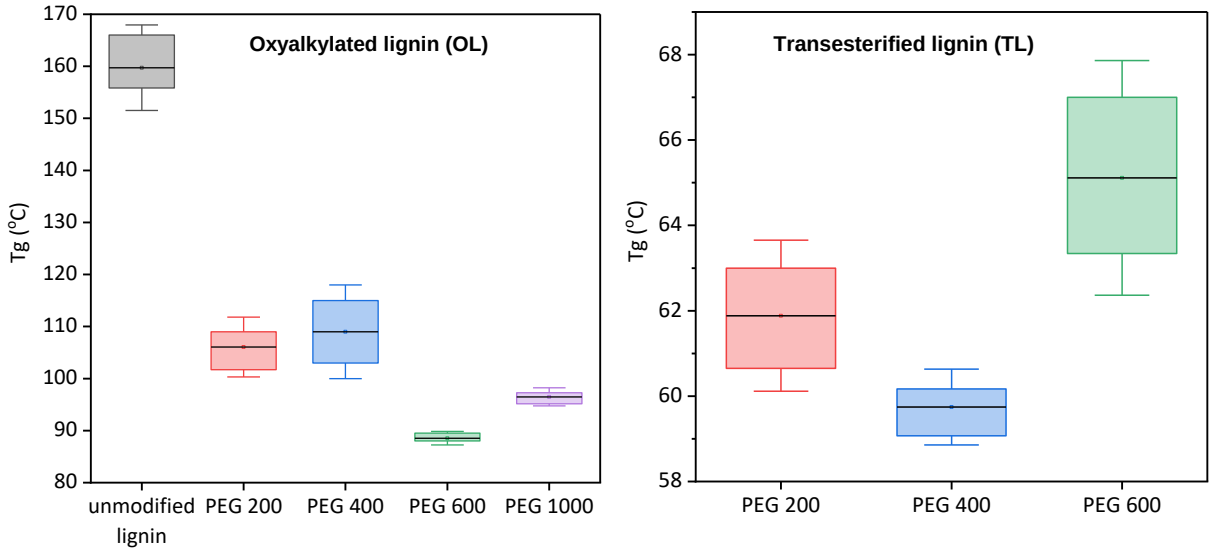

Figure C17: One-way ANOVA ($P \leq 0.05$) statistical analysis of glass transition temperature (*Tg*) of precipitated propylene carbonate oxyalkylated lignin (left) and dimethyl carbonate transesterified lignin (TL).